

https://dspace.org/

# Baseline Hydrogeology of Dolerite Dykes in Lesotho, Mafeteng District as a Case Study

**Monyane, Napo Shadrack**

**2024-06-10**
University of the Witwatersrand, Johannesburg
https://hdl.handle.net/10539/45291
Monyane, Napo Shadrack. (2024). Baseline Hydrogeology of Dolerite Dykes in Lesotho, Mafeteng District as a Case Study. [Master's dissertation, University of the Witwatersrand, Johannesburg]. WIReDSpace. https://hdl.handle.net/10539/45291

Downloaded from a DSpace repository. https://dspace.org/

# Baseline Hydrogeology of Dolerite Dykes in Lesotho, Mafeteng District as a Case Study

By: Napo Monyane

A research report submitted to the Faculty of Science, University of the Witwatersrand, Johannesburg, in partial fulfilment of the requirements for the degree of Master of Science in Hydrogeology

Supervisor: Prof. Tamiru Abiye

Co-Supervisor: Dr. Teboho Shakhane

[Senior Scientist: Resource Planning and Operations, Inkomati-Usuthu Catchment Management Agency]



University of the Witwatersrand
Johannesburg, 2024

# DECLARATION OF ORIGINAL WORK

I, **Napo Shadrack Monyane,** Student number: **1826690**, am a student registered for **GEOL7028A** in the year **2023**. I hereby declare the following:

I am aware that plagiarism (the use of someone else's work without their permission and/or without acknowledging the original source) is wrong.

I confirm that the work submitted for assessment for the above course is my own unaided work except where I have explicitly indicated otherwise.

I have followed the required conventions in referencing the thoughts and ideas of others.

I understand that the University of the Witwatersrand may take disciplinary action against me if there is a belief that this is not my unaided work or that I have failed to acknowledge the source of the ideas or words in my writing.

Signature: N.Monyane Date: **10 June 2024**

# ABSTRACT

Groundwater is a vital alternative resource due to the increasing demand for water supply in Lesotho's rural and urban areas as surface water faces threats from population growth and climate variability. For instance, groundwater serves the demands of Lesotho's growing textile industry and agricultural sectors. The 3D form of the dolerite dykes widespread throughout the Karoo rocks in Lesotho may have an impact on the groundwater occurrence, flow, and yield characteristics of the region. However, specific research on their hydrogeology has not been extensively undertaken.

This study aimed at characterising the hydrogeology of the dolerite dykes in the lowlands of Lesotho using selected places namely, Boluma-Tau, Ha Lumisi, Ha Mofota, Ha Maoela, Ha Mofo, Malumeng, Qalabane, Matlapaneng, Thabana Mohlomi, Ha Mohlehli, Malimong, Tsoeneng and Ha Lenonyane as case studies for the research. This research adopted the desktop and walkover survey in developing information on the region's broad geological and hydrogeological setting within the Karoo lithologies. Included also was the use of ground magnetics in ascertaining the existence and determining the geometry of the dykes, using the D-8 algorithm for flow directions, and drilling and pumping tests for aquifer analysis. The dykes dominating the focal area in the Mafeteng District generally trend NE-SW, NNE-SSW and NW-SE. The magnetic results outlined negative anomalies along the dyke's contact with the country rocks as surveyed from Qalabane, Mafeteng Lesotho, these magnetic lows imply fracture gaps along the strike of the dyke. A generalised dip, width, and depth could not be easily inferred due to inconsistent magnetic anomaly shapes, but forward modelling indicated a thin (10 m wide) shallow (10°) dyke trending NE-SW intruding both the Burgersdorp and Molteno Formations at Qalabane, Mafeteng. As per the D-8 results, the dolerite dykes in Mafeteng are distributed in the intermediate basin flow values due to a gentle hydraulic gradient. Certain dyke sites exhibit a groundwater flow direction towards the north, whilst others display a radial groundwater flow direction. The derivative analysis revealed the boreholes were drilled in a fractured dyke system, also the dominant radial flow regime and double porosity dip at different pumping durations, and the possible recharge boundary were revealed in some drilled dyke sites. Further analysis from the drawdown versus time curves resulted in average yields of 0.1 – 1.25 l/s with transmissivities ranging from 1 – 14 $m^2$/day, insinuating that a limited extraction of the local water supply is suggested from the dolerite dyke lithologies in the lowlands of Mafeteng Lesotho, given the groundwater yielding capacity and magnitude of the transmissivities. Even though the drilled boreholes from the dyke sites indicated a fractured dyke setting, estimated transmissivity values are variable and low, this is indicative of the inconsistent apertures and lack of interconnectivity of the available secondary hydrogeological features in the lowlands of Lesotho.

# ACKNOWLEDGMENTS

Firstly, I would like to thank God, for letting me through all the difficulties I experienced throughout my research journey.

I would like to thank Dr Teboho Shakhane (Co-Supervisor) for his unwavering support throughout the research. I would like to appreciate further Dr Shakhane for providing information regarding the Drilling and pumping test from some of his projects done in the same district, such as the project; Shared Water System (PTY) Ltd (SWS) which UNICEF commissioned to undertake a groundwater resource development for selected villages in Mafeteng (Lesotho) as part of the rehabilitation of water systems (six (6) Districts) and borehole drilling (three (3) Districts), Ref No: TB 9163447.

Additionally, I would also like to acknowledge and give my warmest thanks to my supervisor Professor Tamiru Abiye for his pivotal role and continuous guidance throughout this project.

A heartfelt acknowledgement also goes to Prof. Susan Webb and Dr. Stephanie Enslin from the Wits School of Geophysics for their assistance in field training for ground magnetic surveys and for letting me use some of the geophysical equipment to complete my research report.

I extend my gratitude to my family and friends whose love, belief, and encouragement helped at every stage of the research report writing and during the fieldwork visits.

# Table of Contents

**DECLARATION OF ORIGINAL WORK** ..... **i**
**ABSTRACT** ..... **ii**
**ACKNOWLEDGMENTS** ..... **iii**
**LIST OF FIGURES** ..... **vi**
**LIST OF TABLES** ..... **viii**
**ACRONYMS AND ABBREVIATIONS** ..... **ix**
**1. CHAPTER 1: INTRODUCTION** ..... **1**
1.1. General Introduction ..... **1**
1.2. Problem Statement ..... **2**
**1.3. Aim and Objectives** ..... **3**
1.3.1. Aim ..... 3
1.3.2. Objectives ..... 3
**2. CHAPTER 2: LITERATURE REVIEW** ..... **4**
2.1. Introduction ..... **4**
2.2. The Karoo Supergroup ..... **4**
2.3. Karoo Dolerites and Magmatism ..... **7**
2.4. Geophysics: Ground Magnetics ..... **7**
**2.5. Hydrogeology of Karoo Basin** ..... **8**
2.5.1. General Aquifers of Karoo ..... 8
2.5.2. Secondary Groundwater Occurrence ..... 10
2.5.3. Dykes ..... 11
2.5.4. Fractures and Matrix ..... 12
**3. CHAPTER 3: DESCRIPTION OF THE STUDY AREA** ..... **14**
3.1. Introduction ..... **14**
3.2. Locality ..... **14**
3.3. Physiography and Climate ..... **15**
**3.4. Geology** ..... **15**
3.4.1. Regional-Lesotho ..... 15
3.4.2. Local-Mafeteng ..... 17
**3.5. Hydrogeology** ..... **19**
**4. CHAPTER 4: METHODOLOGY** ..... **22**
4.1. Introduction ..... **22**
**4.2. Geological mapping of dolerite dykes** ..... **22**
4.2.1. Geometry characterisation ..... 22

4.2.2. Drilling ..... 25
**4.3. Groundwater flow properties of dolerite dykes ..... 26**
4.3.1. Groundwater flow direction ..... 26
4.3.2. Pumping Test ..... 28
4.3.3. Groundwater flow characterisation ..... 28
4.3.4. Groundwater yields and aquifer parameters ..... 29
**5. CHAPTER 5: RESULTS AND DISCUSSION ..... 31**
5.1. Introduction ..... **31**
**5.2. Geological mapping of dolerite dykes ..... 31**
5.2.1. Geometry Characterisation ..... 31
5.2.2. Forward Modelling ..... 39
**5.3. Groundwater flow properties of dolerite dykes ..... 42**
5.3.1. Groundwater flow direction ..... 42
5.3.2. Groundwater Flow Behaviour ..... 48
5.4. Estimation of Aquifer Parameters ..... 58
**6. CHAPTER 6: CONCLUSION AND RECOMMENDATIONS ..... 68**
**6.1 Conclusion ..... 68**
**6.2 Recommendations ..... 70**
**7. REFERENCES ..... 71**
**8. APPENDIX ..... 78**
**8.1. GROUND MAGNETIC PROFILES AND MAPS ..... 78**
**8.2. CONSTANT DISCHARGE DATA SHEETS ..... 84**

# LIST OF FIGURES

**Figure 1:** Map of Lesotho with the hydrographic network and slope distribution across all the districts in Lesotho. 2

**Figure 2:** Distribution of the Karoo Basin across Southern Africa (Tokumaru, 2014). ..... 5

**Figure 3:** The geological map of the main Karoo Basin and the extent of the main lithostratigraphic units (Source: Rubidge, 1995). ..... 6

**Figure 4:** South African general groundwater productivity map that shows the predicted yields from boreholes in various hydrogeological units (Created using ArcGIS)..... 10

**Figure 5:** The Digital Elevation Model (DEM) of Mafeteng District, Lesotho (Created using ArcGIS). 14

**Figure 6:** The average annual precipitation and the average temperature of Lesotho and Mafeteng inclusive (Source: Leketa et al. 2018)..... 15

**Figure 7:** Simplified Geological map of Lesotho (Created using ArcGIS)..... 16

**Figure 8:** A dolerite dyke intruding into both the Molteno and Elliot Formations in the lowlands of Lesotho (Source: Davies, 2003)..... 16

**Figure 9:** A portion of Lesotho's chronostratigraphy exposed in the Thupa-Kubu Valley, northwest of Sefikeng, the sediment Formations are overlayed by the basalts (Source: Davies, 2003)..... 17

**Figure 10:** Simplified geology map of Mafeteng district, Lesotho (Created using ArcGIS) ..... 18

**Figure 11:** The dolerite dykes intruding the Burgersdorp Formation, north of the focal area in the Mafeteng District, Lesotho. (Source: Davies, 2003)..... 19

**Figure 12:** The three major catchments of Lesotho are the Mohokare, Makhaleng, and Senqu catchments (Created using ArcGIS)..... 20

**Figure 13:** Background information on the aquifer types as well as their productivity in terms of their potential to sustain and abstract groundwater as extracted in ArcGIS. ..... 21

**Figure 1:** The magnetic survey grid at Qalabane in the district of Mafeteng, Lesotho (Plotted using Global Mapper). ..... 23

**Figure 15:** Dolerite dyke intruding through the Burgersdorp (Tarkastad Subgroup) and Molteno Formations and forming a ridge-like feature at Qalabane, Mafeteng District. ..... 24

**Figure 16:** Flow chart providing sequential processes for the magnetic data processing and results. ..... 25

**Figure 17:** A flow of the Arc-Hydro Tool methodology was used in delineating the drainage network and groundwater flow directions. ..... 26

**Figure 18:** The eight-direction (D8) algorithm for the determination of flow direction and flow accumulation (Source: Tong et al. 2021). ..... 27

**Figure 19:** Graphs of the first logarithmic derivative of drawdown in a borehole for a few types of geometries and boundaries (Source: Van Tonder et al. 2001). ..... 29

**Figure 20:** Unfiltered magnetic field intensity (nT) in 2D contours with assigned UTM coordinates as generated from the raw magnetic data through MagMap2000. ..... 31

**Figure 21:** Total magnetic intensity and spectrum profiles after 1D Fast Fourier Transform (FFT) and reduction to magnetic pole (RTP). ..... 32

**Figure 22:** Unprocessed observed magnetic data processing images of line 17 anomaly in response to geological features' contribution to the overall magnetic flux density present after exposure to a magnetic field in the XZ plane. ..... 32

**Figure 23:** Filtered and smoothed data processing images of line 17 anomaly in response to geological features' contribution to the overall magnetic flux density present after exposure to a magnetic field in the XZ plane. ..... 33
**Figure 24:** The magnetic intensity data was recorded along line 3 (L_3) with the traverses in the NW-SE directions. ..... 34
**Figure 25:** The magnetic intensity data was recorded along lines 4 (L_4) with the traverses in the NW-SE directions with the linear structure positions indicated. ..... 34
**Figure 26:** TMI (nT) image overlayed on Google Earth image in Qalabane, Mafeteng district Lesotho. . 35
**Figure 27:** An RTP map with calculated geomagnetic inclination and declination of -63 and -24.7° respectively. ..... 36
**Figure 28:** A Residual Magnetic Intensity (RMI) after subtraction of regional field from the TMI. ..... 37
**Figure 29:** On the left (A), 1st vertical derivative map from the focal area of study, Qalabane, Mafeteng Lesotho with the survey lines 2 and 6 across the lineament (A-A'). On the right (B), magnetic intensity profiles of lines 2 and 6 show positive and negative anomalies along the linear dyke feature (A-A') and its contacts. ..... 38
**Figure 30:** Forward modelling of the dyke body to reveal its geological structure and geometry using PDYKE software ..... 40
**Figure 31:** Forward model of the dyke fitted on the magnetic response observed in the field to estimate the width and depth using MAG2DC. ..... 41
**Figure 32:** Interpretation of Total Magnetic Intensity with the magnetic anomaly profile of line-6 overlain on Google Earth. ..... 42
**Figure 33:** Mafeteng drainage basin flow map delineated from identifying ridge and relief-like lines and pour points from the study area. Shown also are the dykes distribution and locations of the drilled boreholes used as case studies concerning the drainage flow model derived from DEM Arc-Hydro Tool in ArcGIS. ..... 43
**Figure 34:** The flow accumulation maps for the selected hydrogeological boreholes. [A] shows flow accumulation for boreholes sited on the dykes at Thabana Mohlomi, Ha Lenonyane, and Ha Mofota villages. [B], flow accumulation for boreholes sited on the dykes at Qalabane, Matlapaneng, Ha Lumisi, and Malumeng. Flow accumulation value of 0 and 1 shows no flow and presence of flow respectively... 44
**Figure 35:** Spatial distribution of the groundwater level contour map and the locations of the selected hydrogeological boreholes, derived by IDW interpolation and D8 algorithm in ArcGIS. ..... 46
**Figure 36:** Flow direction map from the villages, Thabana Mohlomi and Qalabane which fall under the shallow and intermediate zones of static groundwater level respectively. Highlighted also are the drill borehole locations and the dykes distribution along the SWL map. ..... 47
**Figure 37:** Flow direction map from the villages, Ha Lenonyane and Ha Lumisi which fall under the shallow and deepest zones of static groundwater level respectively. Highlighted also are the drill borehole locations and the dykes distribution along the SWL map. ..... 47
**Figure 38:** Geological extraction of Mafeteng with the locations of the drilled boreholes used as case studies in the pumping analyses for this research 1=Qalabane, 2=Thabana Mohlomi, 3=Ha Lenonyane, 4=Ha Lumisi, and 5=Malumeng ..... 50
**Figure 39:** The Borehole hydrograph for the CDT that was drilled at Qalabane. ..... 51
**Figure 40:** The diagnostic plots for the Qalabane borehole. Semi-log diagnostic plot and log-log plot. .. 51
**Figure 41:** Derivative plot for the Qalabane borehole. The traditional drawdown data is plotted with the derivative data against time elapsed. ..... 52
**Figure 42:** Diagnostic plots for pumping test at Thabana Mohlomi. Semi-log and log-log plot. ..... 52

**Figure 43:** Derivative plot for the drill borehole at Thabana Mohlomi. The traditional drawdown data is plotted with the derivative data against time elapsed. 53
**Figure 44:** Diagnostic plots for pumping test at Ha Lenonyane. Semi-log and log-log plots. 53
**Figure 45:** Derivative plot for the drill borehole at Ha Lenonyane. The traditional drawdown data is plotted with the derivative data against time elapsed. 54
**Figure 46:** Diagnostic plots for pumping test at Ha Lumisi. Semi-log and log-log plots. 54
**Figure 47:** Derivative plot for the drill borehole at Ha Lumisi. The traditional drawdown data is plotted with the derivative data against time elapsed. 55
**Figure 48:** Diagnostic plots for pumping test at Malumeng. Semi-log and log-log plots. 55
**Figure 49:** Derivative plot for the drill borehole at Malumeng. The traditional drawdown data is plotted with the derivative data against time elapsed. 56
**Figure 50:** Cooper-Jacob curve matching of the borehole at Qalabane as extracted from FC Programme. 59
**Figure 51:** Cooper-Jacob curve matching of the borehole at Thabana Mohlomi as extracted from FC Programme. 59
**Figure 52:** Cooper-Jacob curve matching of the borehole at Ha Lenonyane as extracted from FC Programme. 60
**Figure 53:** Cooper-Jacob curve matching of the borehole at Ha Lumisi as extracted from FC Programme. 60
**Figure 54:** Cooper-Jacob curve matching of the borehole at Malumeng as extracted from FC Programme. 61
**Figure 55:** Recovery graphs: borehole drilled at Qalabane as extracted from the FC Programme. 62
**Figure 56:** Recovery graphs: borehole at Thabana Mohlomi as extracted from the FC Programme. 62
**Figure 57:** Recovery graphs: borehole at Ha Lenonyane as extracted from the FC Programme. 63
**Figure 58:** Recovery graphs: borehole at Ha Lumisi as extracted from the FC Programme. 63
**Figure 59:** Recovery graphs: borehole drilled at Malumeng as extracted from the FC Programme. 63

# LIST OF TABLES

**Table 1:** The descriptive summary of the drill boreholes previously constructed, their geographic locations, elevation, depth to water, and static water level within the study area. 45
**Table 2:** Summarise the results derived from the derivative analysis of the pumping test in the five dyke-locations. 56
**Table 3:** Cooper-Jacob results on estimated transmissivities at different dyke sites in Mafeteng, Lesotho. 62
**Table 4:** Estimated transmissivity results from the recovery test analysis at different dyke sites in Mafeteng, Lesotho. 64
**Table 5:** Categorisation regarding the magnitude of the transmissivities (Source: Krasny, 1993). 65
**Table 6:** Summary of the Groundwater flow properties of the dykes from the Pumping test on the drilled boreholes in the lowlands of the Mafeteng District Lesotho. 66

# ACRONYMS AND ABBREVIATIONS

| | |
|---|---|
| CDT: | Constant Discharge Test |
| DEM: | Digital Elevation Model |
| DWA: | Department of Water Affairs |
| D8: | Eight-Direction |
| FFT: | Fast Fourier Transform |
| GPS: | Global Positioning System |
| Hz-RMS: | Hertz-Root Mean Square |
| $Km^2$: | Kilometres Squared |
| $Kg.m^{-3}$: | Kilogram per cubic meter |
| L: | Liters |
| $L.s^{-1}$: | Liters per second |
| $L.s^{-1}.m^{-1}$: | Liters per second per meter |
| Ma: | Mega Annum |
| M.A.S.L: | Meter above Sea Level |
| $m^{-3}.h^{-1}$: | Cubic meters per hour |
| $m^2/d$: | Meters square per day |
| nT: | Nano Tesla |
| SWS: | Shared Water System |
| SWL: | Static Water Level |
| UNICEF: | United Nations International Children's Emergency Fund |

# 1. CHAPTER 1: INTRODUCTION

## 1.1. General Introduction

The characteristic composition and structure of dolerite dykes have a major role in shaping the hydrogeological conditions in the surrounding area. The dolerite dykes are recognised as geological discontinuities which intrude into the pre-existing rocks. They are typically responsible for creating secondary aquifers due to their link to the fracturing of country rocks and the development of baked high permeability zone near the dykes (Davies, 2003). Since groundwater follows the topography gradient, the presence of the dolerite dykes in a given area has a significant impact on the overall flow of groundwater because these dykes can act as conduits or as barriers to groundwater flow (Wyk and Witthueser, 2011). The dykes, according to Woodford and Chevallier (2002), are further important for groundwater exploration because they are noticeable as vertical stretches of greenery and can be easily identified on remotely sensed imagery using comparatively basic geophysical methods. A variety of techniques, including geophysical surveys, borehole drilling and aquifer testing, have been used in previous studies in identifying and examining the hydrogeological properties of the dykes.

The spatial distribution and orientation of the dolerite dykes in Lesotho are considered superior groundwater sources. Lesotho is a small mountainous landlocked country in South Africa (Figure 1) located in the eastern portion of the major Karoo Basin, which is primarily composed of the Karoo sediments and dolerite dyke bodies. These intrusive bodies may influence the occurrence of groundwater in Lesotho however, due to the fracture systems and weathering in the Karoo Formations, the secondary hydrogeologic features related to the Karoo dykes are heterogeneous, anisotropic and not as porous as the primary aquifers hence the apertures are generally inconsistent (Dippennar *et al*. 2009). Nonetheless, specific research on the hydrogeology of the dyke-related aquifer in Lesotho has not been extensively undertaken. Therefore, the hydrogeological characterisation of these dykes is imperative in understanding the overall groundwater in such geological settings. Additionally, the efficient management of groundwater resources depends on a strong understanding of the hydrogeophysical properties of these intrusive dolerite dyke bodies.

The study aims to contribute to the existing body of knowledge by investigating the baseline hydrogeology of dolerite dykes in Lesotho through applications of ground magnetic surveys, borehole drilling, surface and subsurface water flow models, and aquifer testing.

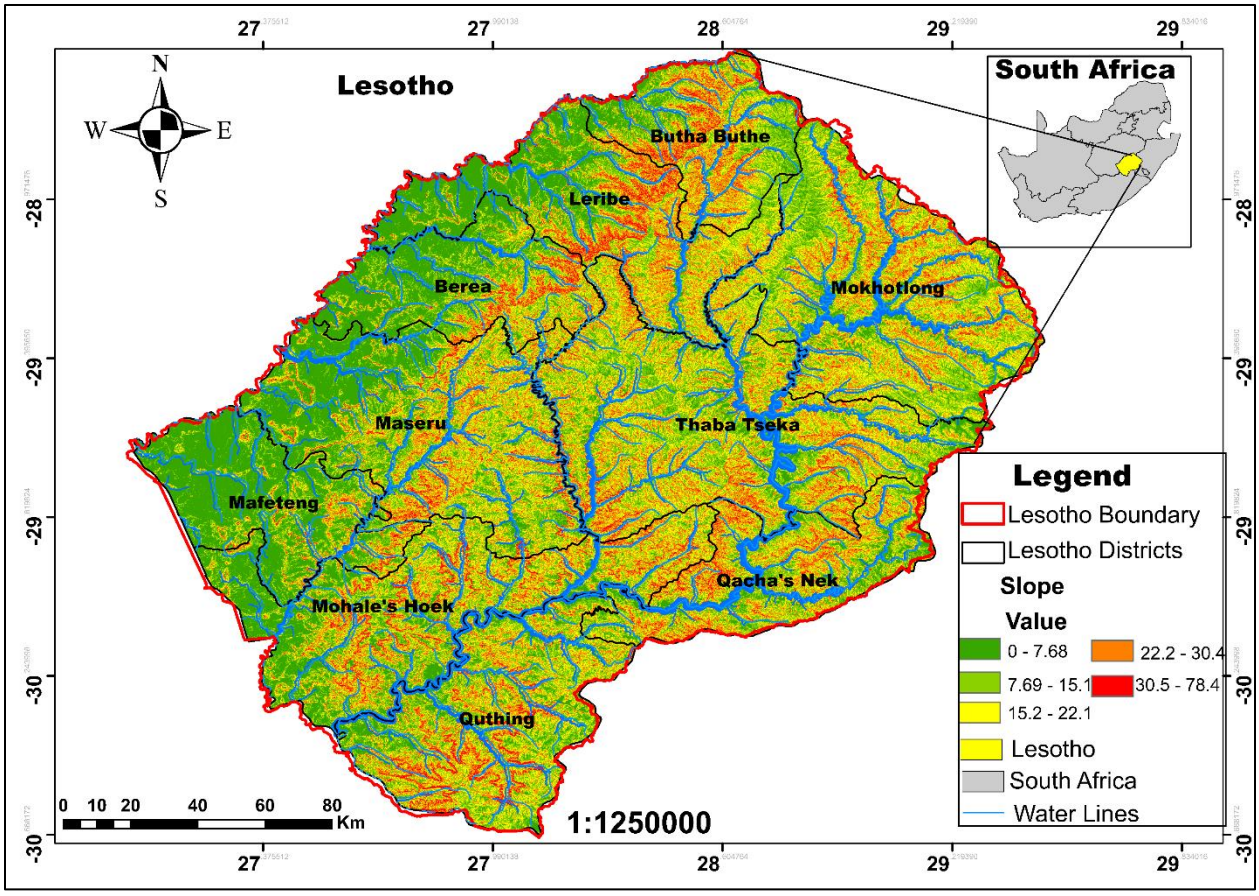



**Figure 1:** Map of Lesotho with the hydrographic network and slope distribution across all the districts in Lesotho.

## 1.2. Problem Statement

Groundwater is a vital alternative resource for increasing demand for water for both Lesotho's urban and rural populations. Davies (2003) highlighted that with the increasing industrialisation and demand for water from the agricultural sector, their needs are met from groundwater sources hence it is an imperative resource of Lesotho's economic infrastructure. Population growth and climate change are threats to the surface water quantity from the Karoo rocks. The presence of the dolerite dykes can impact the groundwater yield across different geological Formations, much as they can within Lesotho's basalts and sediments (Chevallier *et al.* 2001). After, alluvial aquifers, dyke-related aquifers with generally moderate productivity, specific research on their hydrogeology has not been extensively undertaken. Consequently, this study was initiated to characterise the hydrogeology of the dolerite dykes in Lesotho. It is envisaged that the outcome of this study will enhance understanding of how groundwater occurs in dyke-related aquifers, and potentially how dykes in a typical setting control the occurrence of groundwater.

## 1.3. Aim and Objectives

### 1.3.1. Aim

To characterise the hydrogeology of the dolerite dykes in the lowlands of Lesotho using selected places as case studies.

### 1.3.2. Objectives

- Characterise the geometry and geological characteristics of the dolerite dykes.
- To evaluate the hydrogeology (groundwater flow, storage, and yield characteristics) of the dyke-related aquifer in Lesotho within the Mafeteng District.

# 2. CHAPTER 2: LITERATURE REVIEW

## 2.1. Introduction

This section thoroughly evaluates several previous studies (from regional to local) to provide a context baseline hydrogeology of dolerite dykes in Lesotho and to provide insight into the hydrogeophysical characteristics of these dykes. The dolerite dykes are key geological structures that are essential for identifying Lesotho's groundwater resources, nevertheless, research on the hydrogeology of these features has not been extensively undertaken as that limits the efficient management and sustainable groundwater utilisation in the region. This review first synthesises the geological characteristics of the Karoo Formations in understanding the nature of the intrusive bodies' geometry and other geological properties. The chapter further identifies knowledge gaps regarding the use of ground magnetics in mapping these dykes in Lesotho's lowlands, hence this research emphasises the significance of ground magnetic surveys in comprehending the hydrogeophysical attributes of the intrusive bodies. Additionally, provided also is the explanation of the fundamental and secondary hydrogeological features that influence the groundwater occurrence, flow, and aquifer yield within the Karoo lithologies.

## 2.2 The Karoo Supergroup

Karoo Supergroup is a large stratigraphic unit widely spread in Southern Africa (Figure 2) and covers about two-thirds of the surface (Rubidge and Hancox 2002). The stratigraphic thickness of the Karoo is ~12 km and forms a wide-ranging basin in the Southeast of Southern Africa. Baiyegunhi and Liu (2021) outlined that, traditionally the Karoo Basin is believed to be a retro-arc foreland basin, its vast stratigraphy occupies the main Karoo Basin and covers about 300 000 $km^2$ for sedimentation extending from ~300-180 Ma (Baiyegunhi and Liu, 2021).

According to Catuneanu *et al.* (2005), Karoo Basin initially developed during the break-up of Pangea and the first-order cycle of Supercontinent assembly, Baiyegunhi and Liu (2021) further indicate that this development began in front of the Cape Fold Belt in reaction to crustal thickening and shortening brought on by palaeo-Pacific plate's subduction beneath the Gondwana plate during the Late Paleozoic-Early Mesozoic subduction. It has been reported by Davies (2003) that the basin's development was primarily influenced by Carboniferous sediment deposition and the uplift of the Cape Fold Belt. It was further shaped by Karoo basalt and dolerite intrusions, Gondwana breakup, Kimberlite intrusion, mantle upwelling, recent geomorphology, sediment deposition, and tectonic activity.

The main lithostratigraphic units from the Karoo Basin are the Dwyka, Ecca, Beaufort, and Stomberg Groups as shown in Figure 3 (Catuneanu *et al*. 2005). These Karoo Groups resemble different depositional environments where they got deposited, describing the shifting climatic conditions as Gondwanaland

moved from high latitudes to the equator (Baiyegunhi and Liu, 2021). For instance, Woodford and Chevallier (2002) highlighted that the Dwyka and Ecca sedimentary fill were initially deposited through the glacial ice shelf and the marine environments respectively. Overlying the Ecca Group are the Beaufort and Stomberg Groups, their lithologies reveal their palaeo-environmental settings varying from fluvial and aeolian respectively (Baiyegunhi and Liu, 2021). Woodford and Chevallier (2002) also denoted that the Beaufort and Stomberg are the main geological units in Lesotho.

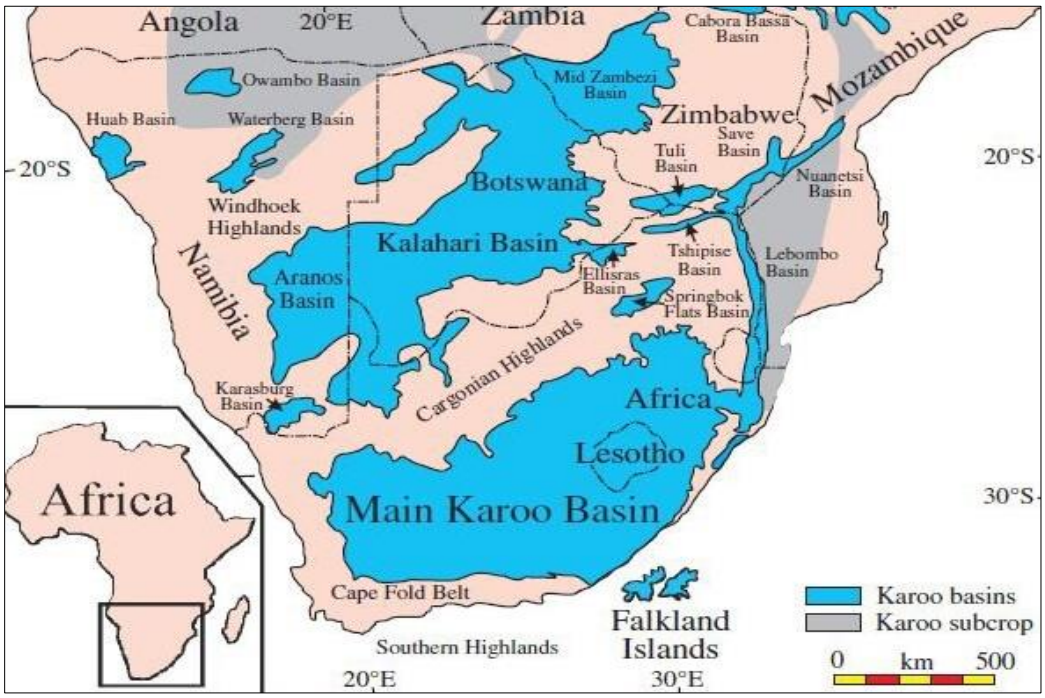



**Figure 2:** Distribution of the Karoo Basin across Southern Africa (source: Tokumaru, 2014).

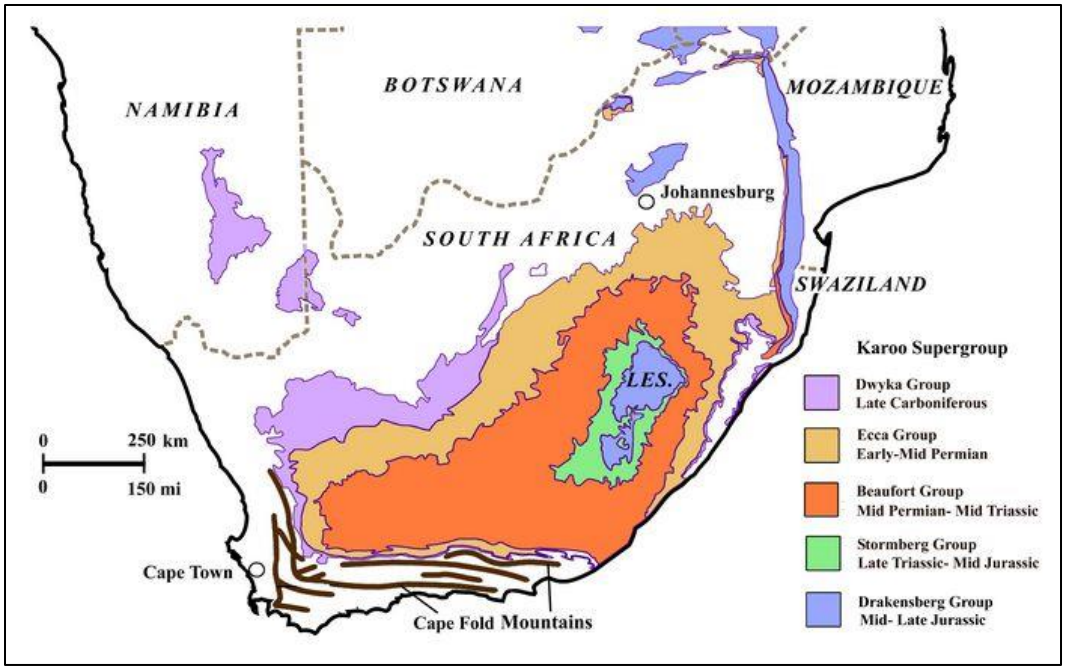



**Figure 3:** The geological map of the main Karoo Basin and the extent of the main lithostratigraphic units (Source: Rubidge, 1995).

The Dwyka Group formed during the underfilled phase of the development of the Karoo Foreland system in the late Paleozoic Ice Age (Catuneanu, 2004). The glaciogenic deposits from the late Carboniferous-Early Permian are characterised by stratified diamictite, with tillite, claystone, and mudstone as the main lithologies of the Dwyka Group (Dietrich and Hofmann, 2019). The Ecca Group, which is Permian-aged, overlies the Dwyka and it is divided into the Lower and Middle-Upper Ecca. Belica *et al.* (2017) noted that the Lower Ecca is dominated by rocks which denotes the transition to postglacial sea level rise. The Middle-Upper Ecca comprises 16 formations grouped into 3 geographical zones which denotes basin floor to deltaic strata (Belica *et al*. 2017; Woodford and Chevallier, 2002). The Ecca Group primarily comprises mudstone, siltstone, sandstone, minor conglomerate, and shale (Johnson *et al*. 2006).

Overlying the Ecca is the Beaufort Group aged in the late Permian-Triassic, this is more established in the Southern segment of Karoo Basin, and its upper sedimentary units consist of thick (>10 m) sedimentary rocks marking a change to faster flowing Rivers (Lanci *et* al. 2013). The main lithologies from Beaufort are mudstones, claystone, and siltstone associated with some sandstones. After Beaufort, it is the deposition of Stomberg Group sediments in the Late Triassic-Early Jurassic, much of the deposition was carried out by the braided rivers flowing from the Cape Fold Belt (Woodford and Chevallier, 2002). The main lithologies of the Stomberg Group include mudstone, claystone, and siltstone which are associated with some shale,

tuff, and sandstone. After Stomberg deposition, continental flood basalts combined with intrusive and extensional tectonics led to the end of deposition in the Karoo Basin (Lanci *et al*. 2013).

### 2.3 Karoo Dolerites and Magmatism

During the mid-Jurassic, an extensive basaltic lava pile from magmatic activity generated fractures, dykes, and sills in the Karoo Basin, the magmatic activity was then followed by the break-up of the Gondwanaland (Woodford and Chevallier 2002). Lesotho is dominated by these lava flows from the magmatic activity of ~180 Ma, the lava pile covers 80% of the country, hence the basaltic lavas contribute to the flow and storage of groundwater in Lesotho. Botha (1998) determined that the basaltic lavas in some areas in Lesotho are about 1400 m thick. According to Woodford and Chevallier (2002), these lava piles are low tholeiitic basalts however, they are heterogeneous and are subdivided into two formations and 11 Stratigraphic units based on a geochemical basis.

The dykes generated from the magmatic activity characteristically define the Karoo Basin as they are widespread within the region. Davies (2003) denoted that the dolerite dykes intruding the Karoo formations in Lesotho trend NW-SE and NNE-SSW and are mostly linear. The development of these linear dykes provides secondary hydrogeological properties to the Karoo sediments and basalts, mainly because they are linked to the country rocks fracturing and the development of a baked high permeability zone close to the dykes (Davies, 2003). The linear dykes dominating in Lesotho are regarded as groundwater sources, better than the ring dykes and sills occurring in parts of the Karoo Basin. Botha (1998) highlighted that the ring dykes and sills intruded the lavas during the extremely active phase (enhanced temperatures) therefore, Karoo Formations got metamorphosed instead of being baked hence minimising their groundwater flow and storage capabilities. This is different with linear dolerite dykes within Lesotho as they baked the country rocks rather than metamorphosing them, thereby improving the hydrogeological properties of the adjacent lithologies hence they are of interest in determining the potential groundwater flow, storage, and occurrence in general.

### 2.4 Geophysics: Ground Magnetics

The magnetic method is one of the geophysical techniques commonly employed in providing subsurface information for the hydrogeological characterisation of geological units. To do further study on groundwater, Conte *et al* (2017) described how ground magnetic surveys are now regarded to be a powerful tool for locating local geological features and tracing dolerite dykes, hence they are an efficient method for assessing and understanding the heterogeneity of various aquifer systems (Abraham *et al*. 2019; Woodford and Chevallier, 2002). Under this technique, variations in the Earth's magnetic field are passively measured

at various points on the surface. Positive and negative anomalies, arising from both the induced and remnant magnetism, are thus produced by the geological units with the highest and lowest magnetic susceptibilities.

The Earth's magnetic field has been measured using a variety of magnetometers (Woodford and Chevallier, 2002). For instance, the earliest studies (Enslin, 1950), particularly in the Karoo Basin, used magnetometers that solely measured the magnetic field's vertical component. Recent proton magnetometers on the other hand measure the total magnetic field. However, the ground magnetic method does not inform on groundwater flows. When used together with water level maps, pumping tests, and hydrogeological models, it enables further understanding of preferential flow paths for surface and subsurface water and the general hydrogeological characteristics of an aquifer. The early research (Enslin, 1955; Botha, 1998) on tracing the orientation of dolerite dykes from the Karoo Basin noted that the magnetic anomaly results could also provide information on the dip direction (less steep slope on the anomaly shape), dip angle and other geometrical parameters (Woodford and Chevallier, 2002). Even so, De Villiers (1961) pointed out that these interpretations are not always accurate because the size and shape of an anomaly depend on several variables, including the dyke's orientation or attitude, the feature's magnetic susceptibility, and the depth at which the intrusive body is buried.

## 2.5 Hydrogeology of Karoo Basin

### 2.5.1 General Aquifers of Karoo

The occurrence of groundwater from Karoo aquifers is generally determined by the complex geometry of its lithologies, and the overburden stress on the sediments from the basalts of which the latter influences the behaviour of groundwater in the secondary hydrogeological features. Botha *et al.* (1998) noted that the complex geometry and the overburden stress largely controlled the sediments' diagenesis, whereby the Karoo sediments got compacted, lithified, and slightly metamorphosed, hence losing their primary porosity.

It is further noted by Botha *et al.* (1998) that the sediments were not affected immediately after the end of the Jurassic era, allowing groundwater to flow within the sediment pores. However, groundwater deposited some secondary carbonate minerals into the voids, and cementation of these minerals further reduced the sediments' porosity, elasticity, hydraulic conductivity, and permeability (Botha *et al.* 1998). During the recharge of Karoo aquifers, the flow mechanism through the unsaturated zones is a preferential flow through the vertical and sub-vertical fractures. At the same time, the Karoo formations act as major storage units of water (Botha and Cloot, 2004).

Generally, Karoo aquifers do not contain large volumes of groundwater hence meagre aquifer yields (Figure 4) however, Botha (1998) highlighted that some boreholes in some formations have high yields (18-72 $m^3 h^{-1}$). Botha and Cloot (2004) explained that most Formations are tight hence low yields, but if drill holes

intersect bedding-parallel fracture, the borehole would have a significant or high yield. This outlines that the poor yields and extremely poor permeabilities are the characteristics that define the Karoo Basin Formations. At the same time, bedding-parallel fractures serve as conduits to groundwater flow in the Basin.

In addition to specific borehole yields, broad primary hydraulic parameters are significant in determining the long-term sustainability of Karoo aquifers, that is the aquifer storativity. Woodford and Chevallier (2002) highlighted that the Dwyka deposits located at the base of the Karoo Supergroup, typically have very low hydraulic conductivity, and since these experienced minimal fracturing, apertures are limited therefore they are not able to store large amounts of groundwater. For that reason, the Dwyka sediments tend to form aquitards instead of aquifers.

The shales and sandstones that comprise most of the Ecca Group are extremely dense and frequently poorly sorted hence they also typically have low permeabilities (Woodford and Chevallier, 2002). In the north of Karoo Basin, the porosity of the shales tends to drop from 0.1% to <0.02% in the south and southeastern regions of the Basin while densities rise from approximately 2000 $Kg.m^{-3}$ to 2650 $Kg.m^{-3}$ (Woodford and Chevallier, 2002). Nevertheless, Woodford and Chevallier (2002) outlined that there are still large volumes of water pumped from the Ecca sediments for instance, in the Petrusburg region in the middle of Free State, about 4500 ha are irrigated from boreholes drilled from the Ecca shales. In addition, the median drill yield of 0.33 l/s of Kwazulu-Natal Vryheid Formation sandstones (Ecca Group) characterises the Formation as permeable (Woodford and Chevallier, 2002).

The Beaufort Group aquifers have complex geometry due to their multi-layered and multiparous nature and their variable thickness. Woodford and Chevallier (2002) described that the sedimentary units typically have low permeabilities due to the lateral migration of meandering streams. For the permeable coarser sediments of Beaufort, a high-yielding borehole may have a limited lifespan if it is not recharged frequently because the sediments are characteristically lens-shaped (Woodford and Chevallier, 2002). The Molteno Formation of Stomberg Group however characteristically forms an “ideal” aquifer, according to Leketa *et al* (2018), this formation possesses specific capacity values that average 1.9 $l.\ s^{-1}.\ m^{-1}$ after 24 hours, and safe yields ranging from 0 to 1.6 l/s. Molteno bodies, because of their greater persistence, these sedimentary Formations (not only pebble conglomerates and coarse-grained sandstones at the base of the Molteno Formation) have better aquifer geometry for storing groundwater (Woodford and Chevallier, 2002).

With regards to the Elliot Formation, Bonney (1975) claimed a porosity of 25 %, and Schmitz and Rooyani (1987) noted that the testing showed that the drilled boreholes yielded between 0.1 l/s and 0.2 l/s, which significantly represents a good semi-confined aquifer of the Elliot Formation. On the other hand, the Clarens

Formation is the most homogeneous in the Karoo Supergroup due to its well-sorted, medium-fine-grained sandstones (Woodford and Chevallier, 2002). With an average uniform porosity of 8.5 % hence low permeability, the Clarens Formation may be able to hold water but not release it rapidly due to its minimal fractures (Woodford and Chevallier, 2002). Leketa *et al.* (2018) pointed out that poor yields of ~0.1 l/s were recorded in this semi-confined aquifer when it was not dry.

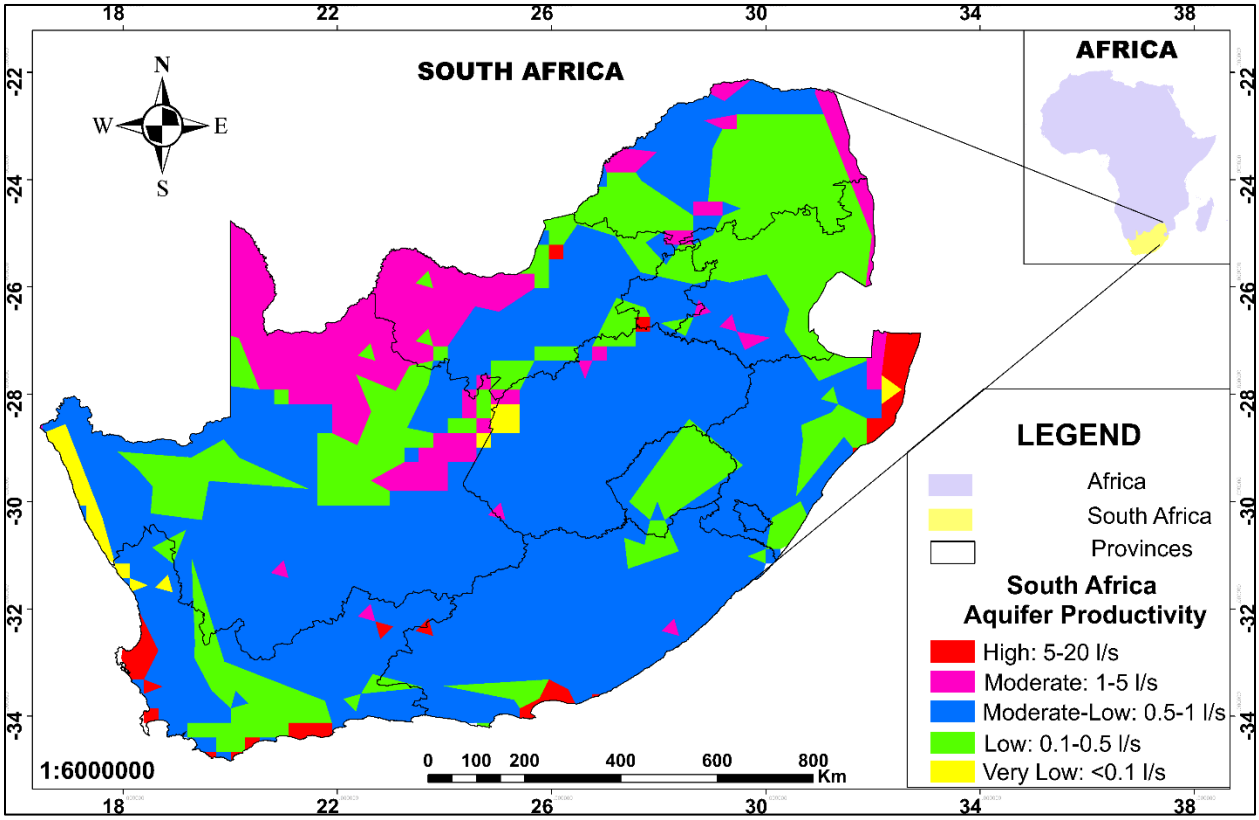



**Figure 4:** South African general groundwater productivity map showing the predicted yields from boreholes in various hydrogeological units (Created using ArcGIS).

### 2.5.2 Secondary Groundwater Occurrence

Regarding groundwater storage and flow in a sedimentary unit, Davies (2003) outlined the two most important points namely:

- The amount of cementation, compaction, and the ratio of sand to shale in the sediment govern the primary interconnected pore space and
- Significantly, the degree of fracture and joint formation during diagenesis, compaction, tectonic activity, metamorphosis, and weathering determines secondary porosity.

Secondary apertures like fractures, faults, edges of intrusive bodies, and bedding planes are where groundwater storage and flow occur, therefore discovering these water-bearing secondary features enhances the success of a borehole drilled into the Karoo rocks (DWA, 2010). Nevertheless, it should be noted that the first blow yields may not necessarily indicate long-term sustainability because these secondary features, with increased confidence for holding groundwater, would need to be interconnected to keep the borehole supplied with water.

The water-bearing secondary features that comprise or make secondary aquifers are characterised by their structural control of groundwater flow, also some of the key characteristics of secondary aquifers from the Karoo Basin are that they are not homogeneous, isotropic, and as porous as primary aquifers (Dippennar *et al*. 2009). In addition, due to the fracture systems and weathering in the Karoo Formations, the apertures are inconsistent hence the hydraulic properties are also largely variable.

### 2.5.3 Dykes

According to Wyk and Witthueser (2011), groundwater flow generally follows the topographic gradient, but it is influenced locally by the existence of geological structures like dykes. The dolerite dykes are discontinuities associated with zones of high permeability because they act as conduits to groundwater, however, the Karoo Dykes can also behave as semi-permeable to impermeable barriers to groundwater flow (Woodford and Chevallier, 2002; and Wyk and Witthueser, 2011).

Considering the primary linear nature of the dolerite dykes in Lesotho, they are considered superior groundwater sources than the ring dykes and sills in some areas of the Karoo Basin (Davies, 2003). Considering the potential for increased storage, yield, and permeability resulting from the fracturing, brecciation, and alteration of the Karoo sediments by these linear discontinuities, groundwater occurrence is therefore promoted along linear dyke zones (DWA, 2010). Botha (1998) stated that the ring dykes and sills intruded the lavas during periods of extremely active phase when temperatures are elevated, Karoo Formations then got metamorphosed instead of being baked hence minimising their groundwater flow and storage.

However, with linear dolerite dykes dominating south of Lesotho, they baked the country rocks rather than metamorphosing them hence that believed to have improved the hydrogeological properties of the adjacent lithologies. Woodford and Chevallier (2002) further highlighted major reasons why Lesotho linear dolerite dykes are preferred for groundwater exploration, these include:

- Drilling a wet borehole in or adjacent to a dyke appears to have a higher chance than drilling in the host rock further away from the dyke.

- Dykes are readily identifiable to both the skilled and unskilled eye in the field and can be easily identified on remotely sensed imagery using comparatively basic geophysical methods (magnetics). They are frequently noticeable as vertical stretches of greenery.
- They are comparatively straightforward to conceptualize and locate an exploratory borehole in the field due to their uniform 3D geometry, and
- Thus, they are economic targets for groundwater.

As stated by Woodford and Chevallier (2002), over 80 % of effective boreholes that have been drilled in the Karoo rocks are associated with the dolerite dykes either directly or indirectly. From Victoria West, over 25 % of the 3194 boreholes surveyed were also drilled next to dolerite dykes (Chevallier *et al*. 2001).

Methods of emplacement for dykes are vital in the improvement of the local hydrogeological properties. For instance, Woodford and Chevallier (2002) described in detail the geometry, structure, and mechanisms of emplacement as well as aspects influencing the occurrence of groundwater and productivity of the boreholes in the Karoo sediments concerning intruding dykes. These aspects include:

- Dip and width of the dyke
- Echelon dyke segmentation
- Transgressive fracturing
- Jointing parallel to dyke contact
- Effect of dyke attitude and drainage
- Dyke intersection
- Contact metamorphism and
- Distance from dyke contact

Geometry, attitude, weathering intensity, and dyke fracture all have an impact on the hydrogeological characteristics of individual structures locally for instance, thick dykes do not always deform the adjacent rocks more than thin dykes, even though the thick dykes may become more porous due to their granularity during weathering (Woodford and Chevallier, 2002). Furthermore, *en-echelon* dyke emplacement is a favourable target for high-yielding borehole drilling because it is linked to complicated stress fields and significant country rock deformation (Woodford and Chevallier, 2002).

### 2.5.4 Fractures and Matrix

Throughout the Karoo Basin, the intrusive dyke bodies are primarily responsible for the development of the fractures in the Karoo Supergroup rocks (Woodford and Chevallier, 2002). Fractures are considered secondary features responsible for groundwater occurrence but as Botha and Cloot (2004) explain, these

fractures only act as preferential flow paths during the aquifer recharge, therefore they should not be thought of as groundwater storage units like it was previously known.

Pumping groundwater from the Karoo Formations could cause a sudden drop in the fractures' piezometric pressure hence forcing water leakage from the matrix into the fracture thereby resulting in what is known as double porosity, this also could deform the horizontal and vertical nature of the fractures (Botha and Cloot, 2004; Botha *et al*. 1998). Earlier studies on single fracture flow dynamics identified key issues including nonlinearity at high Reynolds number, $R_e$ (Lomize, 1951; Room, 1966; Louis, 1967), and the flow through this fractured network considers factors such as fracture morphology and friction factor, $\psi$. The concept of assessing how far the apertures in the fractures might affect the flow in Karoo aquifers was presented by Botha *et al* (1998). The study found that the flux through the fracture strongly depends on the square of the fracture apertures as derived from the discharge rate of a simple parallel plate fracture. Nevertheless, this causes some disparities in the models and other studies during the quantification of the fracture flow since the fractures are typically not parallel, not smooth, and have inconsistent apertures within them (Dippennar *et al*. 2009).

The aquifers' matrix flow was examined in detail in the studies conducted by Botha and Cloot (2004) and Botha *et al.* (1998). Their results indicated that as long as there is a change in the piezometric gradient of the fractures during the well pumping, matrix flow into the fractures will always occur. Furthermore, Botha *et al.* (1998) underlined that because the sediments' bedding-parallel fractures have relatively low hydraulic conductivity ($\sim 10^{-6} - 10^{-8}$ m/s), the rock matrix functions as storage units.

# 3 CHAPTER 3: DESCRIPTION OF THE STUDY AREA

## 3.1. Introduction

This section provides descriptive information on the region's broad geological, topographical, hydrogeological, and some distinctive features within both the Mafeteng district and Lesotho in general. The fundamental understanding of the hydrogeological characterisation of the dolerite dykes in Lesotho is developed by reviewing the existing information related to the regional or sub-regional local hydrogeological and geological maps, as well as the geomorphology of the area.

## 3.2. Locality

Lesotho is divided into different administrative districts, and Mafeteng is one of the 10 districts in Lesotho. Most of the selected places used as case studies for the drilled boreholes and pumping analyses from this research originate in the Mafeteng District. Situated in the Southern region of Lesotho, Mafeteng District has borders with both Maseru and Mohale's Hoek Districts (both in Lesotho), and the Freestate Province in South Africa (Makalo *et al*. 2022).

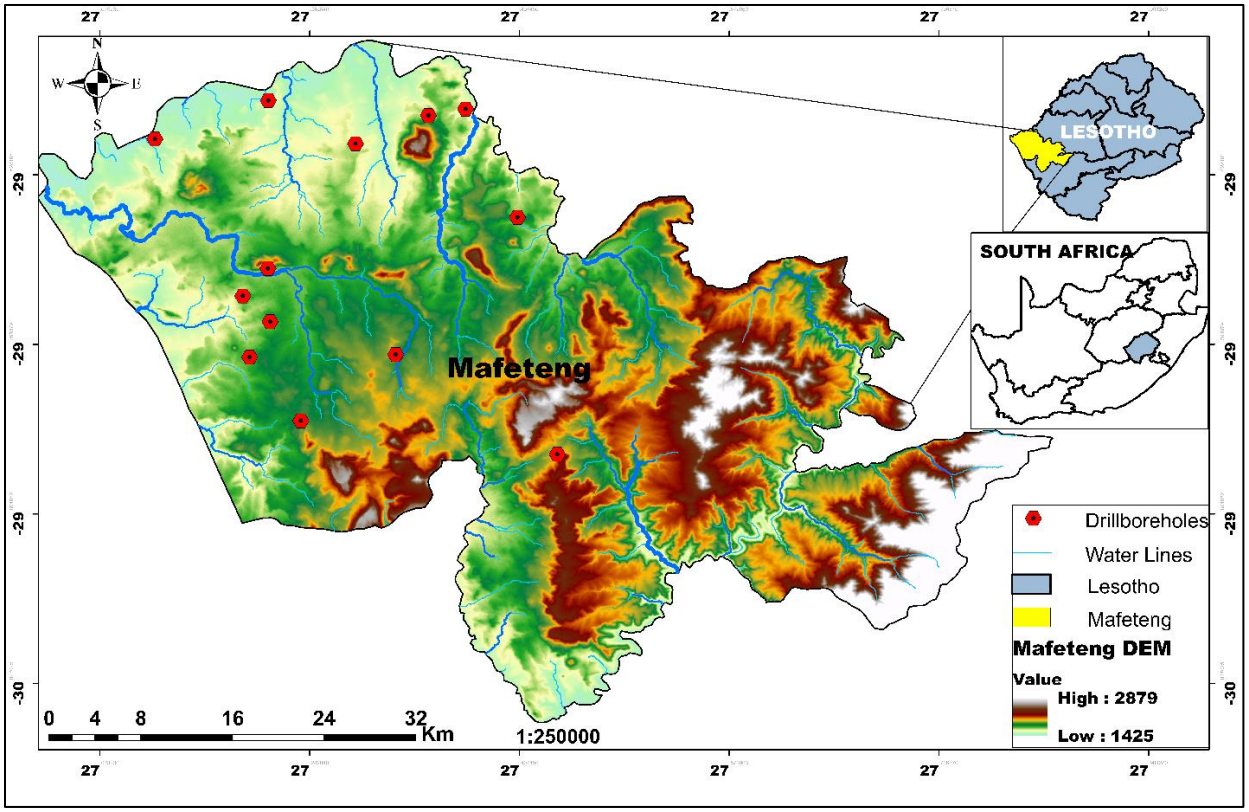



**Figure 5:** The Digital Elevation Model (DEM) of Mafeteng District, Lesotho (Created using ArcGIS).

Hlalele (2017) indicated that the largest areal extent of Mafeteng is occupied by the lowlands (1400 mamsl-1750 mamsl) regions of Lesotho plus a small portion of the foothills (1800 mamsl – 2100 mamsl) as shown from the DEM in Figure 5.

### 3.3. Physiography and Climate

Lesotho is generally considered a semi-arid to temperate region as highlighted in Figure 6 (Davies, 2003). Sene *et al.* (1998) highlighted that the Lesotho Highlands play an important role in both surface and subsurface water as the highlands to the northeast receive about 1600 mm of mean annual rainfall. The country experiences 80% of the average annual rainfall of which it is between October and March, and this is about 750 mm in the low-lying regions (Sene *et al.* 1998). The highest and lowest points in Lesotho are 3500 m and 1500 m above sea level respectively (Sene *et al.* 1998). Regarding temperatures in the region, they usually drop below zero in the highlands during the winter months with the likelihood of snowfall (Sene *et al.* 1998).

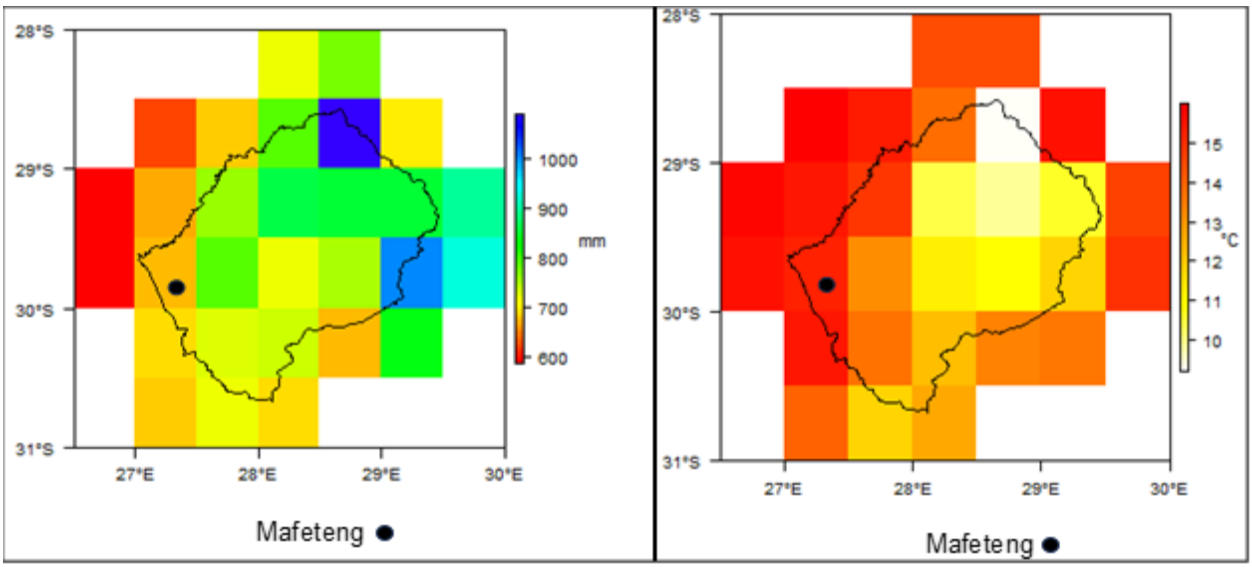



**Figure 6:** The average annual precipitation and the average temperature of Lesotho and Mafeteng inclusive (Source: Leketa et al. 2018).

### 3.4. Geology

#### 3.4.1. Regional-Lesotho

The geology of Lesotho is dominated by the Drakensberg Group basalts of the Karoo Supergroup in the Highlands and by sediments from both the Stomberg and Beaufort Groups in the foothills and lowlands of the country (Figure 7). Davies (2003) highlighted that there are several dykes and sills that intrude into these Formations as indicated in Figure 8. The chrono-stratigraphy of Lesotho is composed of the horizontal to sub-horizontal dipping sediments of the Beaufort and Stomberg Groups, the latter being overlain by the Drakensberg basalts (Davies, 2003). Figure 9 displays the relevant portion of this chronostratigraphy.

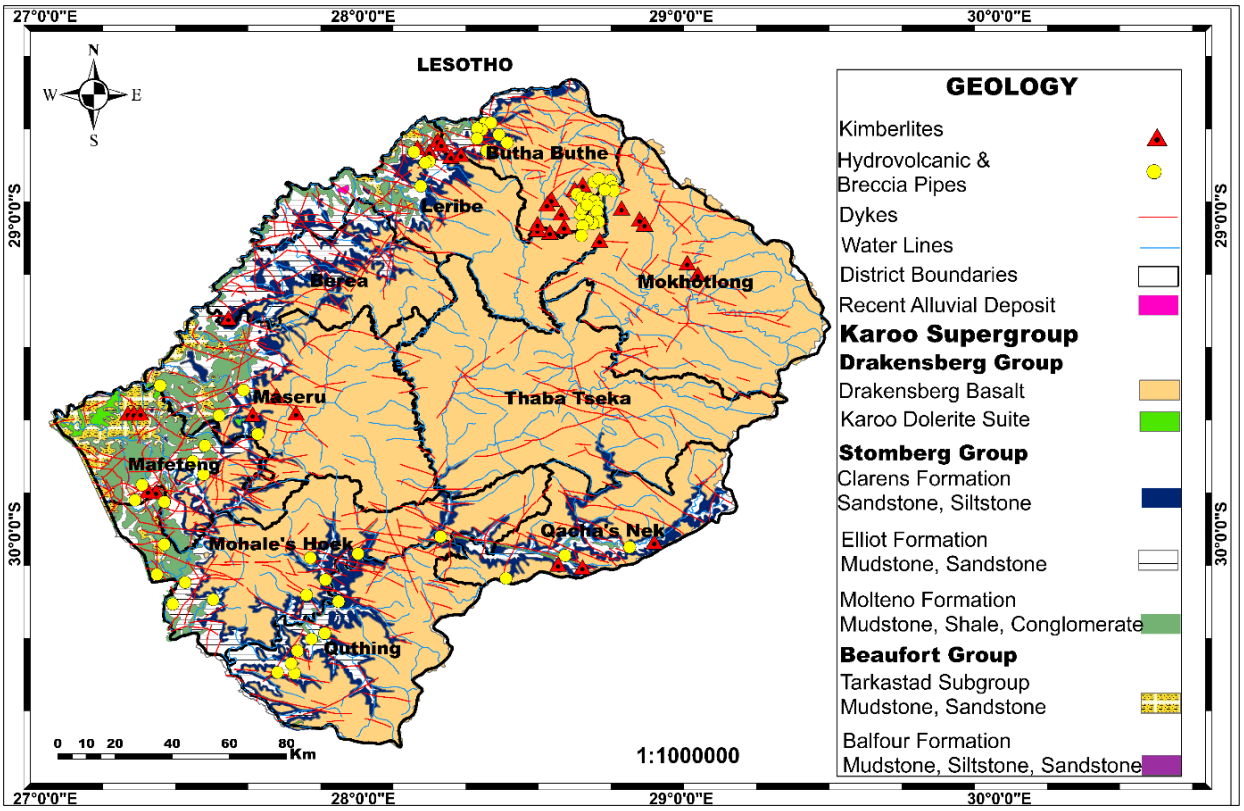



**Figure 7:** Simplified Geological map of Lesotho (Created using ArcGIS).

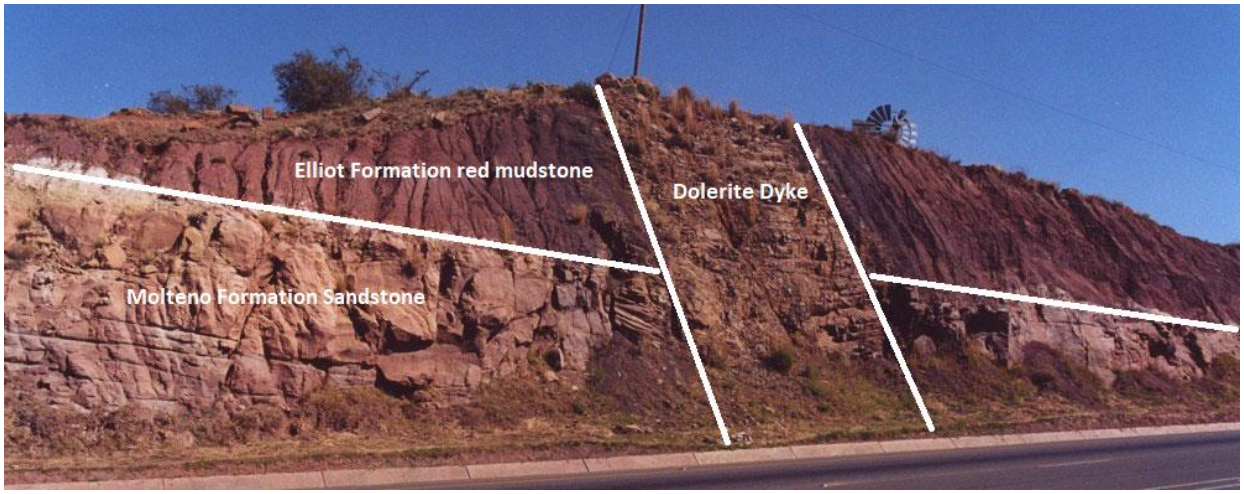



**Figure 8:** A dolerite dyke intruding into both the Molteno and Elliot Formations in the lowlands of Lesotho (Source: Davies, 2003).

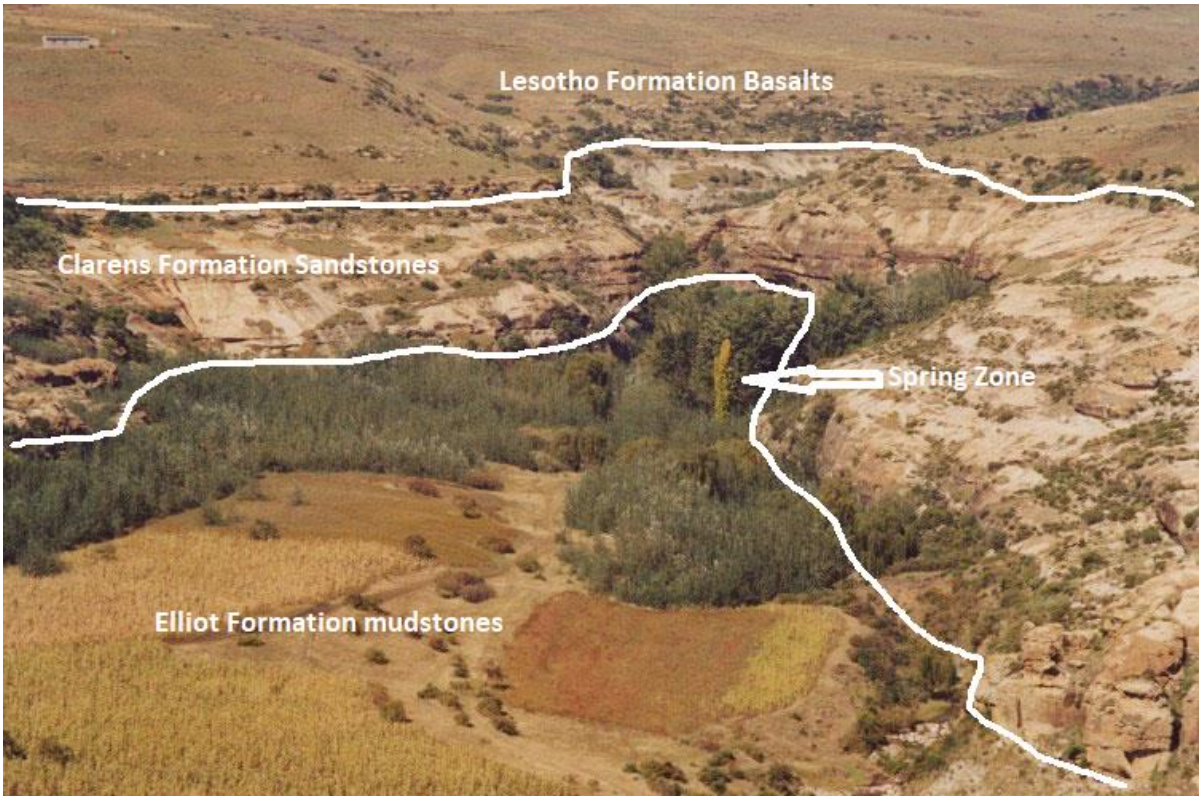



**Figure 9:** A portion of Lesotho's chronostratigraphy exposed in the Thupa-Kubu Valley, northwest of Sefikeng, the sediment Formations are overlayed by the basalts (Source: Davies, 2003).

### 3.4.2 Local-Mafeteng

Mafeteng geology is largely occupied by sedimentary formations and a bit of basaltic lava in the foothills (Figure 10). Leketa *et al*. (2018) and UND (1984) outlined that the oldest sedimentary unit, the Beaufort Group, consists of the Burgersdorp Formation which is characterised by red shales, mudstones, some carbonaceous shales, and buff sandstones, however, these are exposed on the western region in the Mohokare catchment. Similarly, sedimentary rocks from the Molteno (35 m thick in the north to 150 m thick in the south), Elliot (250 m thick in the south to 15 m thick in the north), and Clarens Formations, which belong to the Stomberg Group, consists of fluvial-deltaic mudstones, siltstones, and sandstones (Davies, 2003). The Molteno and Elliot Formations outcrop very well in the western Lesotho catchment (Davies, 2003). Leketa *et al.* (2018) reported that the Clarens Formation occurs from the central and eastern parts of Lesotho but crops well in the central and some valleys in the region.

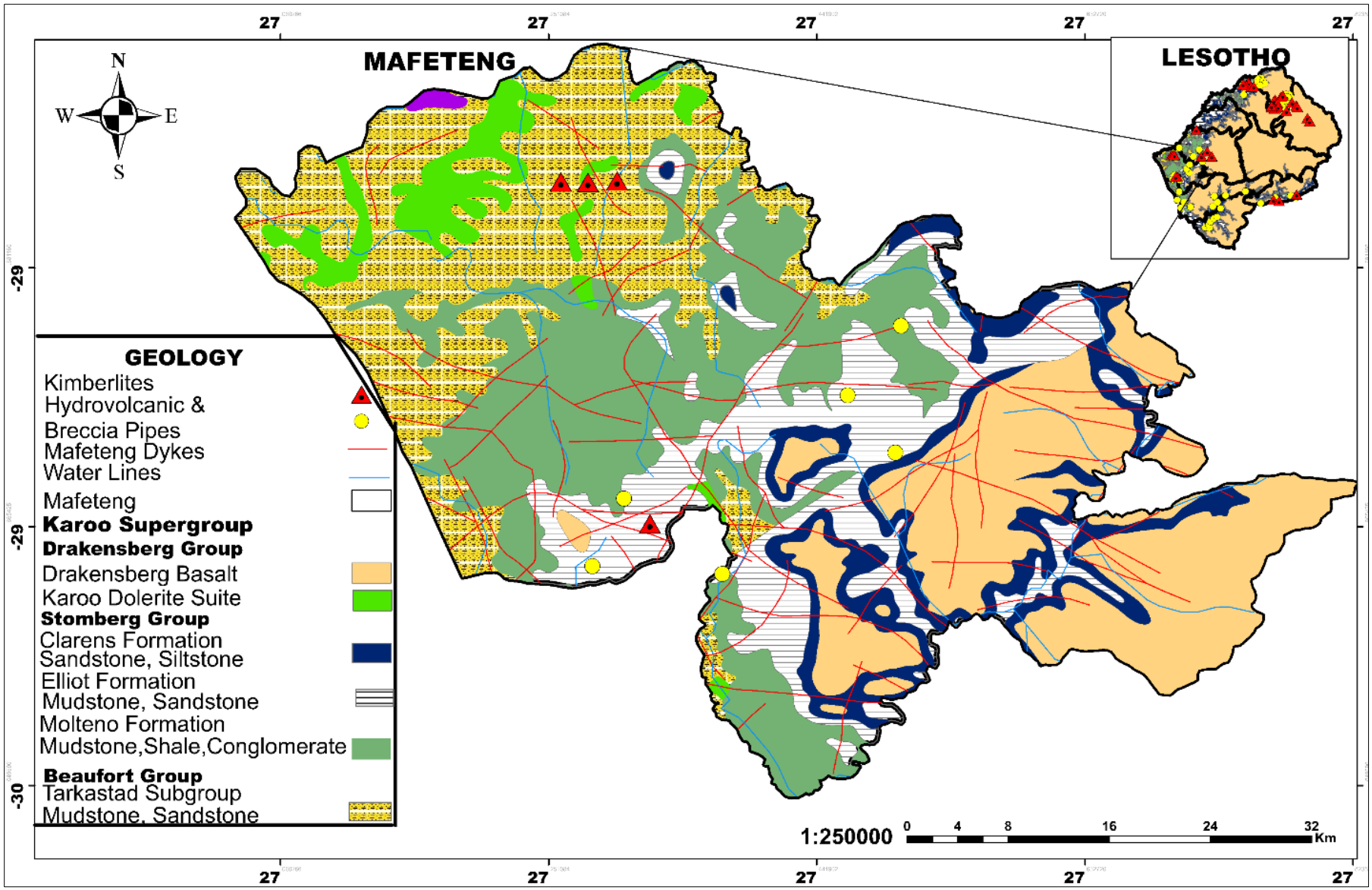



**Figure 10:** Simplified geology map of Mafeteng district, Lesotho (Created using ArcGIS).

The Clarens Formation sediments are further subdivided into different zones based on their structures. The zones include Zone I (thickly-very thickly bedded, silty sandstone and sandy siltstone), zone II (alternating beds of massive and cross-bedded sandstone), and Zone III of massive-very thickly bedded, massive silty sandstone and sandy siltstone (Leketa *et al.* 2018). Generally, no folding or faulting occurs within the sediments in the study area. Clarens Formation is overlain by the amygdaloidal basalt flows (1600 m thick in the north) of the Drakensberg Group (Davies, 2003). Linear dykes, ring dykes and sills intrude the sediment Formations and basalt, with linear dykes resulting in ridge-like features (Figure 11).

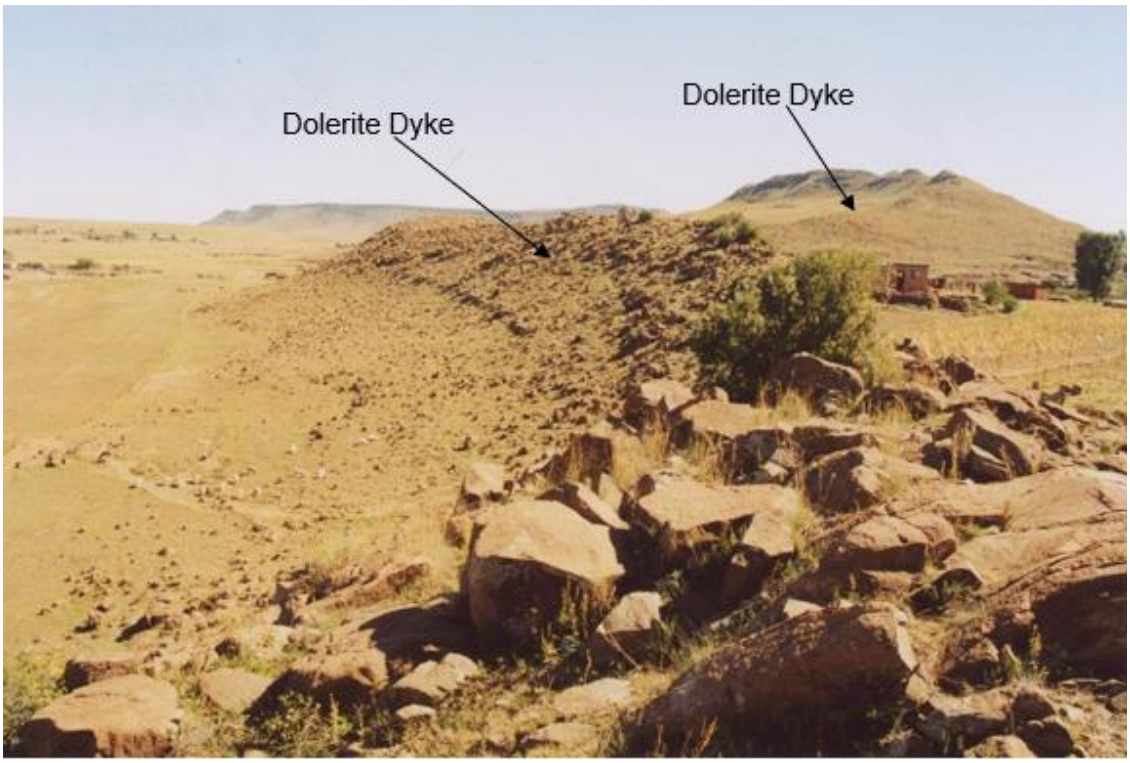



**Figure 11:** The dolerite dykes intruding the Burgersdorp Formation, north of the focal area in the Mafeteng District, Lesotho. (Source: Davies, 2003).

### 3.5. Hydrogeology

Lesotho is composed of 3 main catchment areas (figure 12), the Mohokare (towards the west), Makhaleng (towards the southwest), and the Senqu catchment which occupies most of the Lesotho area. Mohokare catchment is established by the Mohokare River (in English=Caledon River) and marks the border between South Africa and Lesotho. Mohokare catchment covers about 7,000 $km^2$ in Lesotho while the Makhaleng catchment and Senqu catchments cover 3,000 $km^2$ and 20,000 $km^2$ respectively (Grauso *et al.* 2020). The Mohokare, Makhaleng, and Senqu Rivers are tributaries to the extensive Orange River Basin which stretches to South Africa and Namibia (Chatanga *et al*. 2019). Water from these catchments is imperative in Lesotho's districts as it is utilised for various purposes for example, the Makhaleng River supplies 10,000 $m^3$/day to the Maqalika reservoir in cases when the river experiences low flows (Chatanga *et al*. 2019).

Mafeteng District is shared mostly by the Mohokare catchment with portions of both the Makhaleng and the Senqu Catchments, Figure 12.

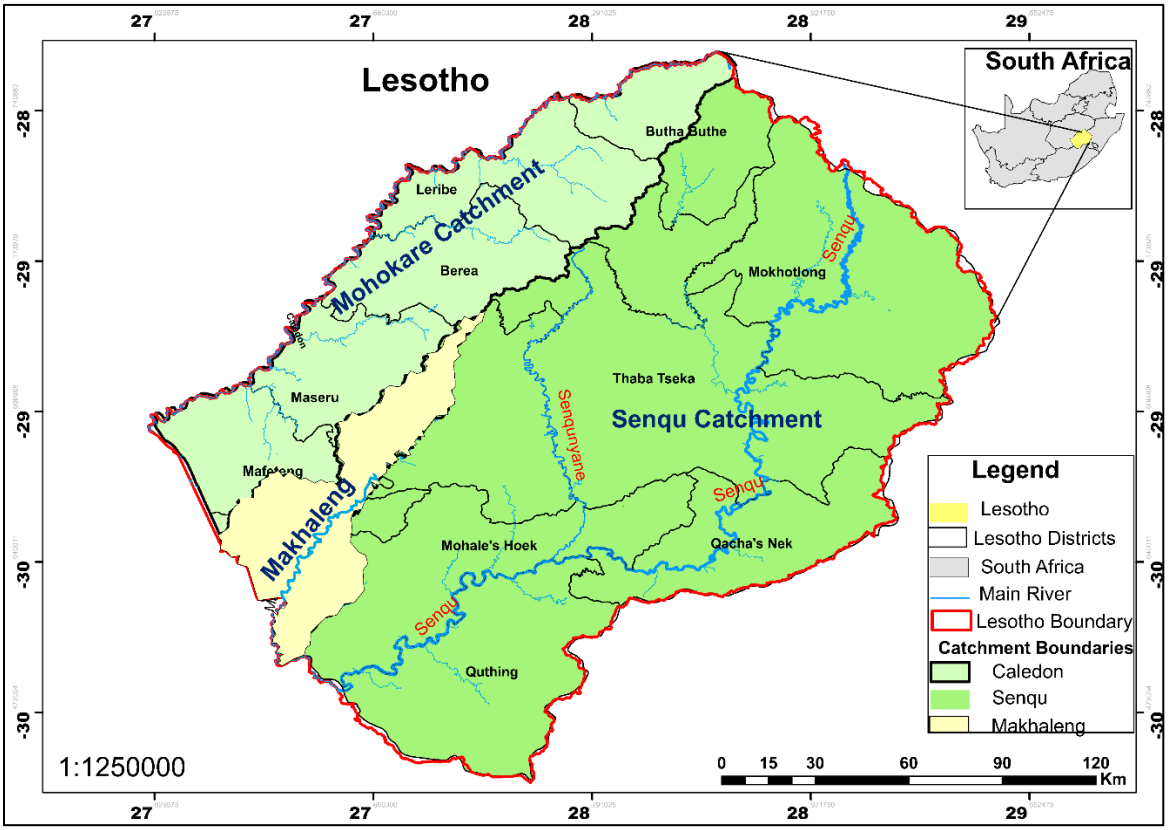



**Figure 12:** The three major catchments of Lesotho are the Mohokare, Makhaleng, and Senqu catchments (Created using ArcGIS).

The occurrence of groundwater in Lesotho is in fractured sedimentary formations, basaltic rock aquifers, alluvial sediments, and dolerite fractures as indicated in Figure 13 below (Davies, 2003). Characteristically, Davies (2003) determined that borehole yields of Burgersdorp could indicate a very low permeable aquifer. On the other hand, the Molteno Formation is the best aquifer as it has good groundwater development potential and, the presence of dolerite fractures could improve the groundwater occurrence of the Formation. Hydraulic characteristics of the Molteno Formation are well developed in the lowlands for example, the total recommended yield for the Roma well field (from the Maseru District) is about 21 l/sec (Davies, 2003). With the Elliot Formation, groundwater occurs in the interbedded sandstone layers. The Clarens Formation is a very poor aquifer because the sandstone from the Formation is very compact, and previous studies highlighted these to be a shallow permeable aquifer (Davies, 2003).

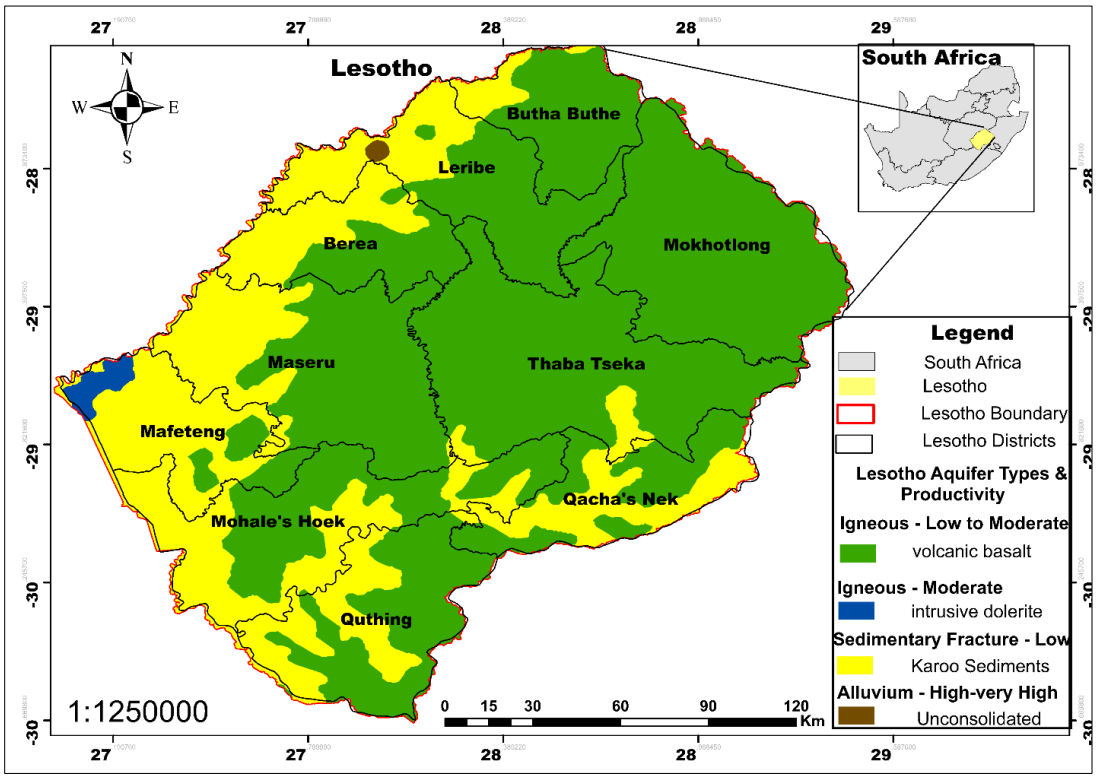



**Figure 13:** Background information on the aquifer types and their productivity in terms of their potential to sustain and abstract groundwater as extracted in ArcGIS.

# 4 CHAPTER 4: METHODOLOGY

## 4.1. Introduction

The methods and procedures used to investigate the baseline hydrogeology of the dolerite dykes in Lesotho are described in this chapter. Both desktop and field investigations were employed to gather and analyse the data in addressing the predetermined objectives outlined in Chapter 1. The methods include ground magnetic surveys for mapping and characterising the geometrical properties of the dykes, digital elevation models, standard percussion drilling for groundwater flow properties and examining the local static groundwater level, and pumping tests to obtain information on transmissivities and aquifer yields as well as understanding the different flow regimes that could be encountered during the pumping process. These methods and procedures were chosen to ensure the reliability and validity of the results.

## 4.2. Geological mapping of dolerite dykes

### 4.2.1 Geometry characterisation

#### 4.2.1.1. Choice of method

The physical properties of geological features can be ascertained by geophysical surveys, provided that these characteristics are substantially different from those of the underlying and overlying rock units. In addition, the geophysical surveys' task is also to define the extent of each component of a hydrogeological structure and categorise it according to its physical attributes. Ground magnetics was utilised in this study in aiding scientifically to locate the intrusive dolerite dyke(s) to be characterised from the focal area of study. In addition, the method was used in determining the geometry and orientation and delineating the strike and width in the determination of the geological characteristics of the intrusive dolerite dykes.

Under the magnetic approach, a magnetometer detects and measures the Earth's magnetic field passively at various points on the surface, the geological features with high magnetic susceptibility cause anomalies that are utilised for site characterisation (Burger, 2006 and Telford, 1990). Positive and negative anomalies are attributed to magnetic minerals contained in rock units and non-magnetic components like voids in the subsurface, respectively (Telford *et al*. 1990). In this study, a Cesium roving magnetometer is used in recording magnetic readings, Mickus (2014) highlighted that the magnetic readings measured from the walk magnetometer result from the subsurface magnetization of magnetizable igneous Formations generated by the Earth's main magnetic field. Significantly, Minner and Dippenaar (2019) pointed out that the magnetometer detects the magnetic field on the surface rather than the magnetic strength directly from the geological feature.

### 4.2.1.2. Data Acquisition

The magnetic data was acquired with up to 17-line profiles covered along the NW-SE (Figures 14 and 15). Following data processing, the minimum curvature algorithm was used to grid the data. The proposed location used for the ground magnetic data is Qalabane, in the Mafeteng district, Long 27.1951, and Lat -29.7711. The magnetic survey lines are designed perpendicular to the geological strike direction to fully determine the magnetic contrast with the adjacent lithology. A total of 17 profiles designed are not of uniform length and spacing due to the inaccessibility of some areas within the designed grid parameters. The grid length covered from line 0 to line 17 is about 644 m with an average line spacing of about 36 m.

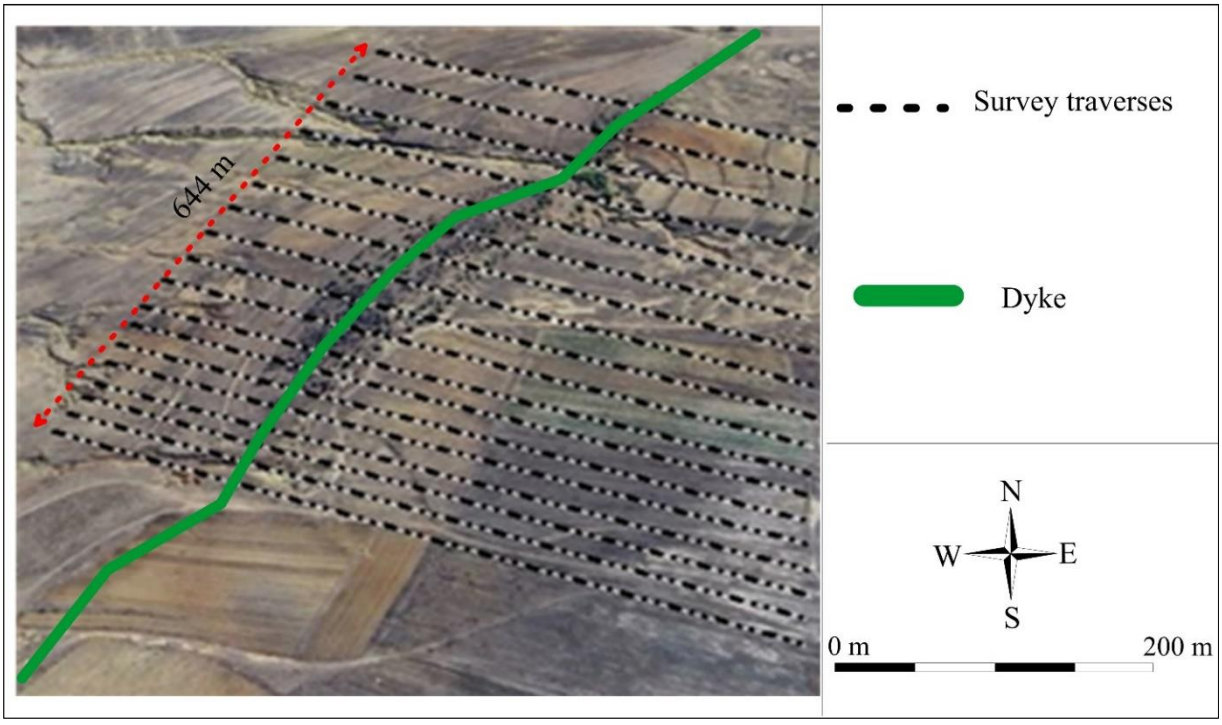



**Figure 14:** The magnetic survey grid at Qalabane in the district of Mafeteng, Lesotho (Plotted using Global Mapper).

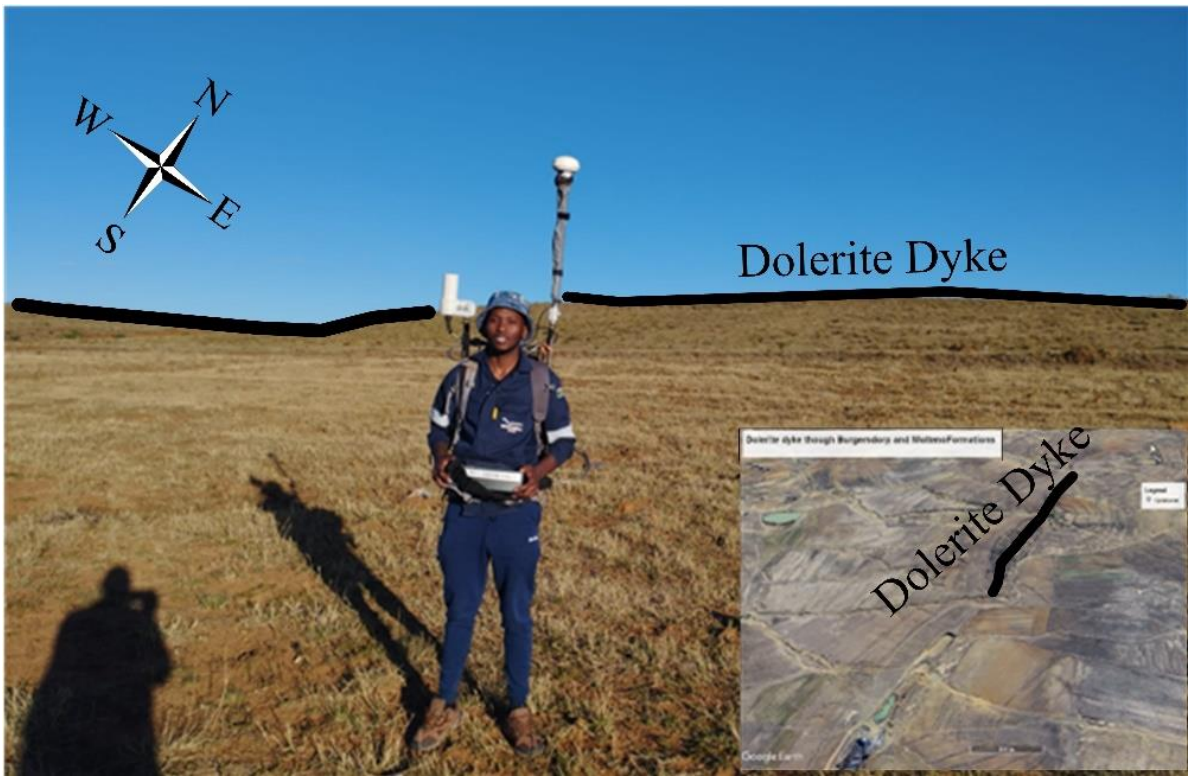



**Figure 15:** Dolerite dyke intruding through the Burgersdorp (Tarkastad Subgroup) and Molteno Formations and forming a ridge-like feature at Qalabane, Mafeteng District.

### 4.2.1.3. Data Processing

Sequential enhancements were done regarding the magnetic data collected (Figure 16). Concerning the measured total magnetic intensity (TMI), Reduction to the Pole (RTP) was employed to assess the impact of potential induced magnetisation and strike on the magnetic anomaly shape. Rajagopalan (2003) explains that the anomaly peak is shifted by RTP to match the magnetic source's margins or core hence it is used. To expose fine-grained geologic features, the regional field was subtracted from the TMI after applying the 2D and 3×3 convolution with a predefined Hanning filter to produce residual magnetic intensity grids (RMI). Further processing included the application of the 1$^{st}$ vertical derivative (VD) on the TMI, Graham (2014) described that the 1$^{st}$ VD allows for eliminating the impact of long wavelengths and big amplitudes for best results hence the reduction was employed. All of these enhancements were done through the programs Geosoft (Oasis Montaj), MagMap2000, and ZondGM3D.

As outlined by Geomatrix (2023), the technical specifications for the Cesium Vapor magnetometer (Geometrics, G-858) used include:

- Operation range, 20 000-100 000 nT
- Noise > 0.008 nT/Hz-RMS

- Gradient tolerance > 20 000 nT
- Heading error 1.5 nT including backpack and GPS
- Sensitivity from 0.01 nT at a 1-sec rate to 0.05 nT at a 0.1-sec cycle rate.

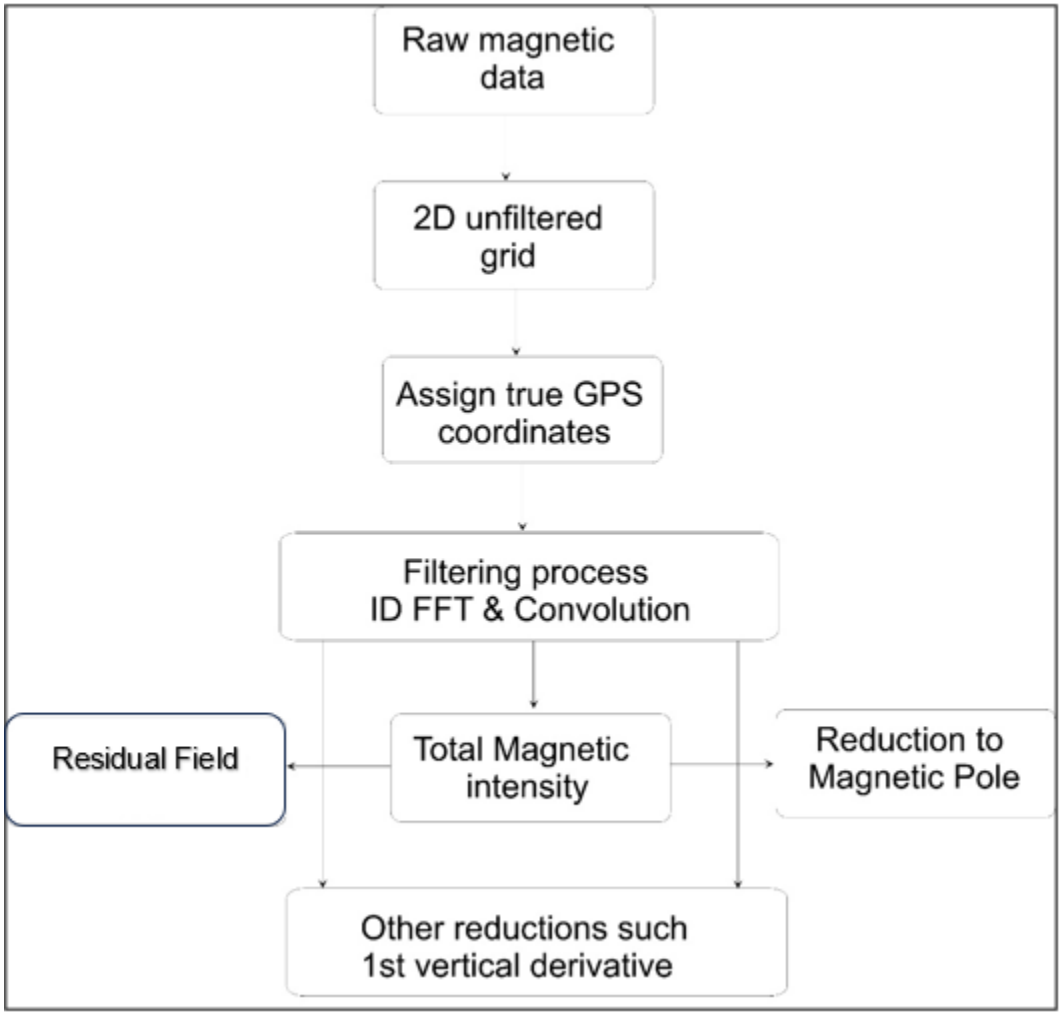



**Figure 16:** Flow chart providing sequential processes for the magnetic data processing and results.

### 4.2.2. Drilling

Drilling is one of the approaches used for groundwater exploration to investigate the potential for boreholes, allowing the hydrogeological conditions of the chosen locations to be examined and the geological features to be hydrogeologically characterised.

The drilling technique used is standard percussion drilling, under the supervision of a qualified Hydrogeologist. Corps (1990) highlighted that this method is a more cost-effective technique of creating holes in the ground using heavy material that is raised and dropped repeatedly during drilling, the holes are then cleaned using high-velocity air or drilling fluid (mud) during the process. According to Shakhane

(2021), the hydrogeologist's supervision includes monitoring the driller's compliance with the bill of quantities and best drilling standards, analysing, and recording the physical and structural characteristics of wash-cutting samples taken at specific depths, as well as penetration rates and a blow yields.

Furthermore, a hydrogeologist's duties were to make recommendations regarding the construction of boreholes and approve the bill of quantities. The boreholes are drilled with a 0.14 m diameter from the chosen places. Eventually, borehole construction followed borehole development, based on the observed hydrogeological characteristics. The rest of the pumping borehole information is in the appendix tables.

## 4.3. Groundwater flow properties of dolerite dykes

### 4.3.1 Groundwater flow direction

The study examined local data regarding the hydrogeological characteristics of the focal area using the 30 m resolution digital elevation model of Lesotho as well as the depth to water data of the boreholes previously constructed, as this information could infer the geological features influencing groundwater flow from the Karoo's sediment aquifers (Deep *et al.* 2021). Using the deterministic eight-node algorithm (D8) that Jenson and Dominique (1988) first suggested, the Arc Hydro Tool was used to describe the drainage pattern, water flow direction, and the static groundwater level for the research area's scope as shown by the step-by-step process in Figure 17 below. Nevertheless, Tong *et al.* (2021) highlighted that for the surface flows the Arc Hydro Tool solely concentrates on the surface water movement to derive the features of drainage systems, such as stream networks, watersheds, and basins, while on the other hand neglecting hydraulic phenomena like evapotranspiration and surface absorption.

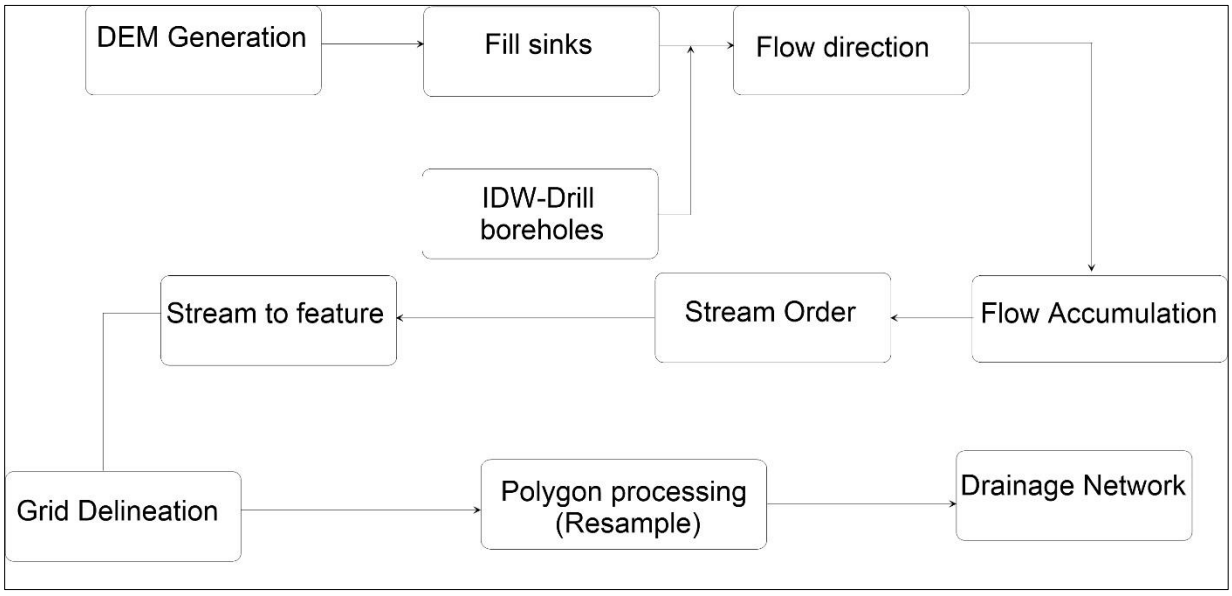



**Figure 17:** A flow of the Arc-Hydro Tool methodology was used in delineating the drainage network and groundwater flow directions.

Water usually flows in the steepest direction, that is, from high to low elevations perpendicular to the equipotential lines. If water may flow from one cell into only eight neighbouring cells, the D8 algorithm examines the flow direction and accumulation using the DEM as an input function; the water flow direction is determined by the steepest slope (Tong *et al*. 2021). Hence, to determine the direction flow, the elevation difference between the central cell and the eight encircling cells is computed, and the cell with the greatest height difference then opts to serve as the source of the water flow (Tong *et al*. 2021). With groundwater flow direction, the Inverse Distance Weighted (IDW) of the boreholes constructed is used as a primary input function, the difference between the depth to groundwater level and the surface is calculated to create the static water level contour map and to determine the direction of groundwater flow (Odipe *et al*. 2020).

To build a new grid model that indicates flow direction, the original elevation numbers are changed to 1, 2, 4, 8, 16, 32, 64, and 128 (Figure 18), these numbers correspond to East, Southeast, South, Southwest, West, Northwest, North, and Northeast directions respectively (Tong *et al*. 2021). It is further highlighted by Tong *et al.* (2021) that each cell has its water quantity assigned a value of 1, and each cell's water flows into the downslope cell for flow accumulation calculations. According to Tarboton *et al.* (1991), regions of concentrated flow in cells with high flow accumulation are utilised to define aquifer and stream networks in water flow.

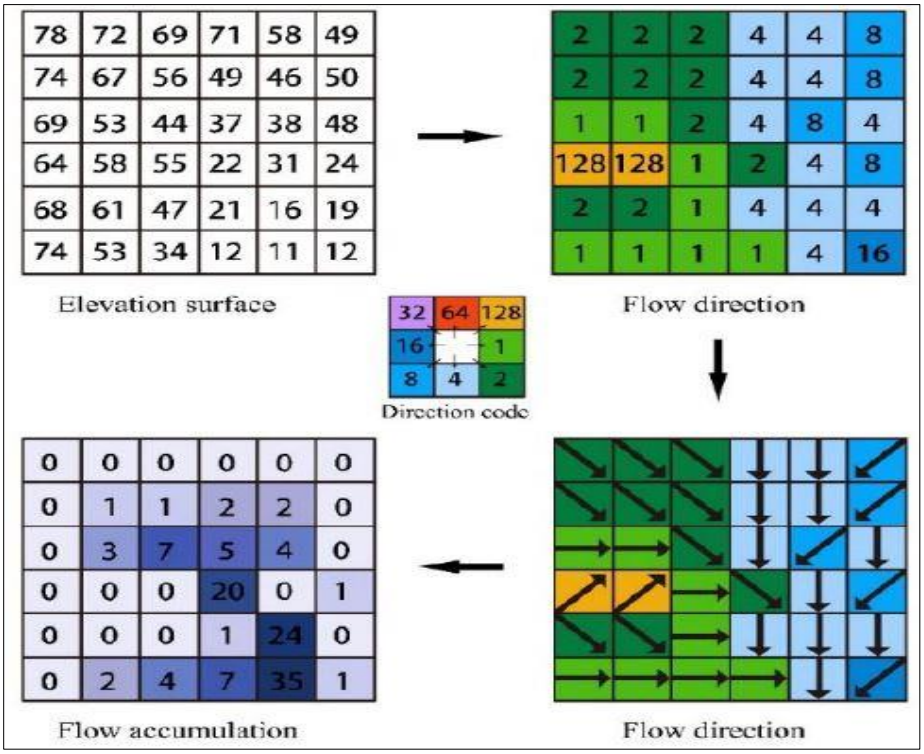



**Figure 18:** The eight-direction (D8) algorithm for determining flow direction and accumulation (Tong *et al.* 2021).

### 4.3.2 Pumping Test

The most popular approach for obtaining hydrogeological characteristics of rock formations is the pumping test, which provides data on storativity, transmissivity, and sustainable yield from hydrogeological research (Xu *et al*. 2019). This approach, according to Mawlood and Ismail (2019), involves pumping groundwater from a wellbore while measuring fluctuations in water level (drawdown) from either an observation well (nearby well) or a control well (pumped well).

The study relies on constant discharge (CDT) and recovery tests from a geological unit of the focal area, in which the pumping rate is maintained at a constant level with CDT throughout. In contrast, the recovery test gauges the residual drawdowns (s') that is, the difference between the water level recorded at a time (t') after the pumping stopped and the initial level before the commencement of the pumping (Gunawardhana, 2021; Atanga, 2014). The residual drawdown is the integral component of the pumping test. Regarding the CDT conducted in the study area, the water level logger and the pump inlet were installed below the reported water strikes. A solinst level logger was also used to track the borehole's subsequent drop in water level as it was exposed to a preset continuous pumping rate. All the measurements were taken from a control well.

### 4.3.3 Groundwater flow characterisation

From the completed pumping and recovery phases (water level recovered to 80%), evaluation of the hydrogeology of the dyke-related aquifer from this research is through pumping tests done by diagnosing different flow regimes that could be encountered from the tests. A derivative analysis is employed by showing the derivative plots whereby the drawdown data is plotted on the same graph as the derivative data. According to Bourdet *et al*. (1989), the derivative plot is derived from the drawdown data utilising the numerical differentiation, the baseline formulation for this calculation is:

$$\left(\frac{\partial S}{\partial \ln T}\right)_i = \frac{(\Delta S_{i-1}/\Delta \ln T_{i-1})\Delta \ln T_{i+1} + (\Delta S_{i+1}/\Delta \ln T_{i+1})\Delta \ln T_{i-1}}{\Delta \ln T_{i-1} + \Delta \ln T_{i+1}}$$

Where T is a time elapsed function. The slopes on either side of *i*, or the right and left weighted average slopes, from the above formulation are expressed as follows:

$$\Delta S_{i-1}/\Delta \ln T_{i-1}$$

and

$$\Delta S_{i+1}/\Delta \ln T_{i+1}$$

Van Tonder *et al.* (2001) highlighted that, throughout a constant rate pumping test, several flow regimes are categorised based on when they occur: early, intermediate, and late (Figure 19).

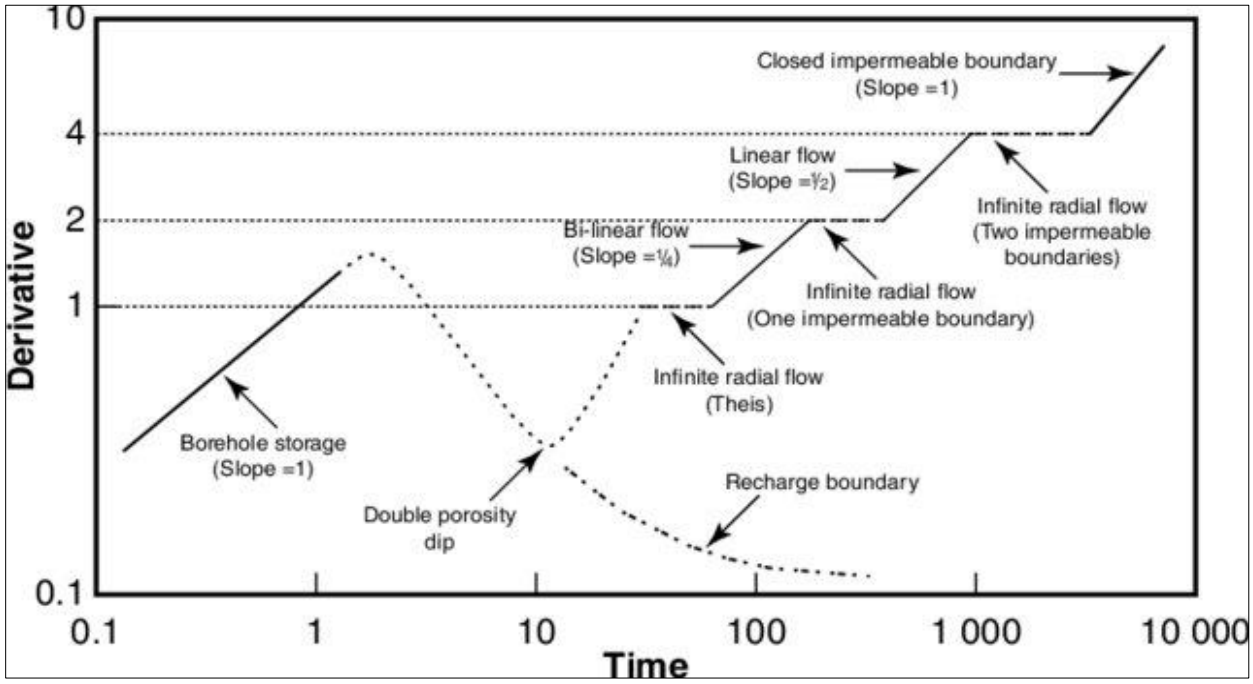



**Figure 19:** Graphs of the first logarithmic derivative of drawdown in a borehole for a few types of geometries and boundaries (Van Tonder et al. 2001).

### 4.3.4 Groundwater yields and aquifer parameters

The CDT data is analysed through various aquifer testing programs such as the Flow Characteristic (FC) program developed by Van Tonder *et al*. (2013). The Cooper-Jacob analysis, which is programmed in the FC Program, is utilised because of its versatility in generating reliable transmissivity (T) values across various geologic settings (Phillips, 1994). The analysis involves matching a straight line to drawdown data plotted as a function of the logarithmic of time since pumping began (Cooper and Jacob, 1946). The baseline formulation of Cooper-Jacob (1946) is simplified from Theis's (1935) drawdown equation:

$$S = \frac{\mathrm{Q}}{4\pi\mathrm{T}}[-0{,}5772 - \ln\mathrm{u} + \mathrm{u} - \frac{\mathrm{u}}{2.2!} + \frac{\mathrm{u}}{3.3!} - \cdots]$$

Based on Cooper-Jacob (1946) assumptions, the drawdown equation is eventually simplified to:

$$\Delta S = \frac{2.3\mathrm{Q}}{4\pi\mathrm{T}}$$

where; $\Delta S$ is the slope of the line per one log cycle, $S$ is the drawdown, Q is the constant pumping test, T is the transmissivity, u is the well constant (Pongmanda and Suprapti, 2020). The baseline formulation for sustainable yield relies on the equation:

$$Q\ (sust) = \left(\frac{\mathrm{Q}}{s'} \times s\right) = SC \times s$$

where; $Q\ (sust)$ is the sustainable yield, Q is the constant pumping test, $s$ is the drawdown, $s$' is the residual drawdown, and $SC$ is the specific capacity. However, the analytical solutions from Theis, Cooper, and Jacob are subject to several assumptions. In this instance, these assumptions include: the control well's water level indicates the aquifer's water level, the aquifer is assumed to be homogeneous and uniformly thick, its areal extent is infinite, and before pumping the potentiometric surface is assumed to be horizontal, and finally, the control well is assumed to fully penetrate the entire thickness (Gunawardhana, 2021).

# 5 CHAPTER 5: RESULTS AND DISCUSSION

## 5.1. Introduction

In the context of the study's objectives, the results and discussions are presented in this chapter following the methods and procedures described in the previous chapter. From the results, a combination of text, tables, figures and maps are used to illustrate the key findings of the research. In addition, the discussions are also provided in analysing the described results observed. The illustrations of the magnetic results establish the study's first objective while the results from the DEM, depth-to-water data models and pumping test data demonstrate the second objective.

## 5.2. Geological mapping of dolerite dykes

### 5.2.1. Geometry characterisation

It is important first to determine accurately what is to be characterised, hence this study argues that for groundwater analyses and characterisation of the dolerite dykes within the focal area, it is significant to utilise geophysics to detect these geomorphic lineaments to ascertain their presence, geometry, and to eventually determine how their geological setting could be controlling the occurrence of groundwater. The ground magnetic data gathered along the survey lines was processed, filtered, and gridded.

As outlined in the previous chapter, to get better results on the detected magnetic anomalies for this current study, magnetic data was processed and some of the processing image results are highlighted below:

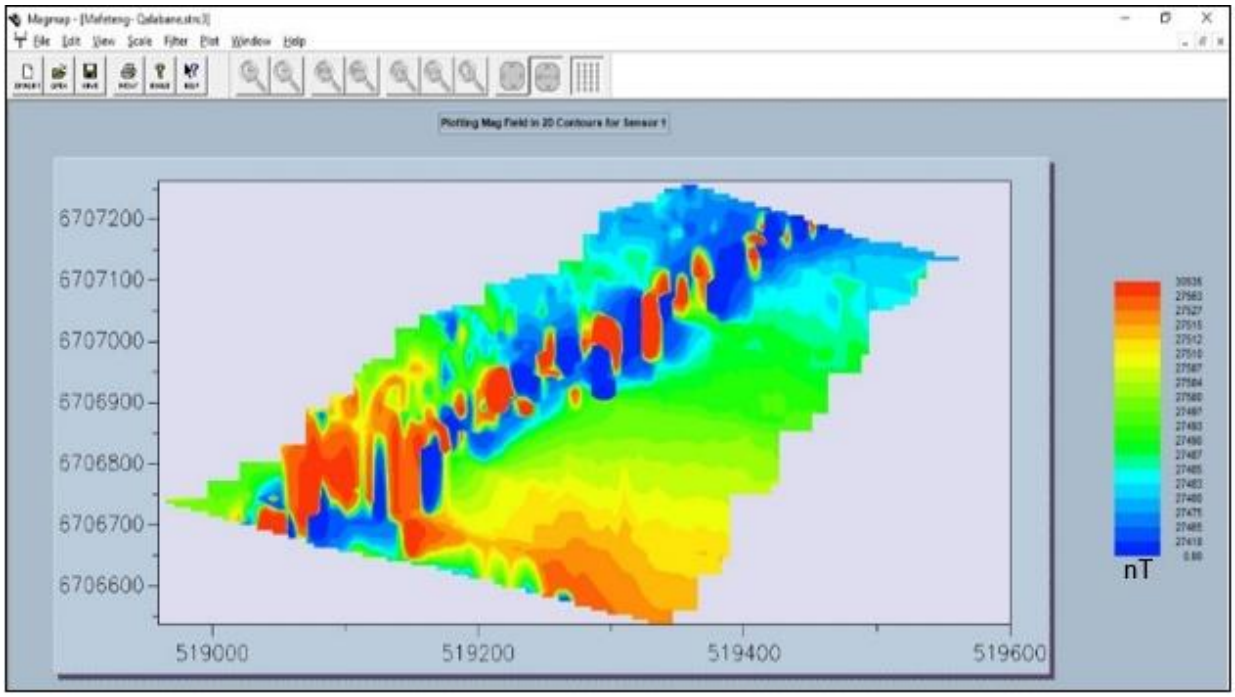



**Figure 20:** Unfiltered magnetic field intensity (nT) in 2D contours with assigned UTM coordinates as generated from the raw magnetic data through MagMap2000.

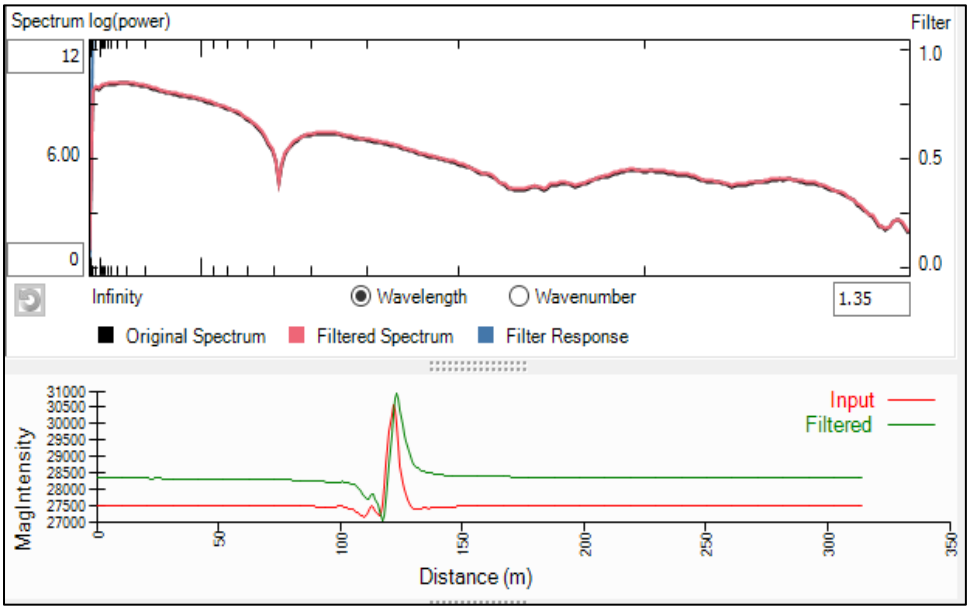



**Figure 21:** Total magnetic intensity and spectrum profiles after 1D Fast Fourier Transform (FFT) and reduction to magnetic pole (RTP).

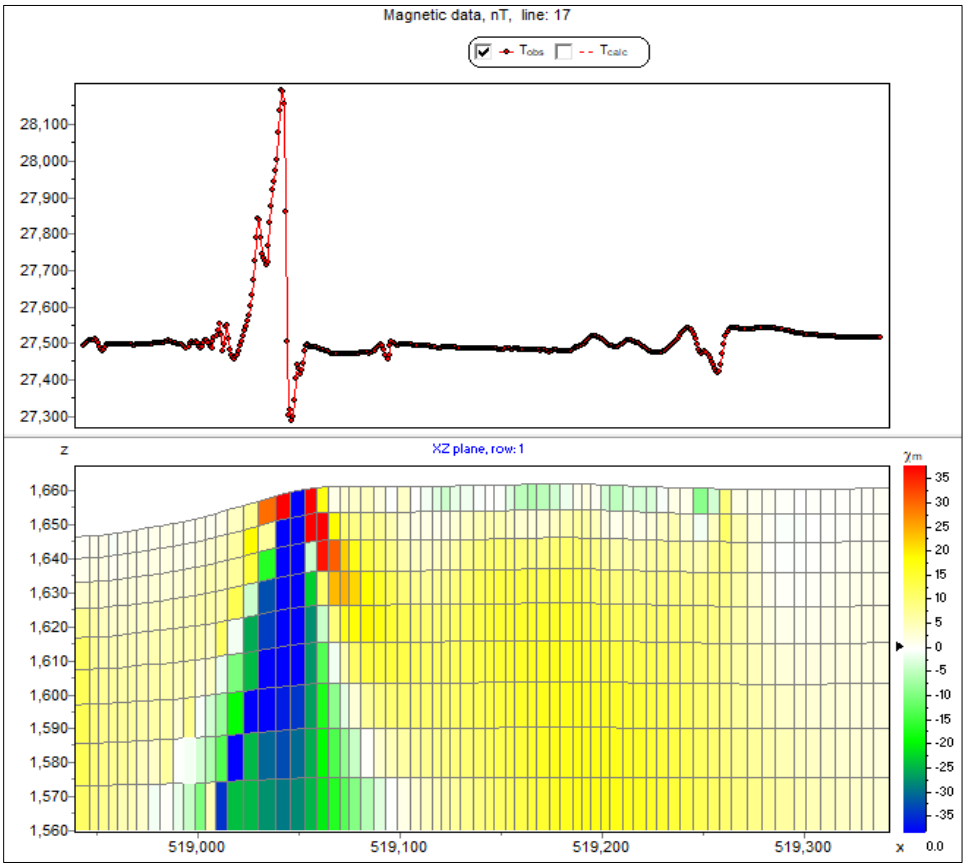



**Figure 22:** Unprocessed observed magnetic data processing images of line 17 anomaly in response to geological features' contribution to the overall magnetic flux density present after exposure to a magnetic field in the XZ plane.

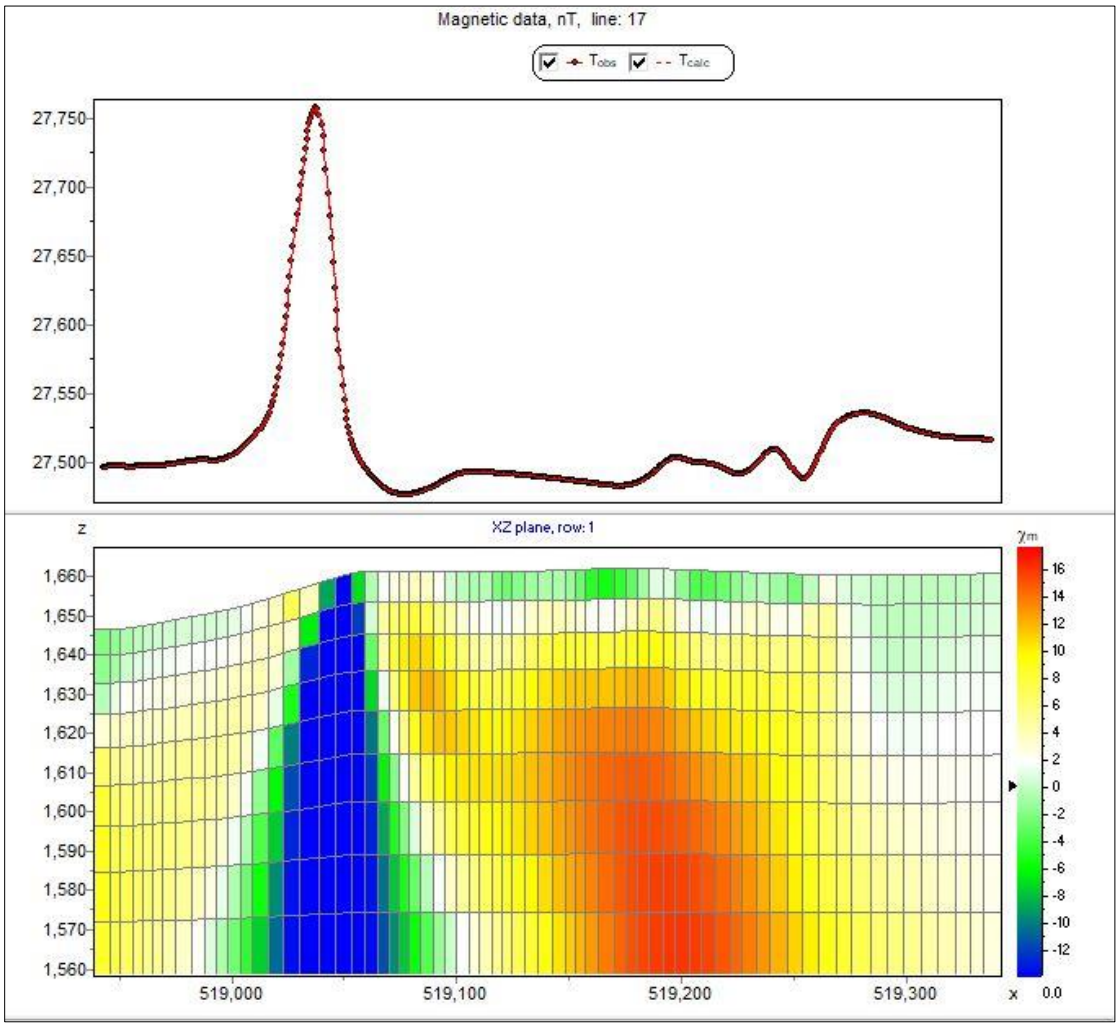



**Figure 23:** Filtered and smoothed data processing images of line 17 anomaly in response to geological features' contribution to the overall magnetic flux density present after exposure to a magnetic field in the XZ plane.

Both the processed and unprocessed data indicate anomalous bodies from the surveyed area, whereby there are substantial variations in magnetic intensity as displayed in the 2D magnetic field map in Figure 20. To precisely align and centre the anomalies, RTP processing is employed as demonstrated in Figure 21. To produce these anomalies through RTP, geomagnetic inclination and declination had to be determined from the collected magnetic data in the study area, these were calculated through Geosoft Oasis Montaj and the determined inclination and declination were -63 and -24.7 respectively. The magnetic intensity variations and anomalies from the area are constantly observed even from zooming in further into the survey grid by selecting and applying filtering processes on one of the magnetic lines, line 17 (Figures 22-23). The walk over-study at Qalabane, in the Mafeteng district, revealed noticeable vertical stretches of greenery with a ridge-like structure as depicted in Figure 14. An example of some of the data recorded along lines 3 and 4, from the traverses done across this linear stretch, is shown as profiles in Figures 24-25 below. The amplitude

of the magnetic anomalies in lines 3 and 4 are visible with ranges from 26010 – 27908 nT, with wavelengths of up to hundreds of meters.

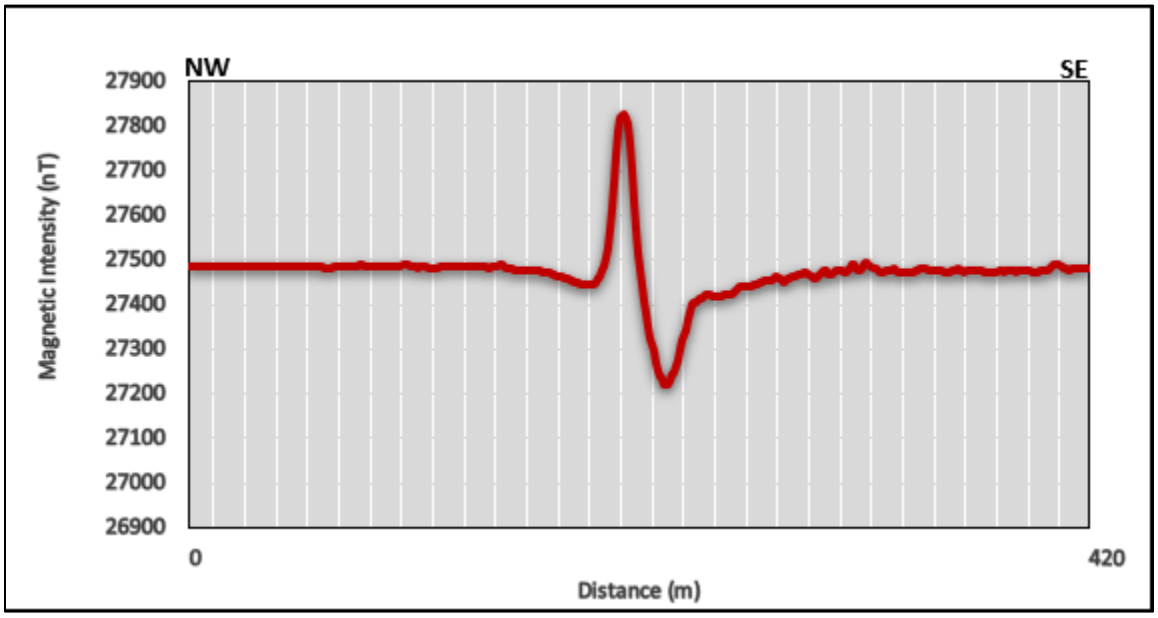



**Figure 24:** The magnetic intensity data was recorded along line 3 (L_3) with the traverses in the NW-SE directions.




**Figure 25:** The magnetic intensity data was recorded along lines 4 (L_4) with the traverses in the NW-SE directions with the linear structure positions indicated.

The linear structure observed as vertical stretches of greenery (Figure 14) is further ascertained by the total magnetic intensity grid (TMI) overlain in the focal area of study in Google Earth (Figure 26). Generally, the total magnetic intensity field is decreasing from the southwest to the northeast of the gridded area.

However, the greatest magnetic intensity values seem to be along the strike of a linear geological structure, even though these values decline towards the northeast of the grid area where the linear structure outcrops at a height roughly equal to the topography surrounding it.

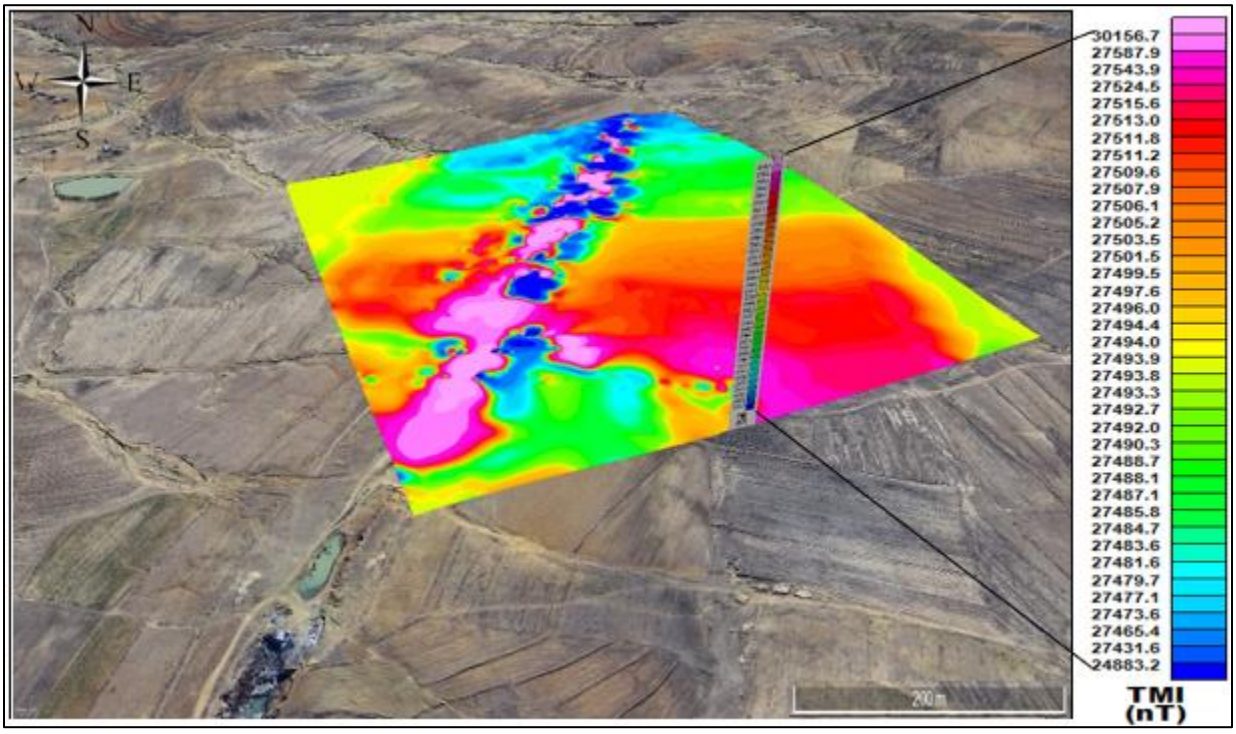



**Figure 26:** TMI (nT) image overlayed on Google Earth image in Qalabane, Mafeteng district Lesotho.

Using a geomagnetic inclination of -64 and a declination of -24.7 of the surveyed area, the TMI grid was reduced to the pole, resulting in the RTP map shown in Figure 27. The reduction in the pole caused the anomalies to shift and coincide with the magnetic source's periphery or core (Rajagopalan, 2003). Very low localised magnetic values (localised negative anomalies) are exposed on the edges of the linear feature's contact, these are marked as "B" both on the eastern and western sides of the linear structure in Figure 27. The residual map shows even more localised magnetic anomalies that are not visible on the TMI grid. After the removal of the regional field, the Residual Magnetic Intensity results in positive and negative anomalies to further substantiate the presence of the linear geological structure striking in the NE-SW directions, and its geophysical magnetization attributes to the adjacent lithology as shown by A-A' line in Figure 28.

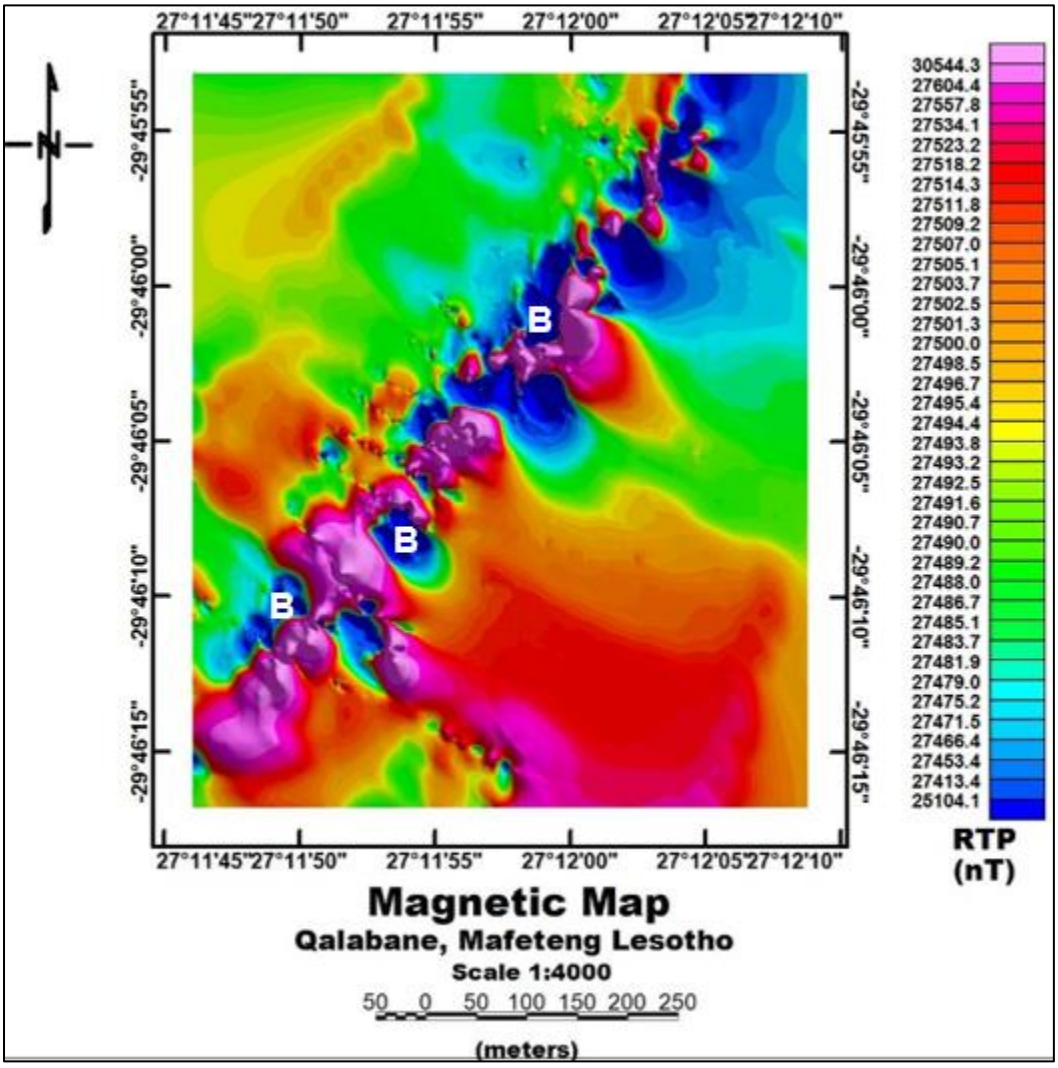



**Figure 27:** An RTP map with calculated geomagnetic inclination and declination of -63 and -24.7° respectively.

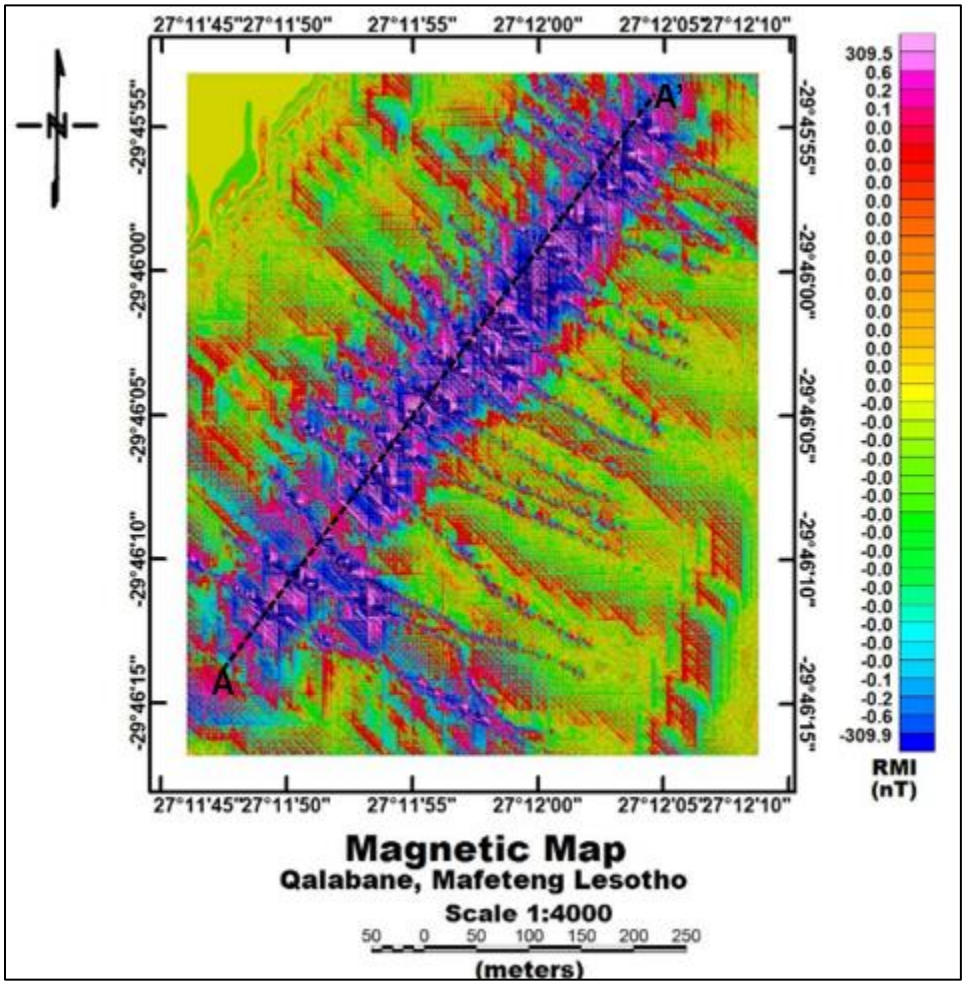



**Figure 28:** A Residual Magnetic Intensity (RMI) after subtraction of regional field from the TMI.

Figure 29 [A] shows the first vertical derivative (1-VD) map on the left, whereby the variations in the magnetic signal as a function of surveyed elevation are quantified. The first vertical derivative aided in increasing the shorter wavelengths and shortening the longer ones of which the latter are from the deeper sources, thus sharpening the edges and accentuating the margins of the anomalies along the linear body's contacts as depicted in Figure 29 [A]. On the other hand, Figure 29 [B] ascertains the maximum values (nT) recorded by each line as measured from the northwest to the southeast across the lineament and the least values on the edges of its contact. The anomaly shape from line 2 is largely dominated by two negative peaks, one in the NW and the other in the SE direction of the positive peak, matching the low magnetism on the edges of a linear body's contact as observed in the derivative map.

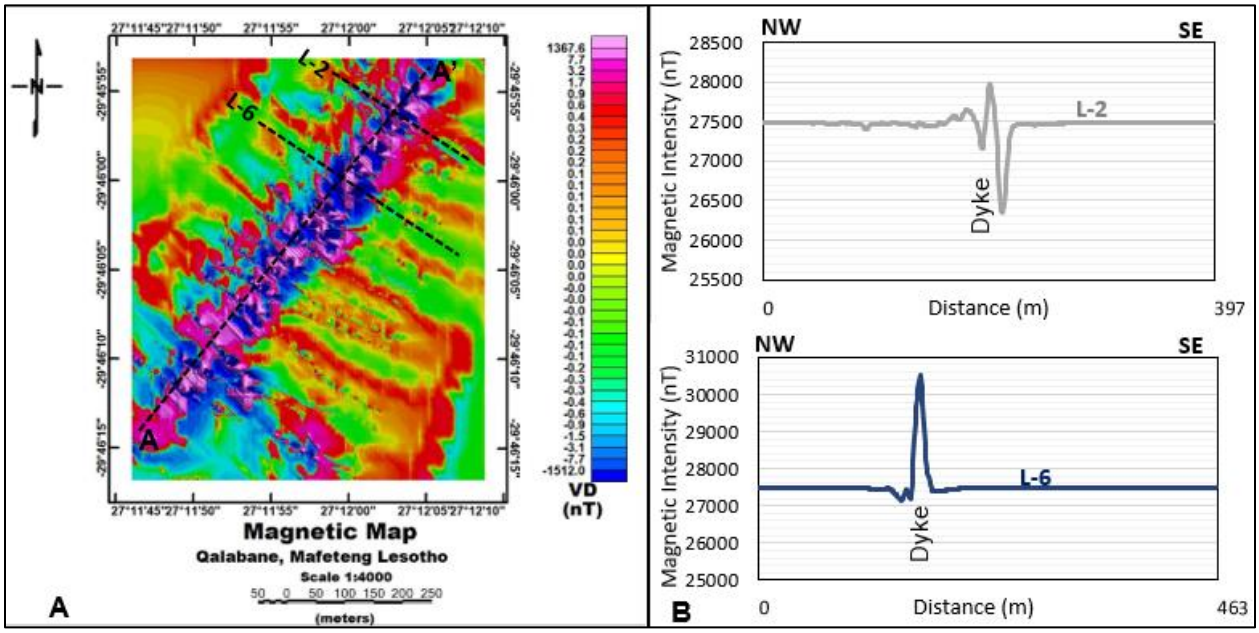



**Figure 29:** On the left (A), 1st vertical derivative map from the focal area of study, Qalabane, Mafeteng Lesotho with the survey lines 2 and 6 across the lineament (A-A'). On the right (B), magnetic intensity profiles of lines 2 and 6 show positive and negative anomalies along the linear dyke feature (A-A') and its contacts.

The magnetic values vary, as shown in the TMI, RMI, RTP, and the first vertical derivative maps created by Geosoft Oasis Montaj. The structure that resembles a ridge and shows vertical stretches of greenery (Figure 14) is magnetically anomalous as seen in Figures 26 – 29. The near-surface mafic-ultramafic igneous intrusion is thought to be the source of the strong magnetic values along the lineament hence, the structure is determined to be a linear dyke. Non-magnetic sources and perhaps thickly bedded sediments from the Stomberg and Beaufort Groups in the region are responsible for the low magnetic values. According to Fourie *et al.* (2019), the strong magnetic values associated with an intrusion over an area are thought to be caused by outcrops that extend over the ground level. As a result, the magnetic intensity values along the dyke that have been shown to decline towards the NE of the surveyed area (Figures 26 – 27) may indicate variations in the depth of the dyke intrusion as it is getting deeper in the NE direction along its strike.

The TMI grid's exposed negative anomalies, which are locally at the dyke's contacts, and these are further accentuated and sharpened on the 1st VD and residual maps. These anomalies at the dyke's edges strongly suggest the presence of fracture gaps on the dyke's contacts, indicating a close relationship between the dyke and the fracture systems on its margins along its strike. Additionally, the lithologies may have been fractured as a result of the magma pulses that initiated the dyke formation, as the Karoo sediments also underwent magmatic activity in the mid-Jurassic (Senger *et al.* 2015; Woodford and Chevallier, 2002). The development of these fractures is also associated with the adjacent lithologies being baked by the intruding

dykes during the less active periods when temperatures are not extreme to initiate metamorphism (Davies, 2003).

### 5.2.2 Forward Modelling

For the research to further accomplish its first objective of characterising and determining the geometry of the dyke from the ground magnetic survey, this subsection incorporates and displays results from Mag2DC and Pdyke programmes used to forward model the dyke.

This is after an observation that, a generalised dip and other geometrical parameters such as width and depth of the linear geological feature cannot be inferred easily from the anomalies since the anomaly shapes from the surveyed lines depicted in Figures 24, 25 and 29 [B] all exhibit inconsistent antisymmetric patterns (The rest of the lines' anomaly shapes are under the Appendix section). This inconsistent shape of the anomalies is further observed in the gridded maps shown above. Forward modelling of the geomagnetic anomalies for line 6 across the liner dyke feature has been done using the Pdyke and the Mag2DC software (Figures 30 and 31). This was done to predict the geometry and other geological parameters of the dyke's structure, which roughly corresponds to the magnetic response that was observed and recorded in the field. Further interpretation of the magnetic anomaly of the modelled dyke shows positive and negative anomaly along line 6 matching with the highest and lowest magnetic intensity values respectively (Figure 32).

As per line 6 across the linear dyke with its physical attributes, the modelled body displayed the estimated properties shown below:

- Width= 10m
- Dip= 10°
- Dip direction towards the South-East
- Geometry= Dyke-like structure

In the focal area of study for this research where boreholes were drilled, the parameters obtained from the modelled dyke at Qalabane suggest the geometry and structure of the other dykes in the area. In terms of width, the modelled dyke is revealed to be thin rather than thick, and it has a shallow depth to the top. This structure substantiates the fracture gaps seen in the magnetic anomaly results given that the adjacent rocks are not necessarily more deformed by thick dykes than thin ones, this structure substantiates the fracture gaps seen in the magnetic anomaly results (Woodford and Chevallier, 2002).

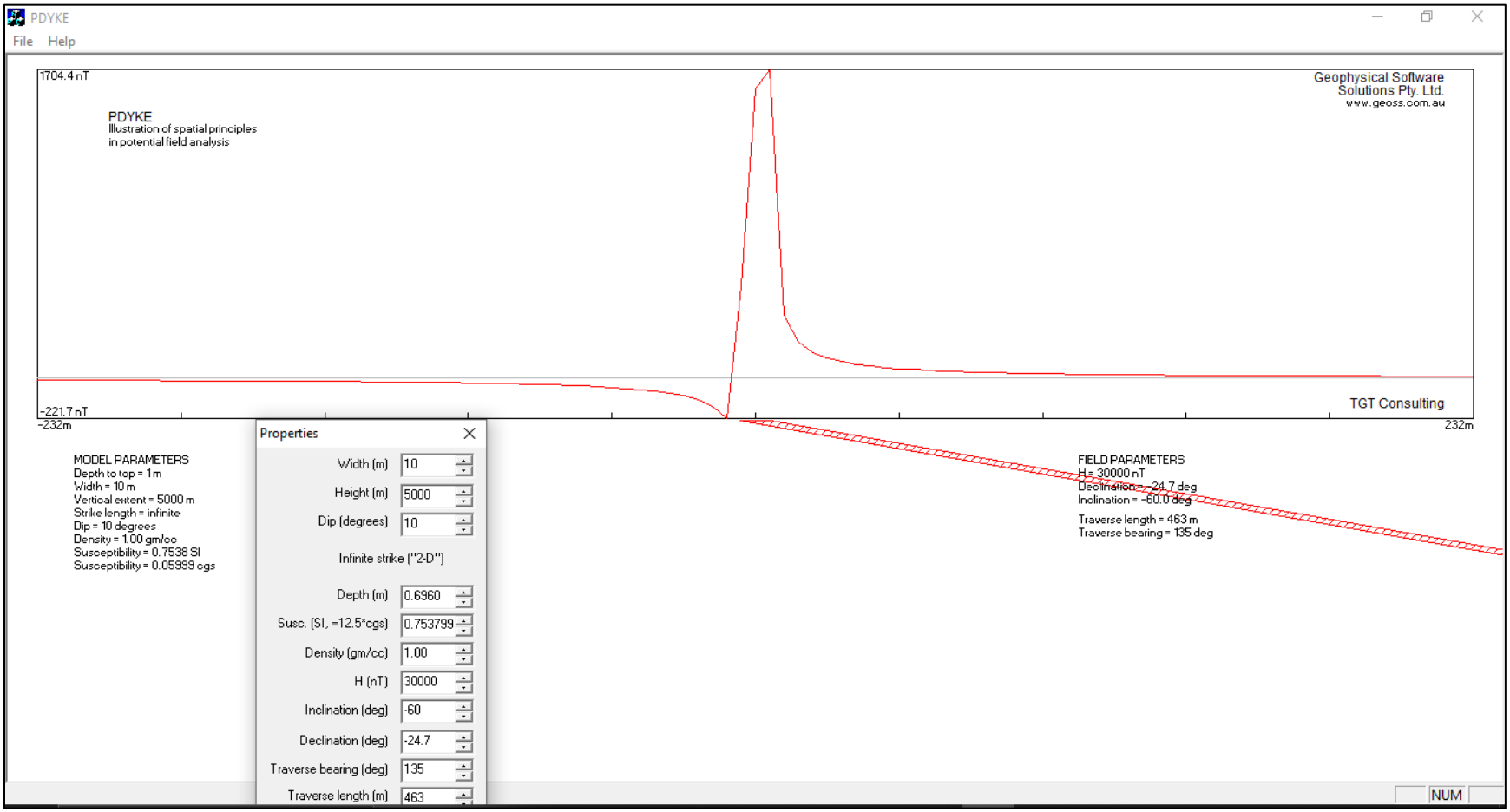



**Figure 30:** Forward modelling of the dyke body to reveal its geological structure and geometry using PDYKE software

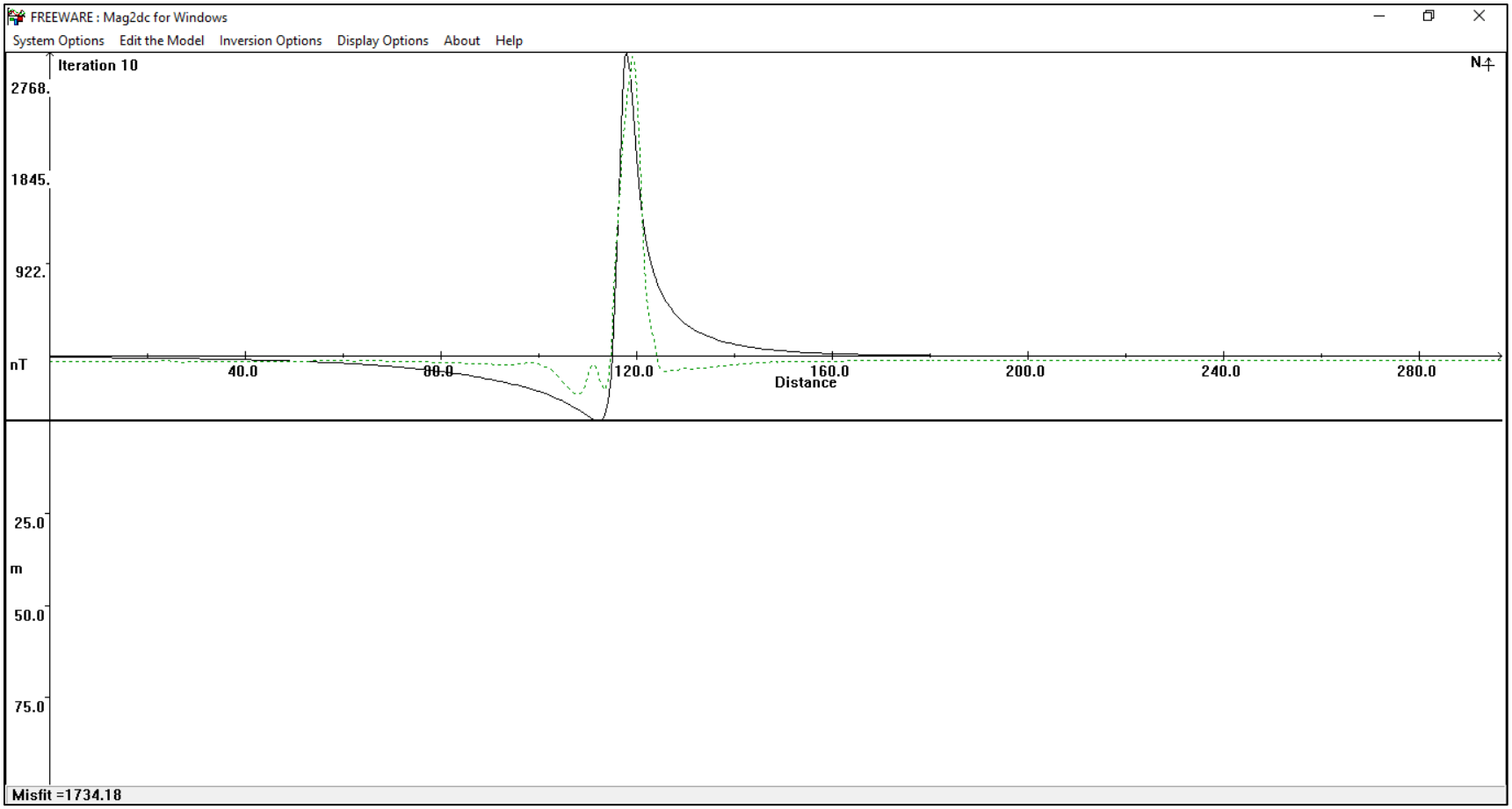



**Figure 31:** Forward model of the dyke fitted on the magnetic response observed in the field to estimate the width and depth using MAG2DC.

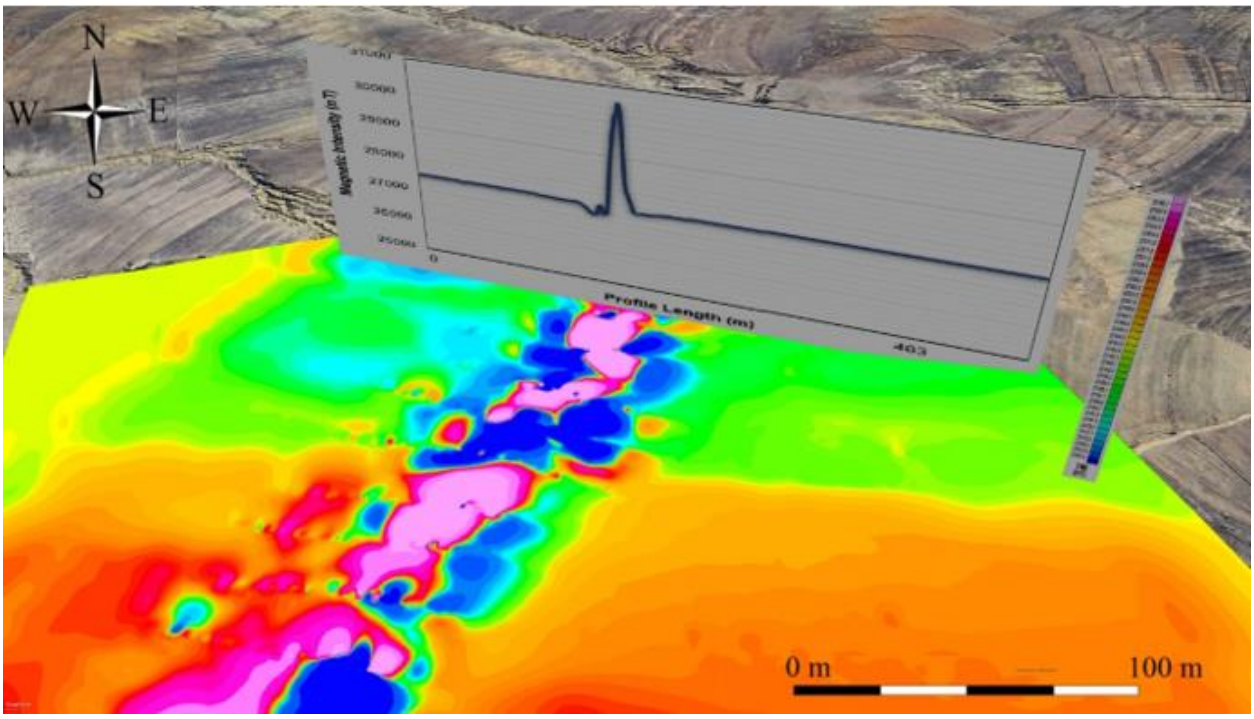



**Figure 32:** Interpretation of Total Magnetic Intensity with the magnetic anomaly profile of line-6 overlain on Google Earth.

## 5.3. Groundwater flow properties of dolerite dykes

### 5.3.1. Groundwater flow direction

The arc-hydro tool is used to analyse and characterise both the surface and subsurface water flow drainage models, with the DEM and IDW interpolation of the boreholes as the main input functions, respectively. The relationship between the drainage pattern and geological features was emphasized and explored by Garcia and Herail (2005), this relation significantly plays a role in water flow directions, accumulation, and groundwater occurrence in general within an area. The dykes intruding the sedimentary formations that are widespread in this study area are among the geological features which create relief and generate fractures on the adjacent lithologies, which further enhances surface and subsurface water flows, thereby allowing the use of the drainage models.

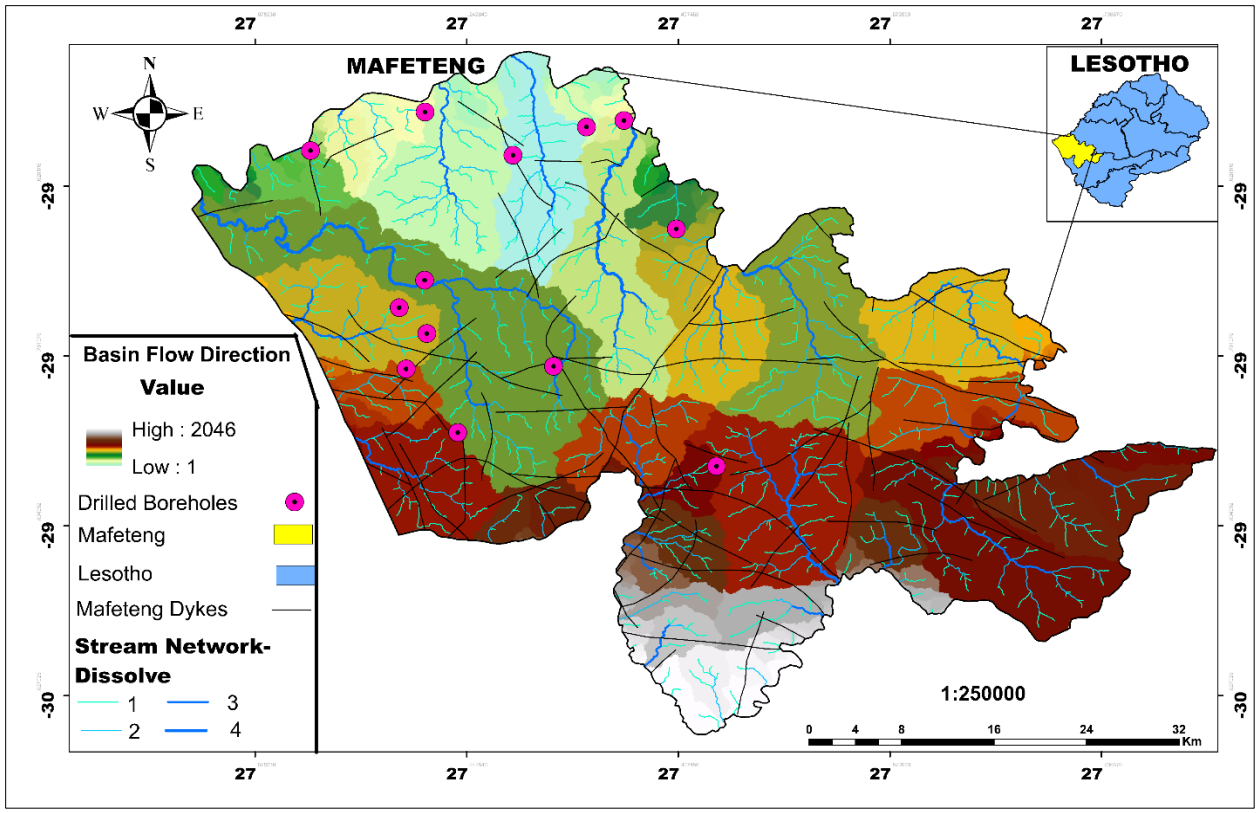



**Figure 33:** Mafeteng drainage basin flow map delineated from identifying ridge and relief-like lines and pour points from the study area. Shown also are the dykes distribution and locations of the drilled boreholes used as case studies concerning the drainage flow model derived from DEM Arc-Hydro Tool in ArcGIS.

The results from Figure 33 show the spatial distribution of the sub-basins with low to high basin flow values. The majority of the boreholes and dykes occupy intermediate flow values. The process of constructing these sub-basins involved locating the edge's pour points, which are places where water may potentially overflow from a sink, thereby determining the contributing area above each pour point (Esri, 2021). In addition, the figure above displays the outcomes of the linear stream network created from the sub-basin cells with higher total flow accumulation. The cells of high accumulation flow that are picked and given a threshold value of 1200 yield stream networks 1, 2, 3, and 4 as shown above. These linear stream networks are then defined by the cells that flow into these high accumulation flows of more than 1200. Using the 1200 threshold value from the established stream networks, a flow accumulation map is created across all the dyke sites as shown in Figure 34.

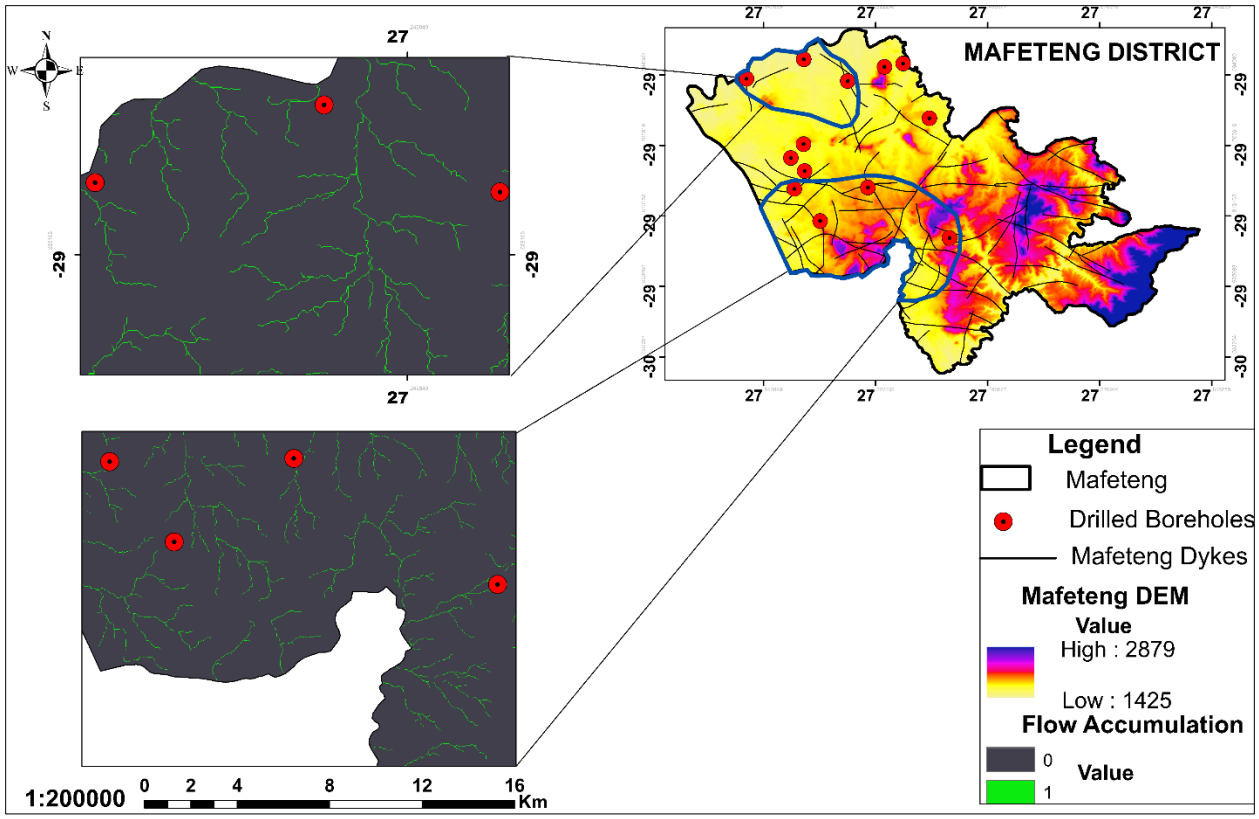



**Figure 34:** The flow accumulation maps for the selected hydrogeological boreholes. [A] shows flow accumulation for boreholes sited on the dykes at Thabana Mohlomi, Ha Lenonyane, and Ha Mofota villages. [B], flow accumulation for boreholes sited on the dykes at Qalabane, Matlapaneng, Ha Lumisi, and Malumeng. Flow accumulation value of 0 and 1 shows no flow and presence of flow respectively.

Groundwater depth (SWL) is usually impacted by the degree of interaction between the percolating surface water and any geological structure functioning as a channel of water from the surface into the subsurface. Therefore, by using an IDW geostatistical method to interpolate the 13 boreholes, a static groundwater level map for the Mafeteng study area was created (figure 35). According to Zouhri and Armand (2019), an IDW geostatistical approach to interpolation procedures enables the creation of surfaces from measured points with greater accuracy depending on the degree of similarity. The interpolation output was then utilized as an input function to ascertain the direction of groundwater flow from the selected boreholes, which were located in different dyke locations. The data is presented in Table 1 below with the surface elevations included.

**Table 1:** The descriptive summary of the drill boreholes previously constructed, their geographic locations, elevation, depth to water, and static water level within the study area.

| Drill-Boreholes | Coordinates | | Elevation (m) | Depth to water (m) | Static Water Level (m.a.s.l) |
|---|---|---|---|---|---|
| | Longitude | Latitude | | | |
| Boluma-Tau | 27.21176 | -29.7434 | 1606 | 7.02 | 1598.98 |
| Ha Lumisi | 27.31032 | -29.7691 | 1675 | 4.55 | 1670.45 |
| Ha Mofota | 27.21039 | -29.5699 | 1531 | 0.1 | 1530.9 |
| Ha Maoela | 27.21007 | -29.7016 | 1599 | 0 | 1599.00 |
| Ha Mofo | 27.33599 | -29.5816 | 1618 | 3.23 | 1614.77 |
| Malumeng | 27.43711 | -29.8474 | 1761 | 5.58 | 1755.42 |
| Qalabane | 27.19571 | -29.7711 | 1620 | 3.15 | 1616.85 |
| Matlapaneng | 27.23587 | -29.821 | 1669 | 19.76 | 1649.24 |
| Thabana Mohlomi | 27.12132 | -29.6001 | 1543 | 14.4 | 1528.6 |
| Ha Mohlehli | 27.19034 | -29.7232 | 1578 | 0.79 | 1577.21 |
| Malimong | 27.4059 | -29.6615 | 1653 | 0.36 | 1652.64 |
| Tshoeneng | 27.36511 | -29.5765 | 1505 | 3.17 | 1501.83 |
| Ha Lenonyane | 27.2788 | -29.6037 | 1560 | 6.84 | 1553.16 |

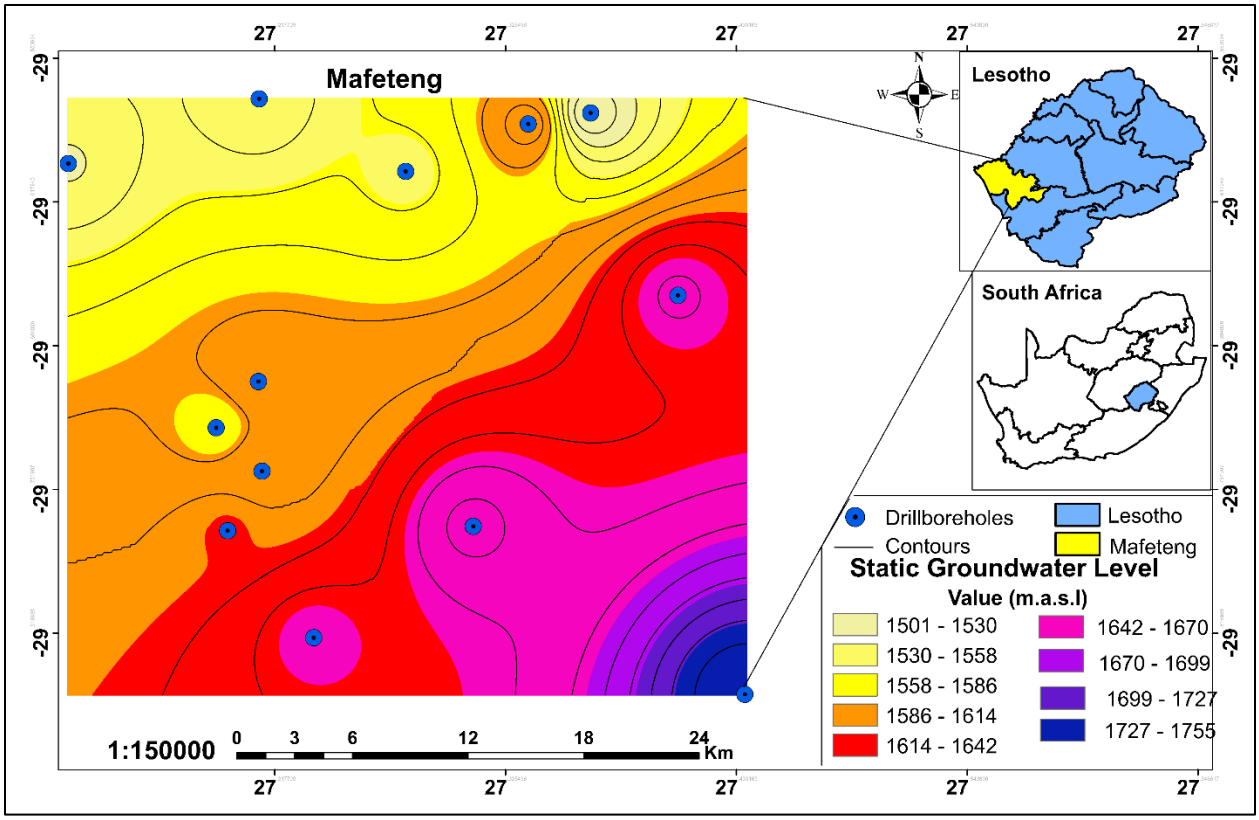



**Figure 35:** Spatial distribution of the groundwater level contour map and the locations of the selected hydrogeological boreholes, derived by IDW interpolation and D8 algorithm in ArcGIS.

Figure 35 shows the shallowest zones and deepest zones, with the latter existing in the southeastern part of the study area recording values between 1727-1755 m.a.s.l of static groundwater level, and the shallow zones towards the northwestern fringes of the area recording values between 1530-1558 m.a.s.l. In addition, flow direction maps from both the shallow and deepest static groundwater zones were created to determine the direction of groundwater flow from the area, through the 13 interpolated boreholes after the highs and lows of SWL by employing the D8 algorithm as explained in Chapter 4. The direction coding (flow direction grid code) is defined by the numbers 1, 2, 4, 8, 16, 32, 64, and 128 which correspond to E, SE, S, SW, W, NW, N, and NE directions respectively. The groundwater flow directions from both Ha Lenonyane and Thabana Mohlomi sites depict a radial flow, while the Qalabane and Ha Lumisi groundwater flow direction is towards the north direction as shown in Figures 36 and 37.

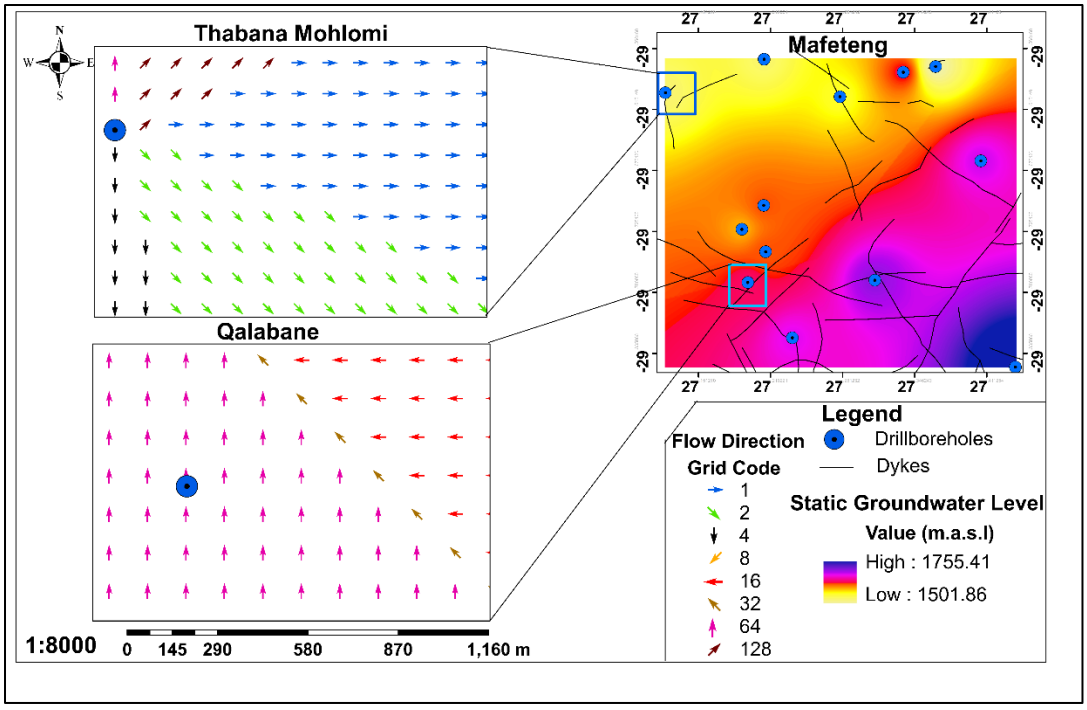



**Figure 36:** Flow direction map from the villages, Thabana Mohlomi and Qalabane which fall under the shallow and intermediate zones of static groundwater level respectively. Highlighted also are the drill borehole locations and the dykes distribution along the SWL map.

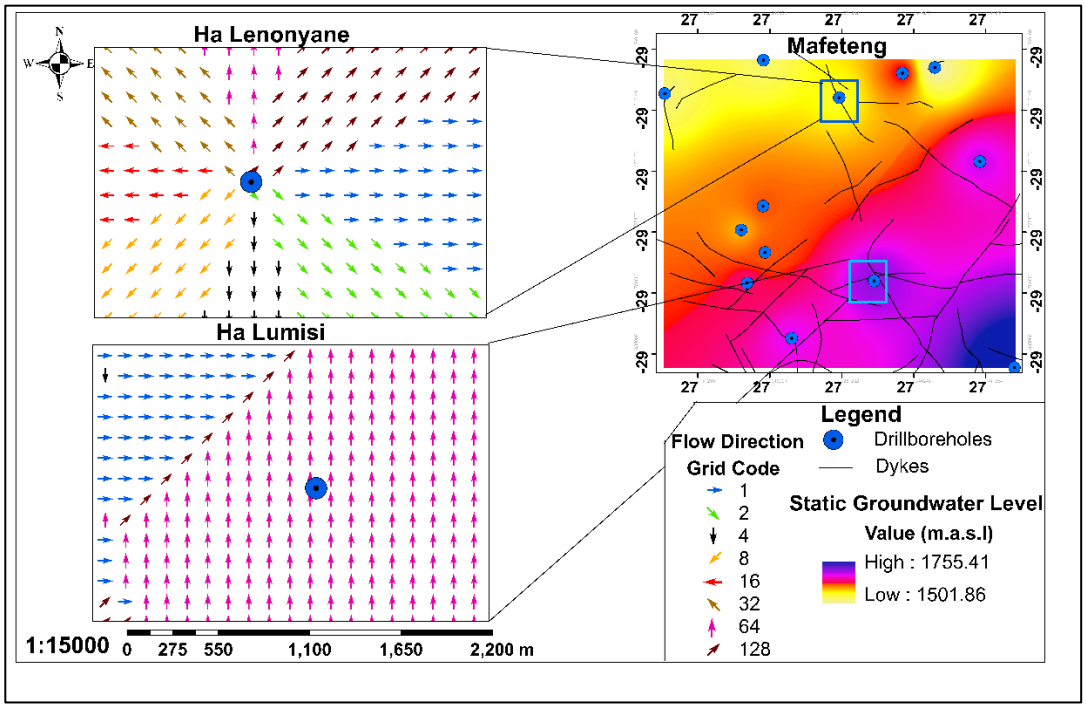



**Figure 37:** Flow direction map from the villages, Ha Lenonyane and Ha Lumisi which fall under the shallow and deepest zones of static groundwater level respectively. Highlighted also are the drill borehole locations and the dykes distribution along the SWL map.

The preceding sub-section conceptualises the geological setting and the development of the dykes in the Mafeteng area concerning the water flows about their observed and analysed geophysical attributes. Water often flows from high to low elevations, perpendicular to the equipotential in the steepest direction. The dykes occupying most of the intermediate basin flow values in Figure 33 are located in the district's lowlands, where the hydraulic gradient is often not very steep resulting in little possibility of surface flows and accumulation. However, according to theory, it is still believed that the surface water that is collected flows preferentially along the edges and into the topographic depressions in the fracture systems of the dyke (Babiker and Gudmundsson, 2004). Given a flow accumulation threshold of 1200 from the grid cells (extracted from the DEM) with potentially high accumulation flow, dyke locations showing a no-flow accumulation in Figure 34 are thought to experience minimum hydraulic gradient with minor relief in their structure, which could be due to the current weathering and erosion. The radial flow experienced in some dyke locations is possibly before the experience of the boundary conditions.

The static groundwater level maps created using information from Table 1 aid in predicting and understanding the flow directions through the local groundwater system at different dyke locations. The hydraulic head is assumed to follow the topography, as described by Babiker and Gudmundsson (2004). The fact that the static groundwater level in the 13 borehole locations varies therefore indicates and ascertains that the Mafeteng District’s groundwater occurs in a variety of topographic features some of which possibly result from the dykes. Based on the horizontal groundwater flow directions in Figures 36 and 37, Qalabane and Ha Lumisi indicate a northward groundwater flow direction, it is perceived that the recharge areas are in the south of the two respective dyke locations. The radial flows at Ha Lenonyane and Thabana Mohlomi however make it difficult to determine the specific discharging and recharging zones.

Furthermore, it is possible to understand the recharge areas for pollutants that may enter the dyke-related aquifer by using the known flow directions that describe the groundwater flows at different dyke sites. This also could help ascertain that there are as few contaminants entering the groundwater system in the lowlands and foothills of Mafeteng by tracing the groundwater contaminants, which tend to flow in the direction of groundwater.

### 5.3.2. Groundwater Flow Behaviour

This section analyses pumping test data from the drilled boreholes in the dyke locations from the Mafeteng District. Initially, the analysis is from a selected place where the geophysical attributes and geometry of the dyke were ascertained and characterised, thus from the Qalabane site. Then, followed by an analysis in places where both the surface and sub-surface flow and accumulation characterisations have been done as per the previous sections.

Pumping tests are the most widely used method for estimating the hydrogeological parameters of rock Formations from a given aquifer and in determining groundwater flow regimes hence, the results from this section enable the study to further achieve its second objective of evaluating the hydrogeology of the dyke related aquifer in Mafeteng, Lesotho. This section includes the derivative analysis of the drawdown data from each of the chosen locations within a dyke-related aquifer with the results summarised in Table 2. This was to characterise any flow regimes that may exist for the baseline flow characteristics around the drilled wells. The diagnostic plots employed in this study include the drawdown vs log time (Semi-log Plot) and the log drawdown vs log time (log-log Plot).

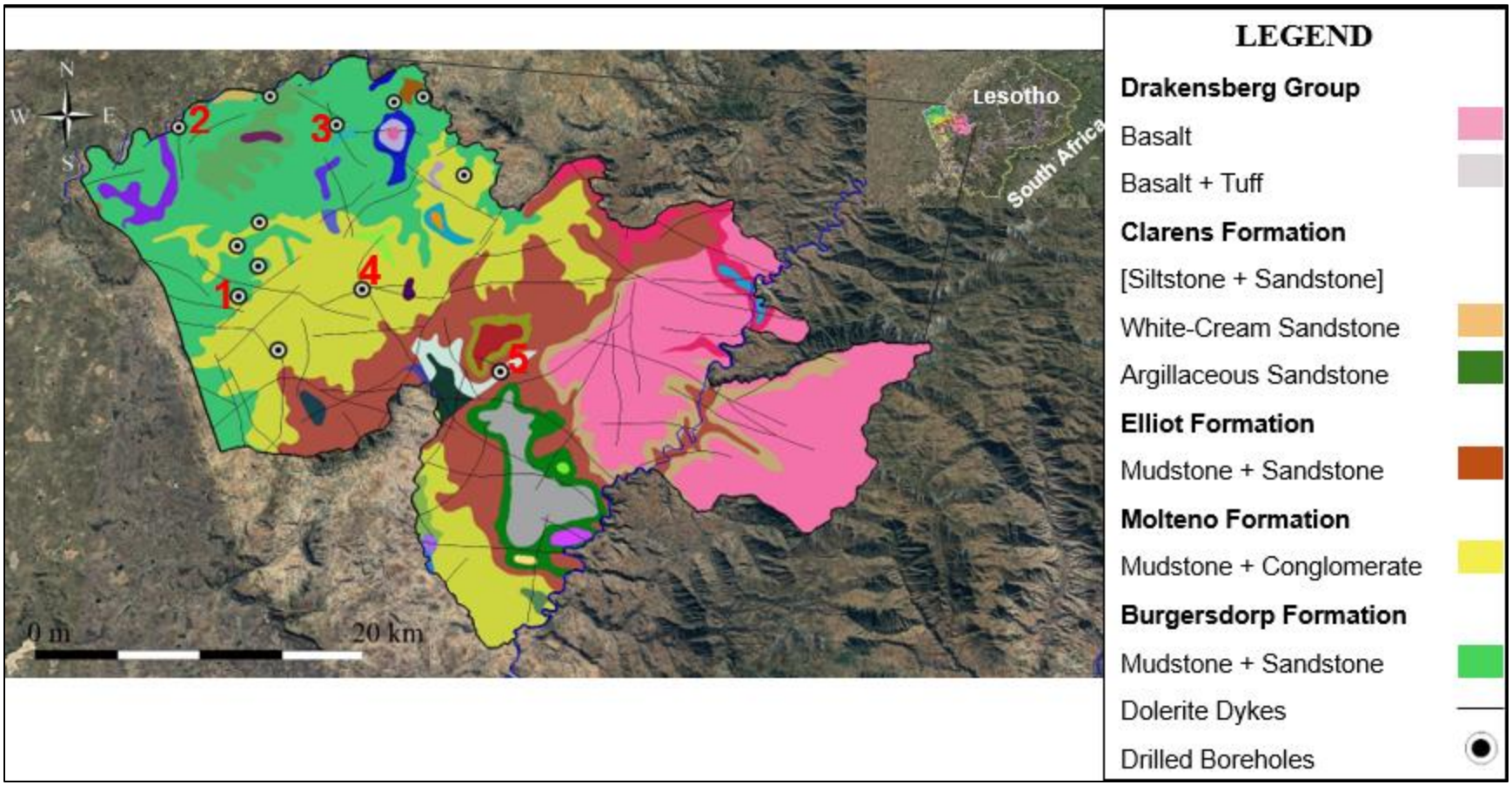



**Figure 38:** Geological extraction of Mafeteng with the locations of the drilled boreholes used as case studies in the pumping analyses for this research 1=Qalabane, 2=Thabana Mohlomi, 3=Ha Lenonyane, 4=Ha Lumisi, and 5=Malumeng

### 5.3.2.1. Qalabane

The water level before the start of pumping (SWL) was 3.15 m for the Qalabane drill borehole (Figure 38 for location). After 720 minutes (12 hours) of constantly pumping at the rate of 1.1 l/s, the total drawdown experienced was 23.06 m, measurements of a well's recovery period were taken after the pumping stopped (Figure 39). The semi-log plot shows a nonlinear relationship between the drawdown and the log time elapsed, but it tends to be linear from intermediate to late pumping times (Figure 40). There are quite various slopes observed in the log-log plot. Additionally, early on in the pumping process, during the 4$^{th}$ and 5$^{th}$ minute (Figure 41), there is a double porosity dip while radial characteristic flow predominates during intermediate-late times of pumping.

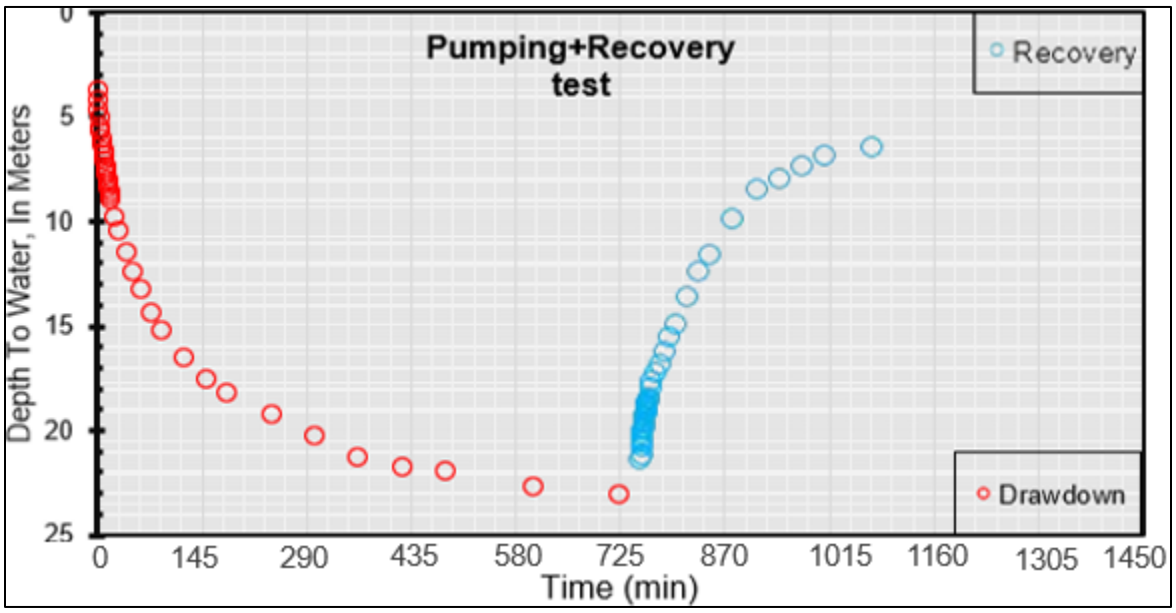



**Figure 39:** The Borehole hydrograph for the CDT that was drilled at Qalabane.

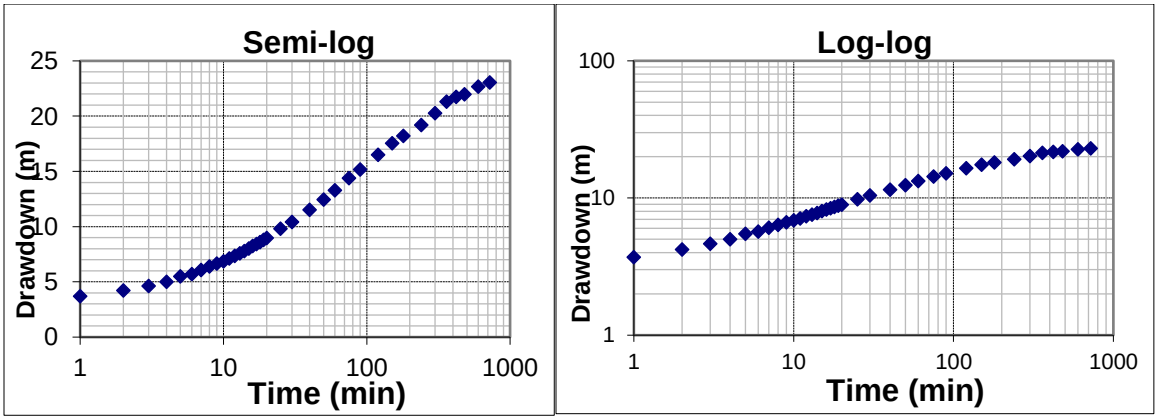



**Figure 40:** The diagnostic plots for the Qalabane borehole. Semi-log diagnostic plot and log-log plot.

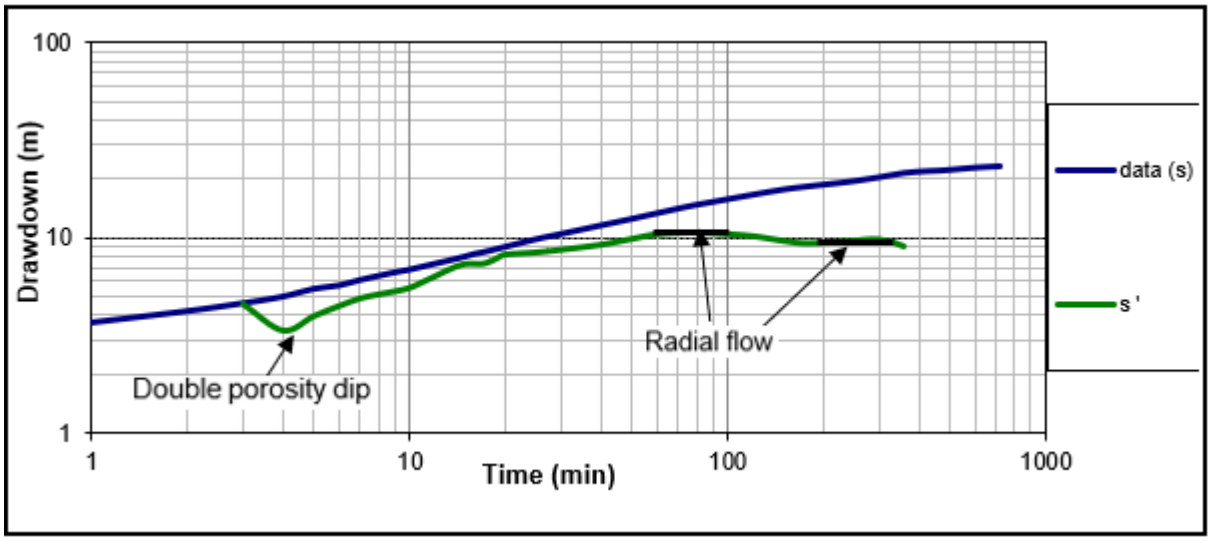



**Figure 41:** Derivative plot for the Qalabane borehole. The traditional drawdown data is plotted with the derivative data against time elapsed.

### 5.3.2.2. Thabana Mohlomi

For the borehole drilled at Thabana Mohlomi (Figure 38), the water level before the start of pumping was recorded as 14.4 m. Pumping was done constantly at the rate of 0.6 l/s for 720 minutes and a total drawdown of 27.5 m was reached. Thereafter, measurements of the recovery data were also taken after the pumping of the borehole stopped. The curve appears to flatten significantly during an intermediate time, as seen in the semi-log plot in Figure 42. A double porosity dip is shown at both early and late times in the derivative plot (Figure 43).

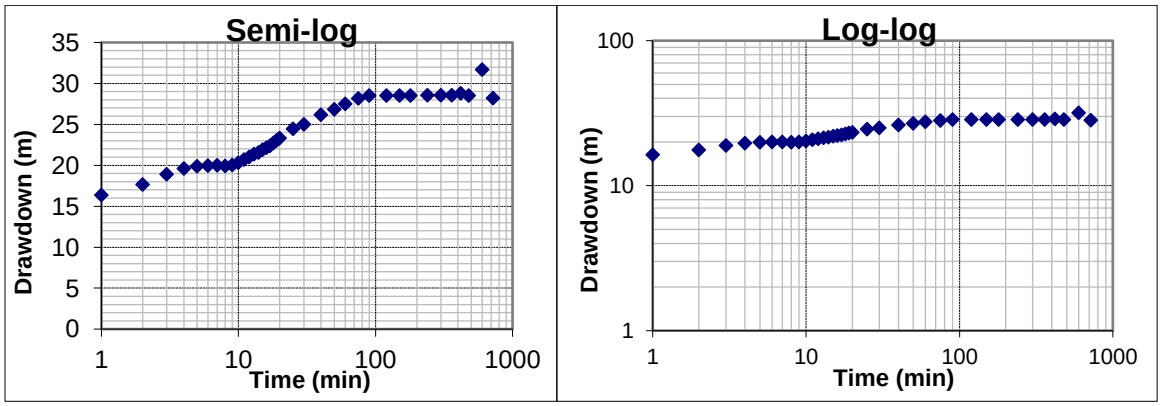



**Figure 42:** Diagnostic plots for pumping test at Thabana Mohlomi. Semi-log and log-log plot.

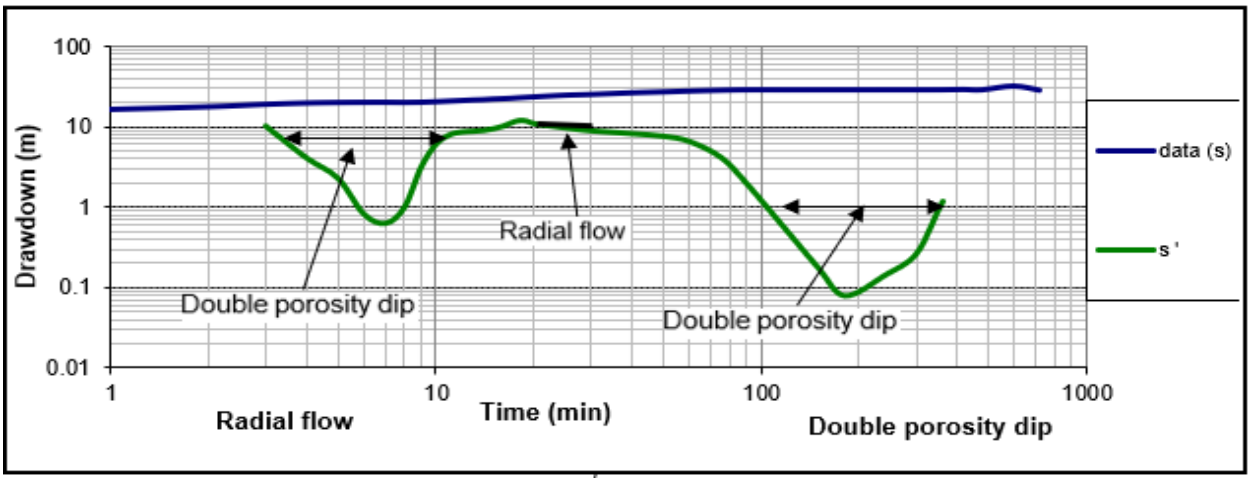



**Figure 43:** Derivative plot for the drill borehole at Thabana Mohlomi. The traditional drawdown data is plotted with the derivative data against time elapsed.

### 5.3.2.3. Ha Lenonyane

The drilling site at the dyke location at Ha Lenonyane (Figure 38) indicated a 6.84 m of water level before the pumping of groundwater. The major water strike was at 42 m. The total drawdown reached by the borehole was 31.25 m after being subjected to a constant pumping rate of 1 l/s for 720 minutes. After the pumping phase, groundwater was left to recover. The slopes indicated in the log-log plot (Figure 44) of the borehole drilled at Ha Lenonyane show 3 different flow characteristics. The derivative plots show a double porosity dip occurring exclusively during the early pumping phases. The radial flow dominance at Ha Lenonyane during an intermediate time is similar to that of Thabana Mohlomi, this is attributed to the flattening of the curve as shown in the log-log plot. The possibility of a recharge boundary at a late time is observed in Figure 45.

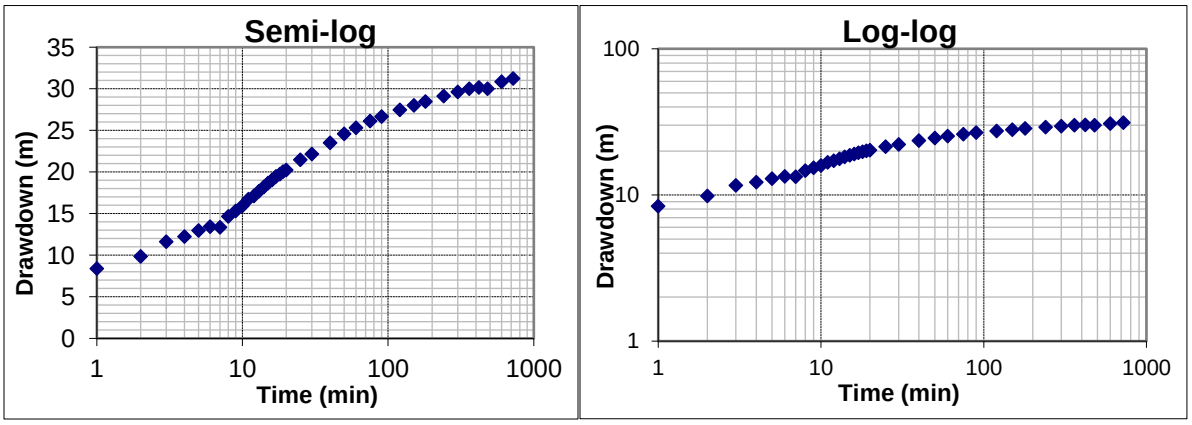



**Figure 44:** Diagnostic plots for pumping test at Ha Lenonyane. Semi-log and log-log plots.

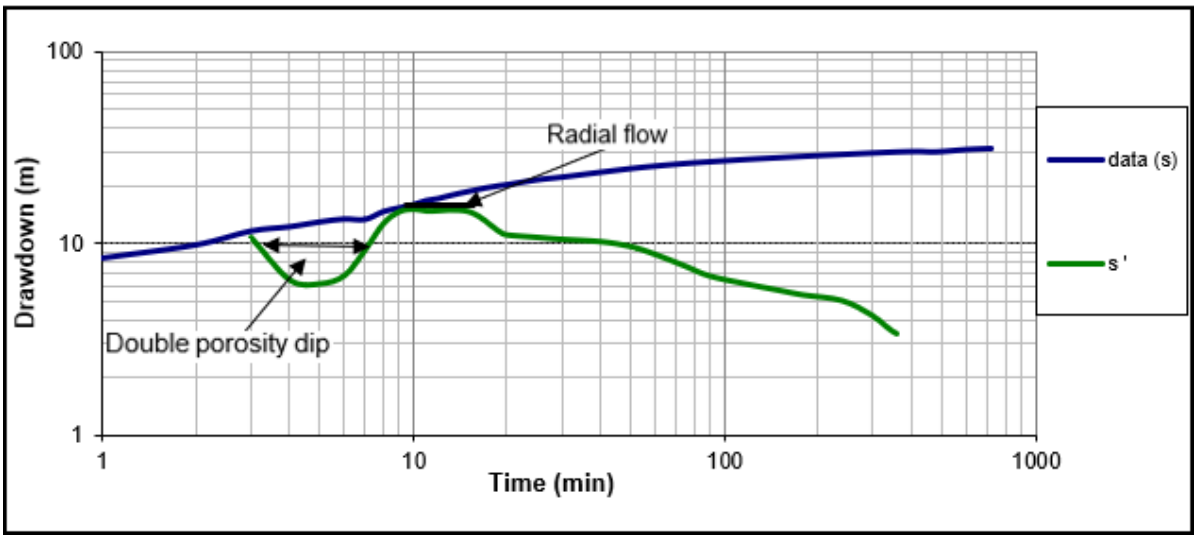



**Figure 45:** Derivative plot for the drill borehole at Ha Lenonyane. The traditional drawdown data is plotted with the derivative data against time elapsed.

### 5.3.2.4. Ha Lumisi

Drilling at Ha Lumisi dyke location (Figure 38) revealed a water level of 4.55 m before the start of pumping. At 36 m, the major water strike was reached. Groundwater was pumped constantly at the rate of 1 l/s for 720 minutes. After that, the borehole was allowed to recover, and the residual drawdowns were measured. Similar to those at Qalabane, the semi-log and log-log plots at Ha Lumisi exhibit non-linear drawdown-time relationships in the early times but are linear eventually at the late phases of pumping (Figure 46). The drawdown data and change in drawdown graphs at Ha Lumisi seem to be parallel towards the intermediate-late times of pumping. Additionally, at the early time, the double porosity dip is encountered, this is at times 3$^{rd}$-5$^{th}$ minute followed by minor oscillations (Figure 47).

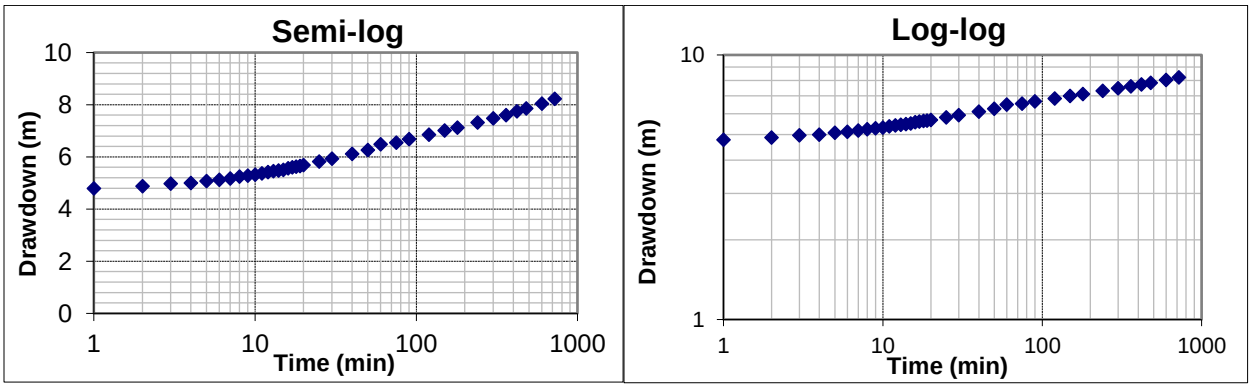



**Figure 46:** Diagnostic plots for pumping test at Ha Lumisi. Semi-log and log-log plots.

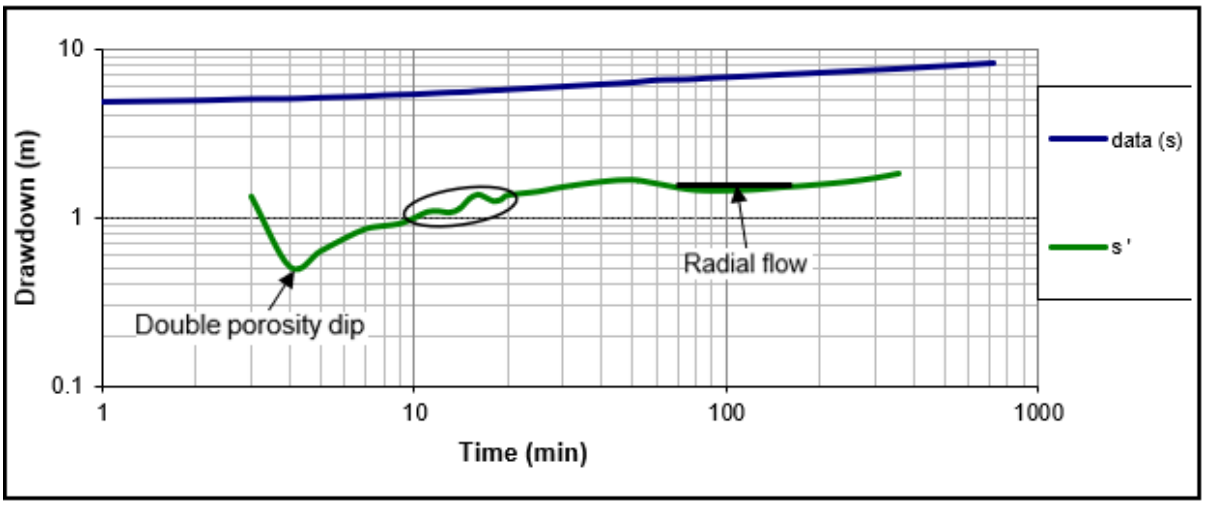



**Figure 47:** Derivative plot for the drill borehole at Ha Lumisi. The traditional drawdown data is plotted with the derivative data against time elapsed.

### 5.3.2.5. Malumeng

At Malumeng, the dyke is observed to be intruding into the Clarens, Elliot, and Molteno Formations (Figure 38). Drilling at this site showed a water level of 5.58 m before pumping with a major water strike at 56 m. After 12 hours of 1.1 l/s pumping rate, the borehole reached a total drawdown of 31.08 m. After the pumping stopped, residual drawdowns were recorded after the borehole was given time to recover. It can be observed (Figure 48 - 49) that the groundwater flow characteristics from the semi-log and derivative curves at the Malumeng borehole behave somewhat differently from the preceding sites. Towards the early-intermediate periods, the drawdown data steepens but thereafter adapts itself in the later times. At this site, the diagnostic plots indicate how radial flows predominate at the later pumping times, whereas the linear flows dominate from early to intermediate times.

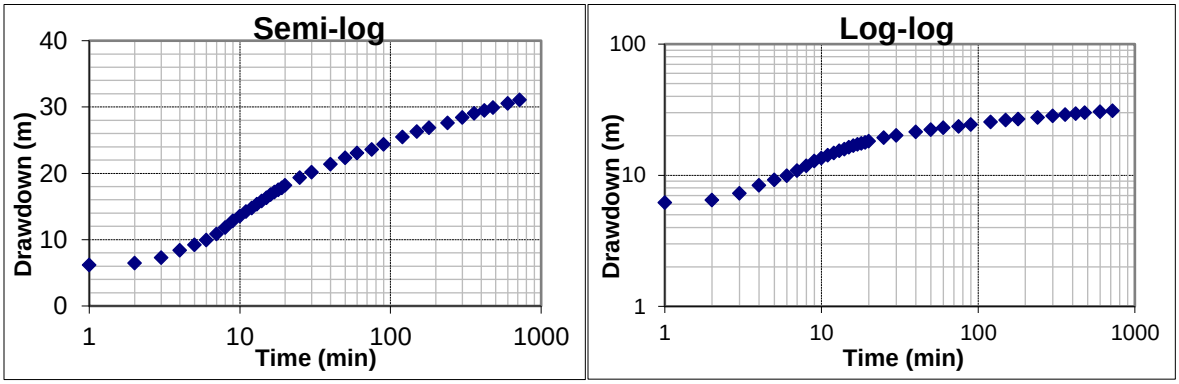



**Figure 48:** Diagnostic plots for pumping test at Malumeng. Semi-log and log-log plots.

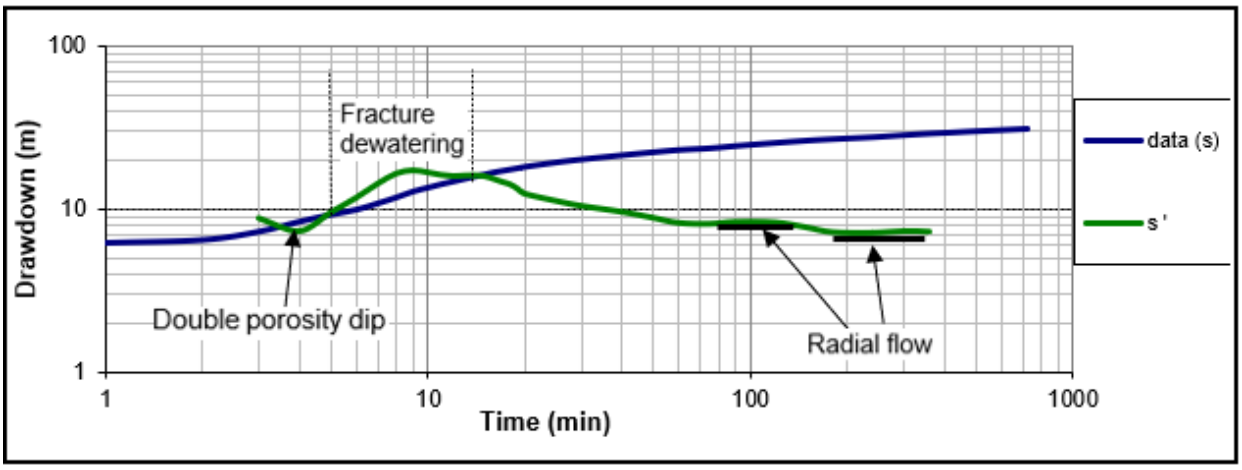



**Figure 49:** Derivative plot for the drill borehole at Malumeng. The traditional drawdown data is plotted with the derivative data against time elapsed.

**Table 2:** Summarise the results derived from the derivative analysis of the pumping test in the five dyke-locations.

| Dyke-Location | Borehole Depth (m) | Analysis | Log Derivative |
|---|---|---|---|
| Qalabane | 80 | Derivative | 0.24 |
| Thabana Mohlomi | 81 | Derivative | 0.10 |
| Ha Lenonyane | 80 | Derivative | 0.21 |
| Ha Lumisi | 45 | Derivative | 0.09 |
| Malumeng | 80 | Derivative | 0.29 |

The preceding sub-section assessment of the hydrogeology of the dyke-related aquifer evaluated the transient drawdown response to pumping at various dyke sites shown in Figure 38. Therefore, it should be noted that ideally, the diagnostic and derivative graphs have nothing to do with either the laminar or turbulent flow conditions. This study's data analysis of the drawdown derivative versus elapsed time during pumping is thought to improve the interpretation of the pumping test because they are sensitive to flow conditions and slight variations in drawdown, making it possible to recognise and understand the heterogeneity within the non-uniform aquifer system (Gringarten, 2008). Additionally, the interpretations of the derivative plots consider the temporal interpretation of the pumping test data. According to Leveinen (2001, 2000), the early-stage pumping response is usually governed by wellbore storage, the intermediate-stage response emphasises the characteristics of the aquifer, and the late-stage responses indicate boundary effects. This does not, however, negate the possibility that aquifer features themselves might offer a multi-stage response. Drawing on the data from the derivative plots within the dyke locations in the focal area, the FC Programme computed the log derivative values (Table 2). This log derivative value shows the relative aquifer's quality. According to Van Tonder *et al.* (2001), the following statement relates to the log

derivative value, log derivative = 0.5 for a single fracture (limited fracture network), log derivative = 0.25 for a good fracture network, and log derivative ≤ 0.1 for a good – very good fracture network.

The double porosity dip is experienced at distinct stages of pumping based on the pumping tests conducted at several dyke sites within the research area, this indicates a fractured system with two zones of opposing flow and hydraulic characteristics. These two zones are the fractures which significantly contribute more to porosity; hence they are permeable but have limited storage capacity. In contrast, the other zone is the matrix blocks which contribute somewhat to porosity but have a substantial storage capacity (Moonen and Carmeliet, 2013). At Qalabane, Figures 40-41, the double porosity dip in the early phases of pumping suggests that pumped groundwater mostly originates from the limited storage of the fracture zone during the $4^{th}$ and $5^{th}$ minute. With a log derivative value of 0.24 at Qalabane, the dyke intruding into the Burgersdorp and Molteno sedimentary formations is regarded as having a good fracture network in the semi-confined aquifer.

As at Qalabane, Thabana Mohlomi dyke location indicates that drilling was done through a fractured system, as shown by the double porosity encountered both at the early and late stages of pumping. However, at Thabana Mohlomi, an infinite radial flow only appears during the intermediate pumping phase (Figure 43) as indicated by the first logarithmic derivative of drawdown in a borehole categorised by Van Tonder *et al.* (2001). Drilling in the dominant Tarkastad Subgroup sandstone may be the cause of this radial flow (Igwebuike *et al*., 2023). Alternatively, the intermediate phase at Thabana Mohlomi may also indicate a phase of groundwater transition when the matrix feeds water into the fractures at an increased rate considering a pseudo-steady state (Kruseman and de Ridder, 1991). The log derivative value of 0.1 from the derivative analysis at Thabana Mohlomi suggests the dyke-related aquifer as having a good – very good fracture network from the unconfined aquifer system. The dyke location at Ha Lenonyane is implied to have flow regimes (Figures 44 - 45) that are quite similar to those reported at Thabana Mohlomi. The primary cause of this is the comparable mudstone and sandstone lithologies found in these locations, which are part of the same geological unit, the Tarkastad Subgroup north of the Mafeteng District, and that drilling was conducted presumably on locations with similar dyke parameters.

A double porosity is encountered in the early times of pumping as well at Ha Lumisi. As Igwebuike *et al.* (2023) have stated, the double porosity dip's trough might be understood as periods when water flows from a highly permeable layer. This is comparable to how it has been experienced even in other dyke sites drilled. The slight oscillations seen in Figure 47 during an intermediate phase further characterise the dyke-related aquifer at Ha Lumisi. These oscillations show the Molteno Formation's distinct lithologies, sandstone, shale, and conglomerate, this is also evidence for geological layering of the geological units in the area.

Additionally, water seems to converge to the well when there is a modest stabilisation of drawdown during the late pumping stage. This might be facilitated by the big, rounded fragments of conglomerate intercalated within the very fine-grained shale of the Molteno Formation. The lowest log derivative value of 0.09, as shown from the derivative analysis at Ha Lumisi, is suggestive of an unconfined dyke-related aquifer with a very good fracture network.

At the Malumeng dyke location, Figures 48 – 49 show quite different aspects of groundwater flow behaviour. The only similarities with other locations are that the early pumping phase still features a double porosity dip, highlighting that we are dealing with a fractured dyke system, and an infinite radial flow also occurs after the conditions boundary in the late pumping phases. However, before reaching an intermediate phase where the matrix supplies water to the fractures, the drawdown data became steeper, implying dewatering of the fracture. This might also suggest the presence of a condition boundary during that pumping period. Subsequently, the drawdown steadily stabilises and reaches the point where water is pumped in the late stages from both the fracture storage and matrix. Lastly, according to Van Tonder *et al.* (2001) 's categorisation under the calculations in the FC Programme, the estimated log derivative value at Malumeng is 0.29, indicating an aquifer with a good fracture network.

## 5.4. Estimation of Aquifer Parameters

The hydrogeological characteristics from the dyke sites in the lowlands of the Mafeteng area are quantitively estimated for additional assessment of the hydrogeology of the dyke-related aquifer in Lesotho. Ha *et al.* (2020) underlined that the present method of predicting aquifer characteristics relies less on manual expertise and more on the use of optimal techniques in conjunction with analytical solutions and models to determine the most accurate estimates. In Lesotho's lowlands, estimating the aquifer's properties is significant not only for flow characteristics but also for groundwater resource management, evaluation, and utilisation. Comprehending these properties also facilitates the awareness of groundwater availability for subsequent decisions about groundwater supplies, particularly in Mafeteng's rural areas that heavily rely on groundwater. This research assessed the Transmissivity (T) and Specific Yield ($S_y$) parameters using the Time-Drawdown data from the pumping tests at the five dyke locations in Mafeteng. To conduct the assessment, the Flow Characteristic (FC) Programme was used.

The depth of the borehole, drawdown, amount of time since pumping began, and the result data of the recovery test is among the data collected from different dyke locations with varying geological features. The aquifer yield and hydraulic parameters of the dyke-related aquifer from this study are determined by matching the observed drawdown data to a straight line. Section 4.2.4 in the preceding chapter outlines the analytical assumptions that underpin this approach. Piscopo *et al.* (2023) defined the sustainable yield of a

borehole as the rate at which groundwater should be extracted, provided that the water level in a given borehole stays above a designated threshold. This parameter hence adds the baseline hydrogeology of the boreholes drilled in the target's area sedimentary Formations additionally, this helps the lowlands of the Mafeteng area in Lesotho with future groundwater management and policy. The Cooper-Jacob method was used in this study in the calculation of the sustainable yield based on the drawdown data (available drawdown inclusive). It is noted that the average sustainable yield from the FC programme can be used in the absence of boundary conditions information.

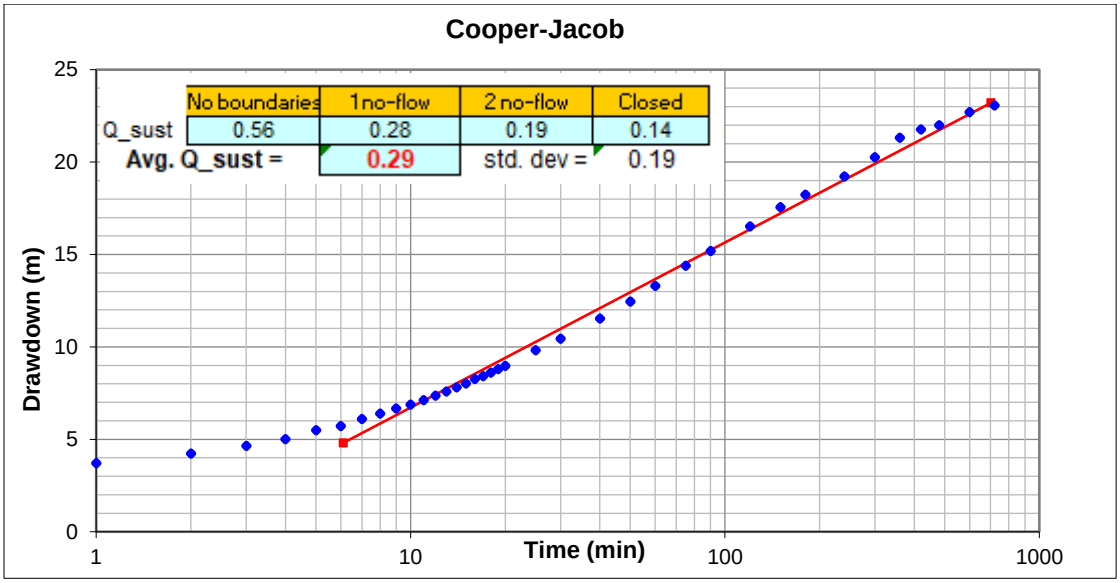



**Figure 50:** Cooper-Jacob curve matching of the borehole at Qalabane as extracted from FC Programme.

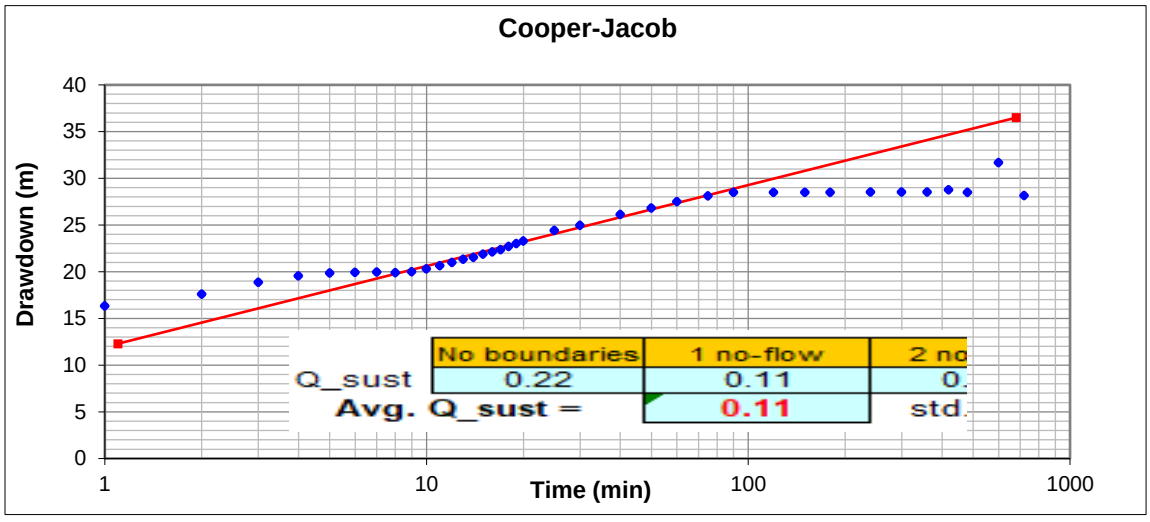



**Figure 51:** Cooper-Jacob curve matching of the borehole at Thabana Mohlomi as extracted from FC Programme.

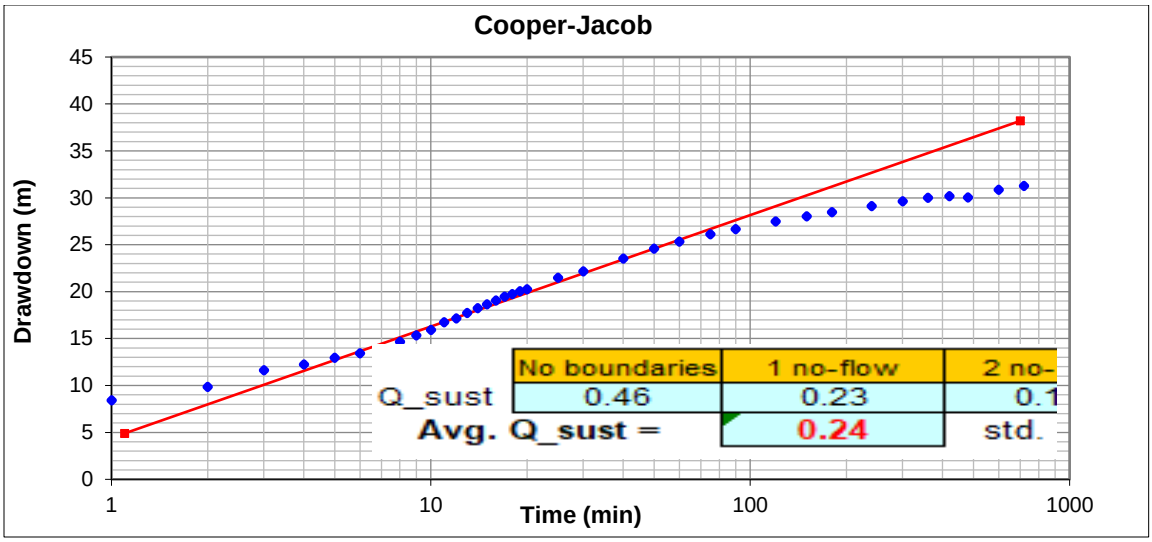



**Figure 52:** Cooper-Jacob curve matching of the borehole at Ha Lenonyane as extracted from FC Programme.

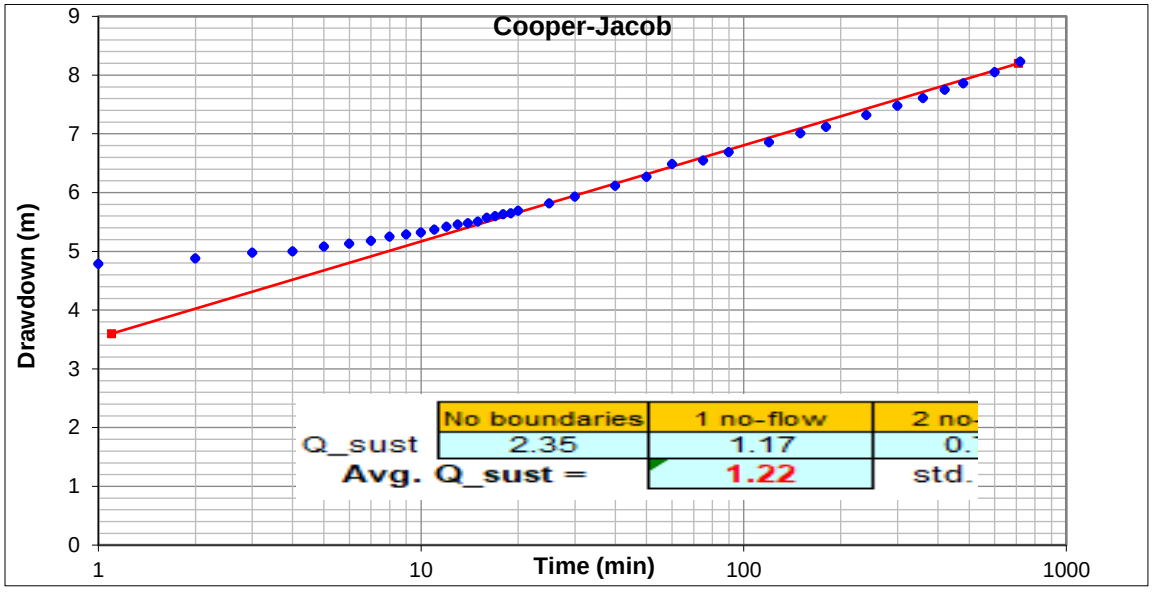



**Figure 53:** Cooper-Jacob curve matching of the borehole at Ha Lumisi as extracted from FC Programme.

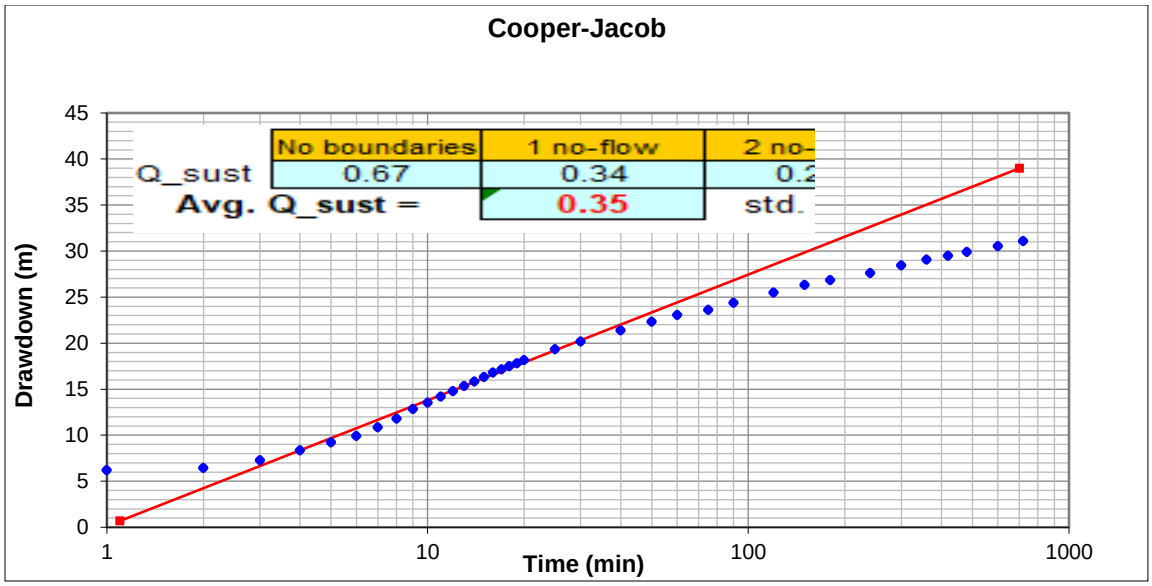



**Figure 54:** Cooper-Jacob curve matching of the borehole at Malumeng as extracted from FC Programme.

The borehole at Qalabane which occurs in the Molteno-Burgersdorp Formations produced an average sustainable yield value of 0.29 l/s (Figure 50). The borehole at Thabana Mohlomi located in the Burgersdorp Formation shows an average sustainable value of 0.11 l/s (Figure 51). Ha Lenonyane borehole which is also from the Burgersdorp Formation yielded an average value of 0.24 l/s (Figure 52). The borehole at Ha Lumisi from the Molteno Formation yielded an average sustainable yield value of 1.22 l/s, while the Malumeng borehole yielded 0.35 l/s of sustainable average yield, Figures 52 and 53 respectively. An estimated sustainable yield from the 5 boreholes drilled at three different dyke locations in Mafeteng shows a range of 0.11 – 1.22 l/s, with the lowest yield estimated at Thabana Mohlomi while the highest yield was from Ha Lumisi. The results further demonstrate a link between the calculated sustainable yield and transmissivity, whereby the high transmissivity values correlate with the high sustainable and average sustainable yield. The results from the Cooper-Jacob solution show transmissivity (T) values ranging from 1 – 10 $m^2$/day (Table 3).

**Table 3:** Cooper-Jacob results on estimated transmissivities at different dyke sites in Mafeteng, Lesotho.

| Dyke-Location | Geology (Formations) | Analysis Method | Transmissivity ($m^2$/day) |
|---|---|---|---|
| Qalabane | Molteno-Burgersdorp | Cooper-Jacob | 1.9 |
| Thabana Mohlomi | Burgersdorp | Cooper-Jacob | 1.1 |
| Ha Lenonyane | Burgersdorp | Cooper-Jacob | 1.3 |
| Ha Lumisi | Molteno | Cooper-Jacob | 9.7 |
| Malumeng | Clarens, Elliot, Molteno | Cooper-Jacob | 1.3 |

The pumping test results for the estimated transmissivities are correlated with recovery estimations from the boreholes drilled to ensure the validity of the predicted transmissivity (Figures 55-59). The recovery tests in this research are thought to be the best estimate for the estimated values as the recorded residual drawdown provides data collected during the period when the aquifer is not under stress from pumping, hence the water level rises naturally (Atangana, 2014). The results are then summarised as shown in Table 4.

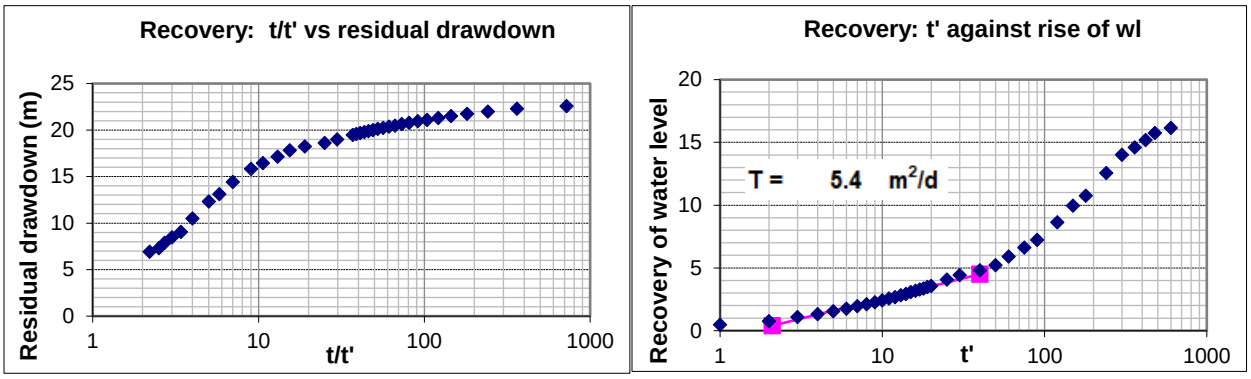



**Figure 55:** Recovery graphs: borehole drilled at Qalabane as extracted from the FC Programme.

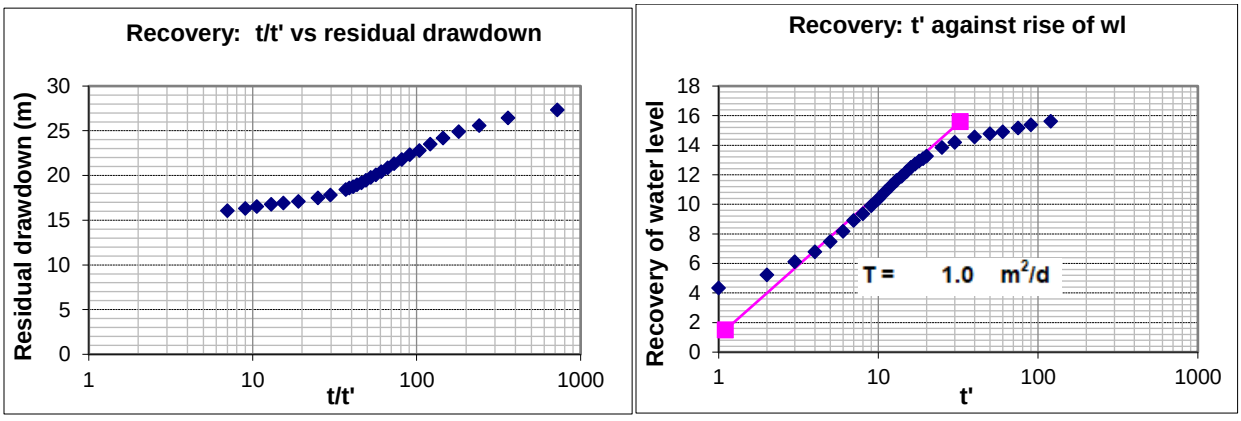



**Figure 56:** Recovery graphs: borehole at Thabana Mohlomi as extracted from the FC Programme.

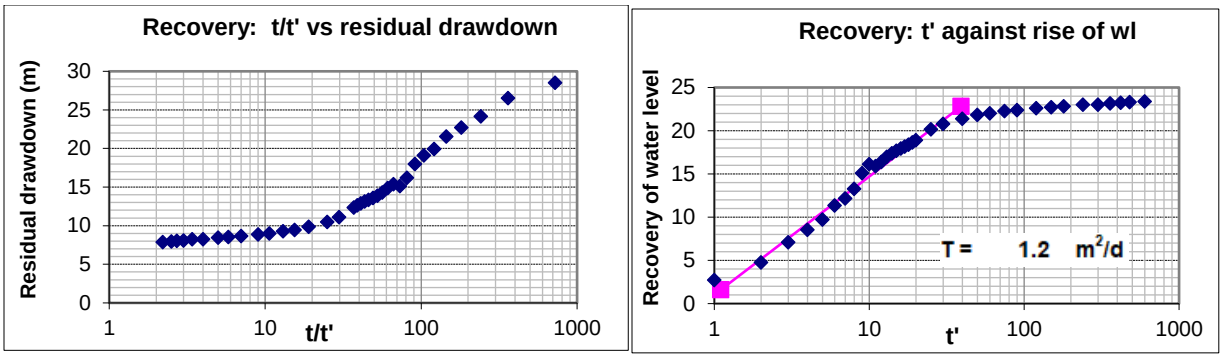



**Figure 57:** Recovery graphs: borehole at Ha Lenonyane as extracted from the FC Programme.

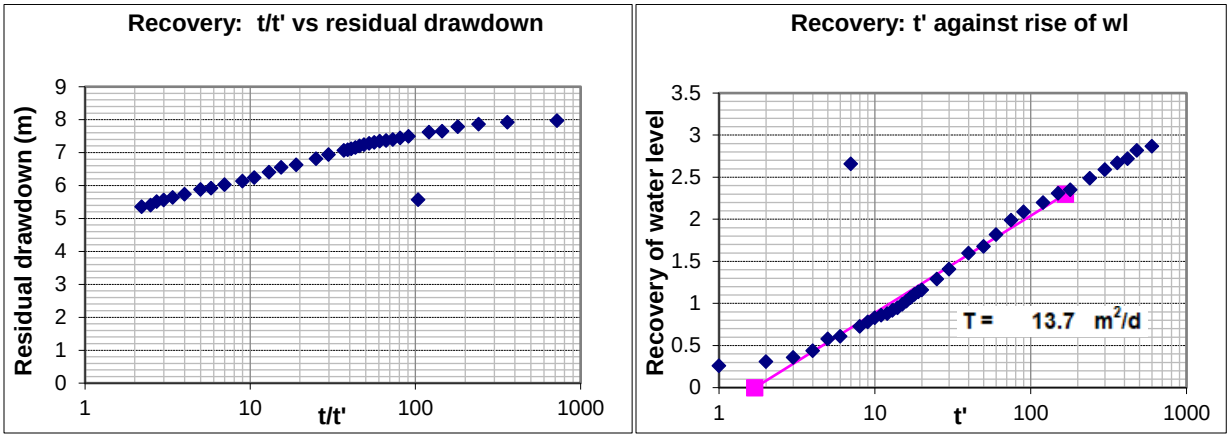



**Figure 58:** Recovery graphs: borehole at Ha Lumisi as extracted from the FC Programme.

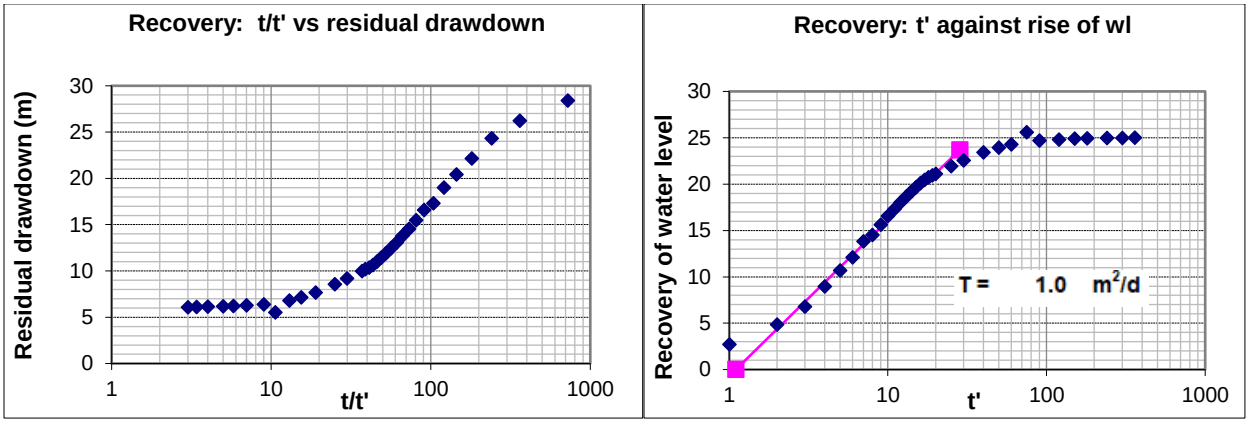



**Figure 59:** Recovery graphs: borehole drilled at Malumeng as extracted from the FC Programme.

**Table 4:** Estimated transmissivity results from the recovery test analysis at different dyke sites in Mafeteng, Lesotho.

| Dyke-Location | Geology (Formations) | Analysis Method | Transmissivity ($m^2$/day) |
|---|---|---|---|
| Qalabane | Molteno-Burgersdorp | Theis Recovery | 5.4 |
| Thabana Mohlomi | Burgersdorp | Theis Recovery | 1.0 |
| Ha Lenonyane | Burgersdorp | Theis Recovery | 1.2 |
| Ha Lumisi | Molteno | Theis Recovery | 13.7 |
| Malumeng | Clarens, Elliot, Molteno | Theis Recovery | 1.0 |

The results from the estimated aquifer parameters were intended to help achieve further the 2nd objective of this study. The parameters which were all estimated using the FC Programme, include transmissivity and sustainable yield. As per the geophysical attributes of the area, two zones of opposing hydraulic characteristics were derived from the focal study area where pumping tests were conducted. These zones are the fractures and the matrix, according to Moonen and Carmeliet (2013), the former has low storage but high transmissivity, whereas the latter has high storage but low transmissivity.

The highest transmissivity values at Ha Lumisi signify high porosity in the Molteno Formation as opposed to the Formations at other dyke locations. The Molteno Formation is dominated by the conglomerate. Since conglomerate has a coarser texture than the very fine-grained mudstone (Burgersdorp and Elliot Formations) and siltstone (Clarens Formation) at other dyke locations, this could potentially explain higher transmissivity values at Ha Lumisi. Zhang *et al.* (2016) ascertained that rocks with very fine-grained textures have the smallest porosity, in their study, they found that mudstone usually has a lower porosity than a conglomerate.

Smaller withdrawal rates for local water supply (private consumption) can be suggested at Qalabane, Thabana Mohlomi, Ha Lenonyane and Malumeng sites because the transmissivities for this study are low regarding the magnitude transmissivity categorisation by Krasny (1993) for groundwater-yielding capacity (Table 5). In contrast, the transmissivities at Ha Lumisi are considered intermediate therefore, withdrawal of the local water supply (small community) is suggested regarding the groundwater-yielding capacity (Krasny, 1993).

**Table 5:** Categorisation regarding the magnitude of the transmissivities (Source: Krasny, 1993).

| Transmissivity ($m^2$/day) | Description | Groundwater yielding capacity |
|---|---|---|
| >1000 | very high | Withdrawal of great regional importance |
| 100-1000 | High | Withdrawal of lesser regional importance |
| 10-100 | Intermediate | withdrawal of local water supply (e.g., small community) |
| 1-10 | Low | Smaller withdrawal for local water supply (private consumption) |
| 0.1-1 | Very low | Withdrawal of local water supply with limited consumption |
| <0.1 | Impermeable | Sources for local water supply are difficult |

Following a thorough analysis of the groundwater flow behaviour, yield and parameters for the dyke-related aquifer in the focal area, a summary of the results are compiled in Table 6 below:

**Table 6:** Summary of the Groundwater flow properties of the dykes from the Pumping test on the drilled boreholes in the lowlands of the Mafeteng District Lesotho.

| Dyke-Location | Geology (Formations) | Estimation Method | Sustainable Yield (l/s) | Average Sustainable Yield (l/s) | Transmissivity ($m^2$/day) | Comments on Flow Regimes and Flow Characteristics |
|---|---|---|---|---|---|---|
| Qalabane | Molteno-Burgersdorp | Cooper-Jacob/Recovery | 0.56 | 0.29 | 2.81 | -Double porosity at early times, characteristics of a fractured semi-confined aquifer. Linear and radial flows at intermediate-late times respectively. |
| | | Basic | 0.51 | 0.27 | | |
| Thabana Mohlomi | Burgersdorp | Cooper-Jacob/Recovery | 0.22 | 0.11 | 1.10 | -Fractured dyke system, double porosity dip at early and late times. Radial flow is dominant. Characteristically unconfined. |
| | | Basic | 0.20 | 0.11 | | |
| Ha Lenonyane | Burgersdorp | Cooper-Jacob/Recovery | 0.46 | 0.24 | 1.25 | -3 distinct flow characteristics. Recharge boundary towards the late pumping phase. Fractured dyke in a semi-confined aquifer. |
| | | Basic | 0.46 | 0.23 | | |
| Ha Lumisi | Molteno | Cooper-Jacob/Recovery | 2.35 | 1.22 | 11.7 | -Fractured dyke system, radial flow dominant before boundary condition. Oscillations defining heterogeneity of the aquifer. |
| | | Basic | 2.06 | 1.25 | | |
| Malumeng | Clarens, Elliot, Molteno | Cooper-Jacob/Recovery | 0.67 | 0.35 | 1.15 | -Fracture dewatering after a double porosity dip in the early-intermediate phases. |
| | | Basic | 0.69 | 0.35 | | |

## 5.5. Summary Chapter

In response to the primary objectives of the research, the key findings of the study on the baseline hydrogeology of the dolerite dykes in Lesotho, notably in Mafeteng District, were resented in this chapter. The main aim was to characterise the hydrogeology of the dolerite dykes in Lesotho using selected places as case studies. Objective 1 of the current study, which was to characterise the geometry and geological features of the dykes per their hydrogeophysical attributes, was accomplished by the use of geophysical methods, the ground magnetic technique. To establish objective 2, additional surface and subsurface water flow models were also provided, which were then followed by the derivative analysis of the pumping test data in determining the groundwater flow behaviour. Additionally, using the Cooper-Jacob method, which is integrated into the FC Programme, hydraulic parameters like transmissivity were evaluated in conjunction with estimates of sustainable yields.

The key findings from the ground magnetic surveys suggested that the negative magnetic anomalies along the dyke's contact with the country rocks imply fracture gaps along the strike of the dyke. The fracture gaps are justified after forward modelling results of the dyke intruding the Burgersdorp and Molteno Formations indicated a thin dyke structure of 10 m wide, and as Woodford and Chevallier (2002) investigated, the thin dykes considerably deform the country rocks more than the thick dyke do, the dyke further indicated a shallow dip angle of 10° and a dip direction towards the NE. The dolerite dyke sites from the focal area are widespread in intermediate basin flow values in response to the gentle hydraulic gradient in the region as per the surface and subsurface water models. Some of these dykes portrayed groundwater flow directions towards the north while others showed a radial groundwater flow. The derivative analysis and diagnostic plots from different dyke sites depicted double porosity dip and radial flow regimes during the pumping phases. The fractured dyke system from the study area is key for the occurrence and flow of groundwater in the area. The drawdown data showed limited yields and very low transmissivity values, the latter implying that limited extraction of local water supply is opted from the dyke sites in Lesotho, particularly in the Mafeteng District.

# 6 CHAPTER 6: CONCLUSION AND RECOMMENDATIONS

## 6.1 Conclusion

Rural areas in the lowlands of Lesotho rely more on groundwater supply from the springs and boreholes (Leketa, 2018). Groundwater in Lesotho generally occurs in the Karoo lithologies, but the complex geometry of these lithologies controls the distribution of groundwater. Additionally, Woodford and Chevallier (2002) stated that secondary features like dykes contribute to the flow and spread of groundwater in the Karoo basin, and also these dykes can either act as barriers or conduits to groundwater. In Lesotho, specific research on these intrusive dolerite dyke bodies, and their hydrogeology has not been extremely undertaken. As such, it is significant to detect and determine the baseline hydrogeology of the Lesotho dolerite dykes.

The hydrogeology of the dolerite dykes in Lesotho was studied and characterised using sites from the Mafeteng District as case studies. To that end, the following objectives were established:

- Characterise the geometry and geological characterisation of the dolerite dykes and
- Evaluate the hydrogeology (groundwater flow, storage, and yield characteristics) of the dyke-related aquifers in Lesotho.

The results from a selected research site enhance our understanding of the groundwater dynamics in dyke-related aquifers in the Mafeteng lowlands, and the potential of the dykes on the overall groundwater distribution from the focal area. The research considered an initial assessment of the region's broad geological, hydrogeological and distinctive features within the region. This was undertaken in the examination of the local information on geological and hydrogeological maps to comprehend the overall hydrogeological characterisation of the area. As per the initial assessment, the dykes dominating in Mafeteng generally trend NE-SW, NNE-SSW and NW-SE.

The ground magnetic survey was employed to ascertain and determine the geometry and existence of the dykes that were mapped as part of the initial characterisation of the focal area through ArcGIS. The dyke's emplacement and nature as it intruded into the sedimentary Formations were outlined by the magnetic results from TMI, RMI, RTP, and VD maps of the Qalabane site. The maps from Qalabane indicated very strong magnetic values of a dyke trending in the NE-SW directions. At the dyke's contact edges along its strike, there are negative anomalies that might be related to the fracture gaps on the dyke's contacts with the Molteno and Burgersdorp sedimentary Formations. A generalised dip angle for the dyke and other geometrical parameters such as width and depth could not be easily inferred due to the inconsistent anomaly shapes. Hence, forward modelling was undertaken on one of the profiles and estimated a thin width of 10 m with a shallow dip angle of 10 degrees and dip direction towards SE for the dyke at Qalabane Mafeteng.

The narrow linear dyke intrusion is thought to have deformed the country rocks, resulting in the fracture gaps seen at the dyke's edges as negative magnetic anomalies. These parameters give a possible idea about somewhat similar geometrical parameters and the nature of dykes in other dyke sites from the same study area.

The Mafeteng lowland's dyke dominated area's relationship to flow directions and accumulation was deduced using the arc-Hydro tool for both the surface and the subsurface models. The majority of the dykes in Mafeteng are distributed in the intermediate basin flow values due to a gentle hydraulic gradient, meaning that the flows and accumulation are unlikely in the borehole locations used for this study. Using the D8 algorithm, groundwater flow directions were obtained from static groundwater flow maps (Figures 36-37). For the Qalabane and Ha Lumisi dyke sites, groundwater flows northward, however, groundwater flows in different directions at Thabana Mohlomi and Ha Lenonyane.

The effect of the pumping test at dyke locations was studied to establish any groundwater flow characteristics, aquifer flow regime and any current boundary conditions to evaluate the hydrogeology of the dykes in the lowlands of Mafeteng, Lesotho. Analysing the diagnostic and derivative plots from the obtained drawdown data allowed for this to be accomplished. The results indicate that every borehole that was examined showed a fractured dyke system. This is corroborated by the log derivative values, which range from 0.09, which denotes a very good fracture network, to 0.29, which denotes a good fracture network. In most boreholes drilled at Mafeteng, the radial flow regime that predominated throughout the intermediate pumping phases may have existed before the sediments experienced boundary conditions. Pumping at Ha Lumisi produced somewhat different results than at other dyke locations, early to intermediate times saw a fracture dewatering, and the derivative plot (Figure 47) exhibited modest oscillations, indicating aquifer heterogeneity.

A quantitative assessment of the hydraulic parameters in the area serves as the basis for further analysis of the hydrogeology of the dykes. The transmissivity and yield characteristics of the boreholes drilled in various lithologies of the Mafeteng lowlands were estimated using the FC Programme. Based on the transmissivity magnitude, transmissivity values in the area are classified as low to very low (Krasny, 1993). Higher values than other boreholes in other dyke locations are found at the Ha Lumisi dyke site, indicating a high porosity from the coarse-grained conglomerate that originated from the Molteno Formation in the region. The recovery test findings confirmed the validity of the transmissivity data, Ha Lumisi continued to exhibit greater transmissivity than other boreholes in other dyke locations. A limited extraction of the local water supply is suggested from the sedimentary and dolerite dyke lithologies in the lowlands of Mafeteng, Lesotho, given the groundwater-yielding capacity and the magnitude of the transmissivities.

## 6.2 Recommendations

- While the dolerite dykes may have intruded on similar geological Formations, their natural emplacement may vary within a given location. Since the ground magnetic survey was only carried out at one site to ascertain the dyke intrusions and the geometrical parameters of the dykes in the area, the results were inferred to the remaining dykes in the lowlands of Mafeteng. Therefore, it is recommended that more geophysical ground magnetics be performed at additional locations as well, to completely establish the broad dyke characterisation that specifies the nature and emplacement of the intrusive bodies in Lesotho's Burgersdorp, Molteno, Clarens and Elliot Formations.
- For additional parameters such as storativity to be estimated, observation wells can be recommended in the pumping test analyses for future hydrogeological characterisation of the dyke related aquifers in the lowlands of Lesotho.
- For the groundwater flow directions derived from the D8 algorithm, an integrated approach in quantifying the interaction between the modelled surface water and the potentiality of groundwater from the surface can be recommended for future research in Lesotho's Lowlands. This would further aid in characterising and assessing the dolerite dyke impact on the incoming water from the surface into the subsurface and how that account to baseflow in the presence of an intrusive body.

# 7 REFERENCES


Abraham, J.D., Minsely, B.J., Bedrosian, P.A., Smith, B.D. and Cannia, J.C., 2012. Airborne Electromagnetic surveys for groundwater characterisation. *ASEG Extended Abstracts, 2012*(1), pp.1-4.

Alley, W. M., Reilly, T. E., and Franke, O. L. (1999). Sustainability of ground-water resources, volume 1186. *US Department of the Interior*, US Geological Survey.

Atangana, A. (2014). Analytical solutions for the recovery tests after constant-discharge tests in confined aquifers. *Water SA*, 40(4): 595–600.

Babiker, M. and Gudmundsson, A. (2004). The effects of dykes and faults on groundwater flow in an arid land: The Red Sea Hills, Sudan. *Journal of Hydrology*, 297: 256–273.

Baiyegunhi, C., Gwavava, O., Liu, K., and Oloniniyi, T. L. (2018). An integrated geophysical approach to mapping and modelling the karoo dolerite intrusions in the southeastern Karoo basin of South Africa. In SEG Technical Program Expanded Abstracts 2018, pages 1474–1478. Society of Exploration Geophysicists.

Baiyegunhi, C. and Liu, K. (2021). Sedimentary facies, stratigraphy, and depositional environments of the Ecca Group, Karoo Supergroup in the Eastern Cape province of South Africa. *Open Geosciences*, 13(1): 748–781.

Belica, M. E., Tohver, E., Poyatos-More, M., Flint, S., Parra-Avila, L. A., Lanci, L., Denyszyn, S., and Pisarevsky, S. A. (2017). Refining the chronostratigraphy of the Karoo Basin, South Africa: magnetostratigraphic constraints support an early Permian age for the Ecca group. *Geophysical Journal International*, 211(3): 1354–1374.

Bonney, G. (1975). Development Fund Project Survey and Design of a Borehole Water Supply at Roma. *Roma Groundwater Investigation Hydrogeologist's Report, Hydrogeology section*, report MGH GB4, DMG. Maseru.

Botha, J. and Cloot, A. (2004). Deformations and the karoo aquifers of South Africa. *Advances in water resources*, 27(4): 383–398.

Botha, J., Verwey, J., Van der Voort, I., Vivier, J., Buys, J., Colliston, W., and Loock, J. (1998). Karoo aquifers: their geology, geometry and physical properties. report to water commission. WRC report no: 487/1/98. *Institute for Groundwater Studies*, South Africa.

Botha, J. F. (1998). Modelling subsurface flow in karoo aquifers. *WIT Transactions on Ecology and the Environment*, 23.

Bourdet, D., Ayoub, J., and Plrard, Y. (1989). Use of pressure derivative in well-test interpretation. *SPE Formation Evaluation*, 4(02): 293–302.

Brown, G. O. (2002). Henry Darcy and the making of a law. *Water Resources Research*, 38.

Burger, H.R., Sheehan, A.F., and Jones, C.H., (2006). Exploration Using the Magnetic Method, Introduction to Applied Geophysics: Exploring the Shallow Subsurface, W.W. Norton & Company, *New York,* p. 429-497.

Catuneanu, O. (2004). Basement control on flexural profiles and the distribution of foreland facies: the Dwyka group of the Karoo Basin, South Africa. *Geology*, 32(6): 517–520.

Catuneanu, O., Wopfner, H., Eriksson, P. G., Cairncross, B., Rubidge, B. S., Smith, R. M. H., and Hancox, P. J. (2005). The Karoo Basins of south-central Africa. *Journal of African Earth Sciences*, 43: 211–253.

Chatanga, P., Ntuli, V., Mugomeri, E., Keketsi, T., and Chikowore, N. V. (2019). Situational analysis of physicochemical, biochemical and microbiological quality of water along Mohokare River, Lesotho. *The Egyptian Journal of Aquatic Research*, 45(1): 45–51.

Chevallier, L. P., Goedhart, M. L., and Woodford, A. C. (2001). Influence of dolerite sill and ring complexes on the occurrence of groundwater in the Karoo fractured aquifers: a morpho-tectonic approach*: Report to the Water Research Commission*. Water Research Commission.

Cole, M. J., Bailey, R. M., Cullis, J. D., and New, M. G. (2018). Spatial inequality in water access and water use in South Africa*. Water Policy*, 20(1): 37–52.

Comte, J.C., Wilson, C., Ofterdinger, U. and González-Quirós, A., 2017. Effect of volcanic dykes on coastal groundwater flow and saltwater intrusion: A field-scale Multiphysics approach and parameter evaluation. *Water Resources Research*, *53*(3), pp.2171-2198.

Cooper, G. (1997). Forward modelling of magnetic data. *Computers & Geosciences*, 23(10): 1125–1129.

Cooper Jr, H. and Jacob, C. E. (1946). A generalized graphical method for evaluating formation constants and summarizing well-field history. *Eos, Transactions American Geophysical Union*, 27(4): 526–534.

Corps, P. (1990). Irrigation reference manual. *Information Collection & Exchange Washington DC*.

Davies, J. (2003). Lesotho lowlands water supply feasibility study–hydrogeology. *British Geological Survey Report* CR/03 C, 176: 2003.

Deep, M. A., Araffa, S. A. S., Mansour, S. A., Taha, A. I., Mohamed, A., and Othman, A. (2021). Geophysics and remote sensing applications for groundwater exploration in fractured basement: A case study from Abha area, Saudi Arabia. *Journal of African Earth Sciences*, 184:104368.

Department of Water Affairs, Republic of South Africa (2010). *A guideline for the assessment, planning and management of groundwater resources in South Africa,* Pretoria: Water Affairs, Edition 2.

De Villiers, S.B., 1961. *Boorplekaanwysing vir water in Suidwes-Transvaal*. Geological Survey, Department of Mines.

Dietrich, P. and Hofmann, A. (2019). Ice-margin fluctuation sequences and grounding zone wedges: The record of the late Palaeozoic ice age in the eastern Karoo Basin (Dwyka group, South Africa). *The Depositional Record*, 5: 247 – 271.

Dippenaar, M. A., Witth¨user, K. T., and Van Rooy, J. L. (2009). Groundwater occurrence in basement aquifers in Limpopo province, South Africa: model-setting-scenario approach. *Environmental Earth Sciences*, 59: 459–464.

Enslin, J.F., 1950. Geophysical methods of tracing and determining contacts of dolerite dykes in Karroo sediments in connection with the siting of boreholes for water. *South African Journal of Geology*, *53*(1), pp.193-204.

Enslin, J.F., 1955. A new electromagnetic field technique. *Geophysics*, *20*(2), pp.318-334.

Esri (2021). *Stream to Feature.* Available at: https://desktop.arcgis.com/en/arcmap/latest/tools/spatial-analyst-toolbox/stream-to-feature.htm (Accessed: 11 November 2023).

Fourie, F., Huber, M., and Kovaleva, E. (2019). Geophysical characterisation of the daskop granophyre dyke and surrounding host rocks, Vredefort impact structure, South Africa. *Meteoritics & Planetary Science*, 54(7): 1579–1593.

Gandhi, S. and Sarkar, B. (2016). Essentials of mineral exploration and evaluation. *Elsevier*.

Garcia, M. and H´erail, G. (2005). Fault-related folding, drainage network evolution and valley incision during the Neogene in the Andean pre cordillera of northern Chile. *Geomorphology*, 65(3-4): 279–300.

Geomatrix (2023). *G-858AP From Geometrics*. Available at: https://www.geomatrix.co.uk/land-products/magnetic/g-858/ (Accessed 20 November 2023).

Graham, K. M., Kwasi, P., Wemegah, D. D., and Boamah, D. (2014). Geological and structural interpretation of part of the Buem Formation, Ghana, using aero geophysical data. *Journal of Environment and Earth Science*, 4(4): 17 – 31.

Grauso, S., Pasanisi, F., and Tebano, C. (2020). Modelling the suspended sediment yield in Lesotho rivers. *Modelling Earth Systems and Environment*, 6: 759–768.

Gringarten, A. C. (2008). From straight lines to deconvolution: The evolution of the state of the art in well test analysis. *SPE Reservoir Evaluation & Engineering*, 11(01): 41–62.

Gunawardhana, L. N., Al-Harthi, F., Sana, A., and Baawain, M. S. (2021). Analytical and numerical analysis of constant rate pumping test data considering aquifer boundary effect. *Environmental Earth Sciences*, 80: 1–13.

Ha, D., Zheng, G., Zhou, H., Zeng, C., and Zhang, H. (2020). Estimation of hydraulic parameters from pumping tests in a multi-aquifer system. *Underground Space*, 5(3): 210–222.

Hlalele, B. (2017). Cointegration analysis of vulnerability index and standardised precipitation index in Mafeteng district, Lesotho. Jamba: *Journal of Disaster Risk Studies*, 9(1): 1–6.

Igwebuike, N., Muchingami, I., and Kanyerere, T. (2023). Application of hydrogeophysics and diagnostic plots in setting up a sustainable managed aquifer recharge scheme, West Coast, South Africa. *Journal of African Earth Sciences*, 206:105039.

Jenson, S. K. and Dominique, J. O. (1988). Extracting Topographic Structure from Digital Elevation Data for Geographic Information System Analysis. *Photogrammetric Engineering and Remote Sensing*, 54 (11): 1593–1600.

Johnson, M., Visser, J., Cole, D., de Wickens, H., Christie, A., Roberts, D., and Bradle, G. (2006). Sedimentary rocks of the karoo supergroup, in "Johnson, MR, Anhaeusser, CR, and Thomas. 2006). *The Geology of South Africa. Geological Society of South Africa, Johannesburg/Council for Geoscience, Pretoria*, 691p.

Kelly, W. E. and Mares, S. (1993). Applied geophysics in hydrogeological and engineering practice. *Elsevier*.

Krasny, J. (1993). Classification of transmissivity magnitude and variation. *Groundwater*, 31(2): 230–236.

Kruseman, G.P. and de Ridder N.A. eds. (1991). *Analysis and Evaluation of Pumping Test Data Second Edition (Completely Revised)* ILRI publication 47. Intern. Inst. for Land Reclamation and Improvements, Wageningen, Netherlands, p. 377. Available at: https://gw-project.org/books/analysis-and-evaluation-of-pumping-test-data/ (Accessed 10 January 2024).

Kusangaya, S., Warburton, M. L., Van Garderen, E. A., and Jewitt, G. P. (2014). Impacts of climate change on water resources in southern Africa: A review. *Physics and Chemistry of the Earth, Parts a/b/c*, 67: 47–54.

Lanci, L., Tohver, E., Wilson, A., and Flint, S. (2013). Upper Permian magnetic stratigraphy of the lower Beaufort group, karoo basin. *Earth and Planetary Science Letters*, 375: 123–134.

Leketa K, Migwi M, Crane E, Upton K, Ó Dochartaigh BÉ and Bellwood-Howard, I. (2018). Africa Groundwater Atlas: Hydrogeology of Lesotho. British Geological Survey. Available at: http://earthwise.bgs.ac.uk/index.php/Hydrogeology_of_Lesotho (Accessed 18 April 2023).

Leveinen, J. (2001). Conceptual and analytical modelling of fracture zone aquifers in hard rock-Implications of pumping tests in the Pohjukansalo wellfield, east central Finland (No. YST-105). *Geological Survey of Finland, Nuclear Waste Disposal Research*.

Leveinen, J. (2000). Composite model with fractional flow dimensions for well test analysis in

fractured rocks. *J. Hydrol*, 234, 116–141.

Lomize, G.M., 1951. Flow in fractured rocks. *Gosenergoizdat, Moscow*, *127*(197), p.635.

Louis, C.A., 1969. Study of groundwater flow in jointed rock and its influence on the stability of rock masses. *Imperial College Rock Meck. Res.*, (10), pp.1-90.

Makalo, M. J., Mtshali, K., Tsotetsi-Khambule, A. M., Mofokeng, L. S., Taioe, M. O., Onyiche, T. E., and Thekisoe, O. M. (2022). First report of gastrointestinal nematodes and coccidia parasites from free-range chickens in Mafeteng district, Lesotho. Veterinary Parasitology: *Regional Studies and Reports*, 36:100798.

Mawlood, D. and Ismail, S. (2019). Comparison between Neuman and Dupuis for pumping test in water table aquifer. *ZANCO Journal of Pure and Applied Sciences*, 31(3): 385–391.

Mickus, K. (2014). Magnetic method. *Geophysics*, 45: 1640–1658.

Minnaar, R. C. and Dippenaar, M. A. (2019). Hydrogeological characterisation of regional faults and dolerite dykes in the Precambrian basement and Karoo Supergroup (Tete province, Mozambique). *South African Journal of Geology*, 122 (3): 343-356.

Moonen, P. and Carmeliet, J. (2013). Modelling moisture transport in intact and fractured concrete. In Weerheijm, J., (eds). Understanding the Tensile Properties of Concrete, Woodhead Publishing Series in Civil and Structural Engineering, *Woodhead Publishing*. pp 98–122.

Odipe, O. E., Sawyerr, H. O., and Adewoye, S. O. (2020). Static water level and elevation analyses of shallow hand-dug wells in Ilorin metropolis, Nigeria. *Asian Journal of Geographical Research*, 3(3): 48–53.

Phillips, T.J. (1994). The determination of a mathematical relationship between aquifer parameters calculated from a conventional porous rock analytical technique and a fractured rock method for analysing pumping test data. *Unpubl B.Sc. Hons. thesis,* Rhodes University, Grahanisfown, South Africa.

Piscopo, V., Sbarbati, C., Dinagde, T. D., and Lotti, F. (2023). Practical approach for defining the sustainable yield of wells in low permeability fractured rocks. *Sustainability*, 15(13).

Pongmanda, S. and Suprapti, A. (2020). Performing application of Cooper-Jacob method for identification of storativity. Conference Series: *Earth and Environmental Science*, 419(1):012128.

Rajagopalan, S. (2003). Analytic signal vs. reduction to pole: Solutions for low magnetic latitudes. *Exploration Geophysics*, 34(4): 257–262.

Romm, E.S., 1966. Flow characteristics of fractured rocks. *Nedra, Moscow*, *283*.

Rubidge, B. S. and Hancox, J. P. (2002). The karoo supergroup. *Rocks & Minerals*, 77:54 – 59.

Rubidge, B. S. (ed.) (1995). Biostratigraphy of the Beaufort Group. South African Commission on

Stratigraphy. *Bio stratigraphic Series* 1, pp. 1-45.

Schmitz, G. and Rooyani, F. (1987). Lesotho: geology, geomorphology, soils. *National University of Lesotho*.

Sene, K. J., Jones, D. A., Meigh, J. R., and Farquharson, F. A. K. (1998). Rainfall and flow variations in the Lesotho Highlands. *International Journal of Climatology*, 18(3): 329–345.

Senger, K., Buckley, S. J., Chevallier, L., ˚Ake Fagereng, Galland, O., Kurz, T. H., Ogata, K., Planke, S., and Tveranger, J. (2015). Fracturing of doleritic intrusions and associated contact zones: Implications for fluid flow in volcanic basins. *Journal of African Earth Sciences*, 102: 70–85.

Shakhane, T. (2021). Rehabilitation of water systems (six (6) districts) and borehole drilling (three (3) districts) siting, drilling, and pumping tests in Mafeteng. Ref no: itb 9163447.

Siemon, B., Christiansen, A.V. and Auken, E., 2009. A review of helicopter-borne electromagnetic methods for groundwater exploration. *Near Surface Geophysics*, *7*(5-6), pp.629-646.

Tarboton, D. G., Bras, R. L., and Rodríguez-Iturbe, I. (1991). On the extraction of channel networks from digital elevation data. *Hydrological Processes*, 5: 81–100.

Telford, W. M., Geldart, L. P., and Sheriff, R. E. (1990). Applied Geophysics. Cambridge University Press, 2 editions.

Tokumaru, K. (2014). The Kalahari impacts hypothesis for the birth of the moon: Did Morokweng meteorite impact (145 ma) break up the Gondwanaland and ignite volcanic explosion to form the moon? *Journal of Geological Resource and Engineering*, 2(2016):73 – 80.

Tong, Z., Luo, Y., and Zhou, J. (2021). Mapping the urban natural ventilation potential by hydrological simulation. *Building Simulation*, 14: 351–364.

UNDP (1984). Exploration for Diamonds (phase 1) and Exploration for Minerals (Phase 2). *Geology and Mineral Resources of Lesotho*, technical report DP/UN/LES-71-503/8 and DP/UN/LES-73-021/9, for the Government of Lesotho.

Van Tonder, G., Botha, J. F., Chiang, W.-H., Kunstmann, H., and Xu, Y. (2001). Estimation of the sustainable yields of boreholes in fractured rock formations. *Journal of Hydrology*, 241: 70–90.

Woodford, A. and Chevallier, L. (2002). Hydrogeology of the main Karoo Basin: Current knowledge and future research needs. *Water Research Commission Report, No. TT, 179* (02): 482.

Wyk, Y. V. and Witthueser, K. (2011). A forced-gradient tracer test on the Hansrivier Dyke: Beaufort West, South Africa. *Water SA*, 37: 437-444.

Xu, J., Chen, M., Hong, H., Xu, X., and Liu, B. (2019). Differences of hydraulic conductivities from pumping and draining tests with intensity effects. *Journal of Hydrology*, 579:124165.

Zhang, N., He, M., Zhang, B., Qiao, F., Sheng, H., and Hu, Q. (2016). Pore structure

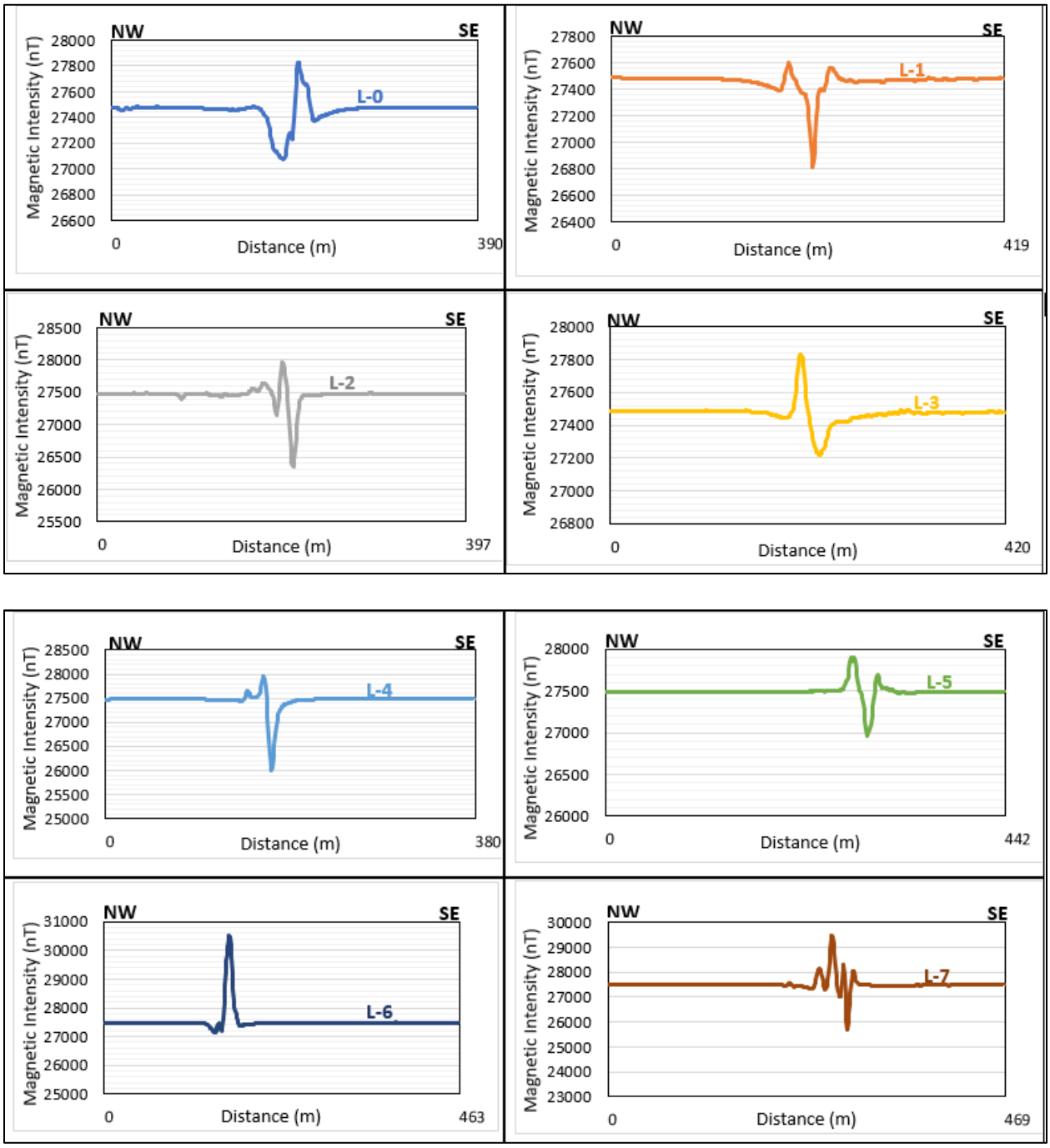
characteristics and permeability of deep sedimentary rocks determined by mercury intrusion porosimetry. *Journal of Earth Science*, 27: 670–676.

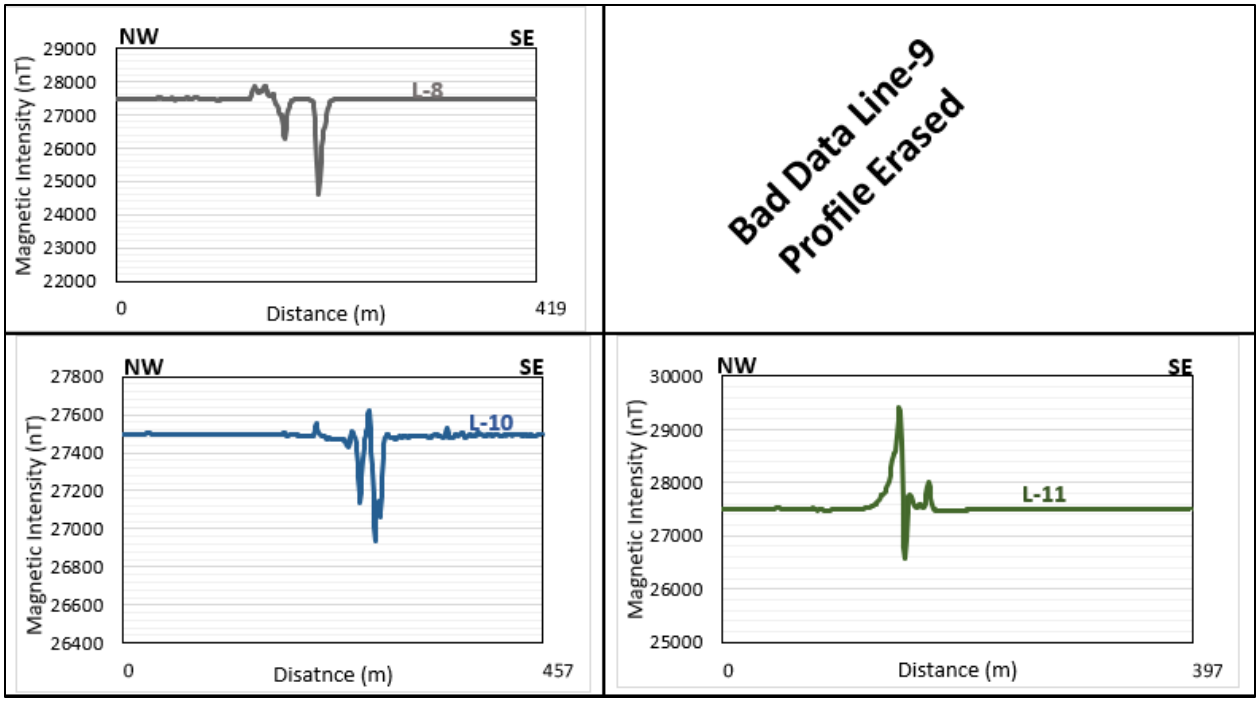
Zouhri, L. and Armand, R. (2019). Groundwater vulnerability assessment of the chalk aquifer in the northern part of France. *Geocarto International*, 36: 1193 – 1216.

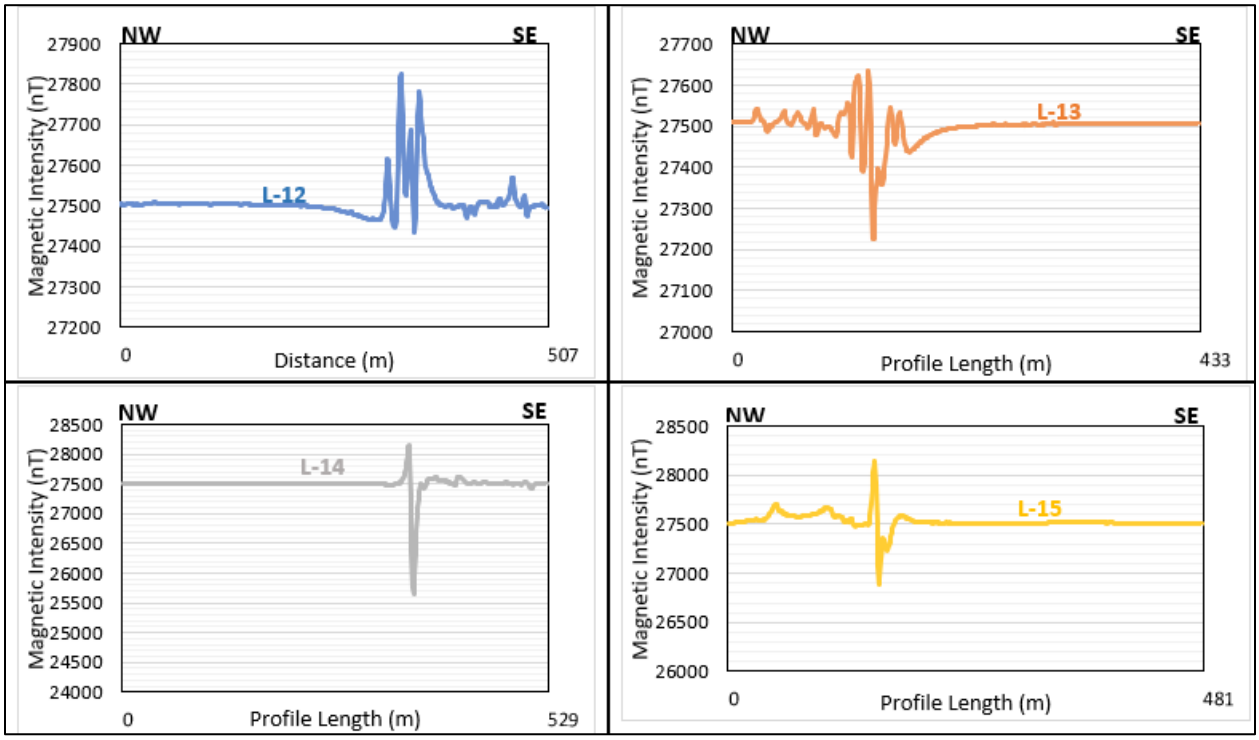
# 8. APPENDIX

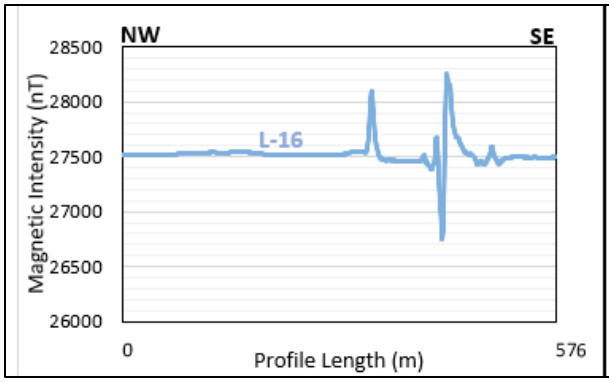
## 8.1 GROUND MAGNETIC PROFILES AND MAPS

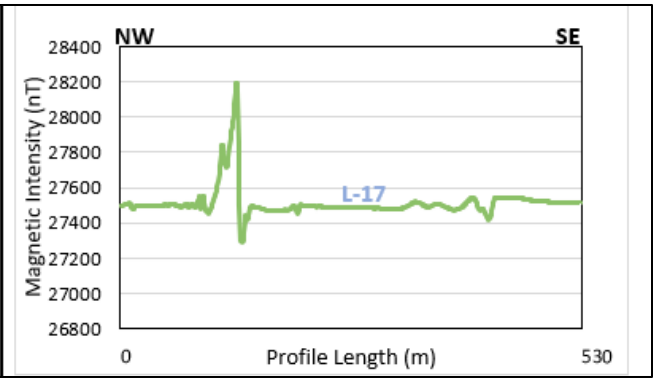
Below are the line profiles, Magnetic grids, and maps for the ground magnetic survey undertaken at Qalabane, Mafeteng District, the kriging maps still show similar anomalies to those presented in the results section.

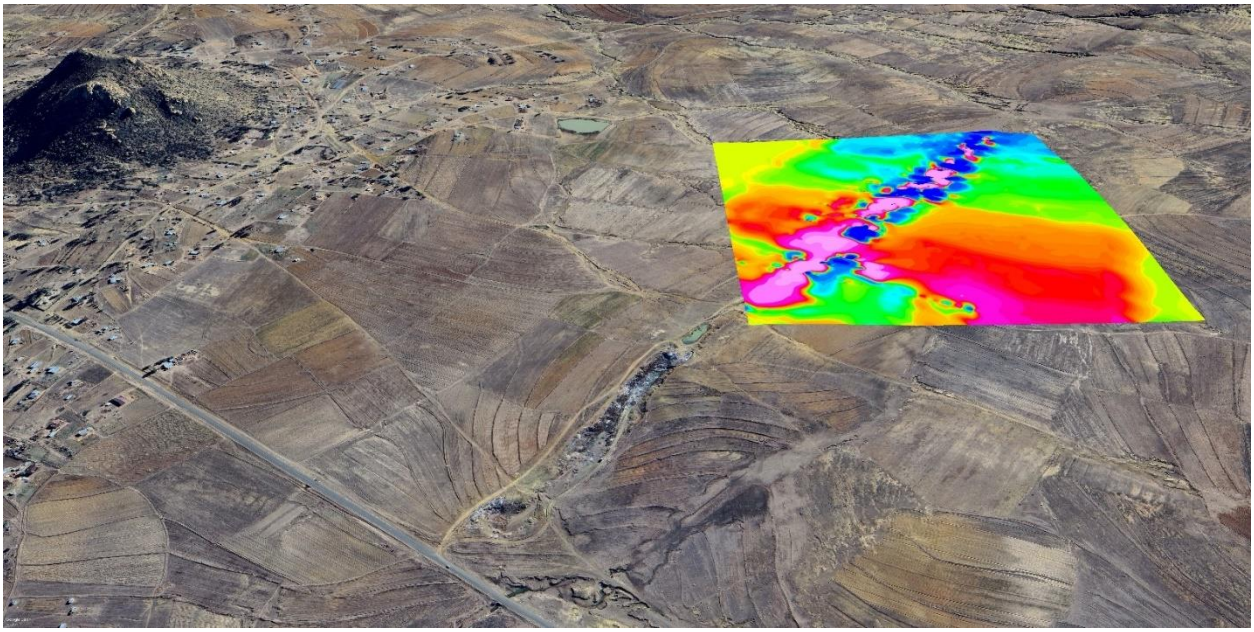


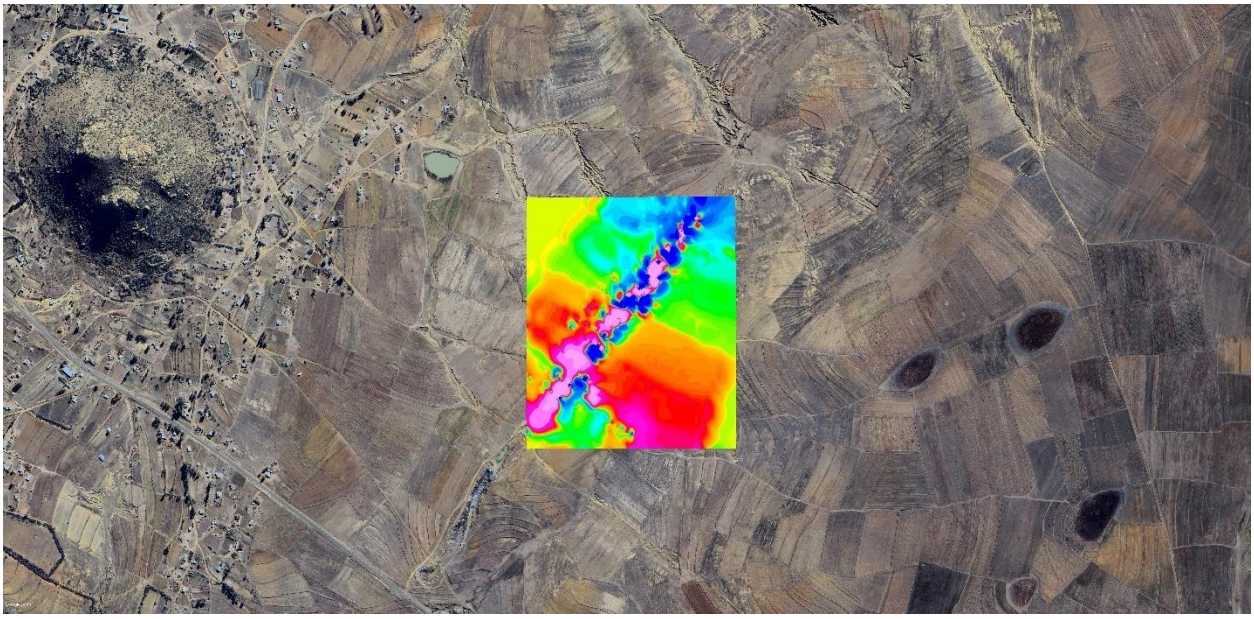

NW
SE
L-8
Magnetic Intensity (nT)
29000
28000
27000
26000
25000
24000
23000
22000
0
Distance (m)
419
Bad Data Line-9
Profile Erased
NW
SE
L-10
Magnetic Intensity (nT)
27800
27600
27400
27200
27000
26800
26600
26400
0
Disatnce (m)
457
NW
SE
L-11
Magnetic Intensity (nT)
30000
29000
28000
27000
26000
25000
0
Distance (m)
397

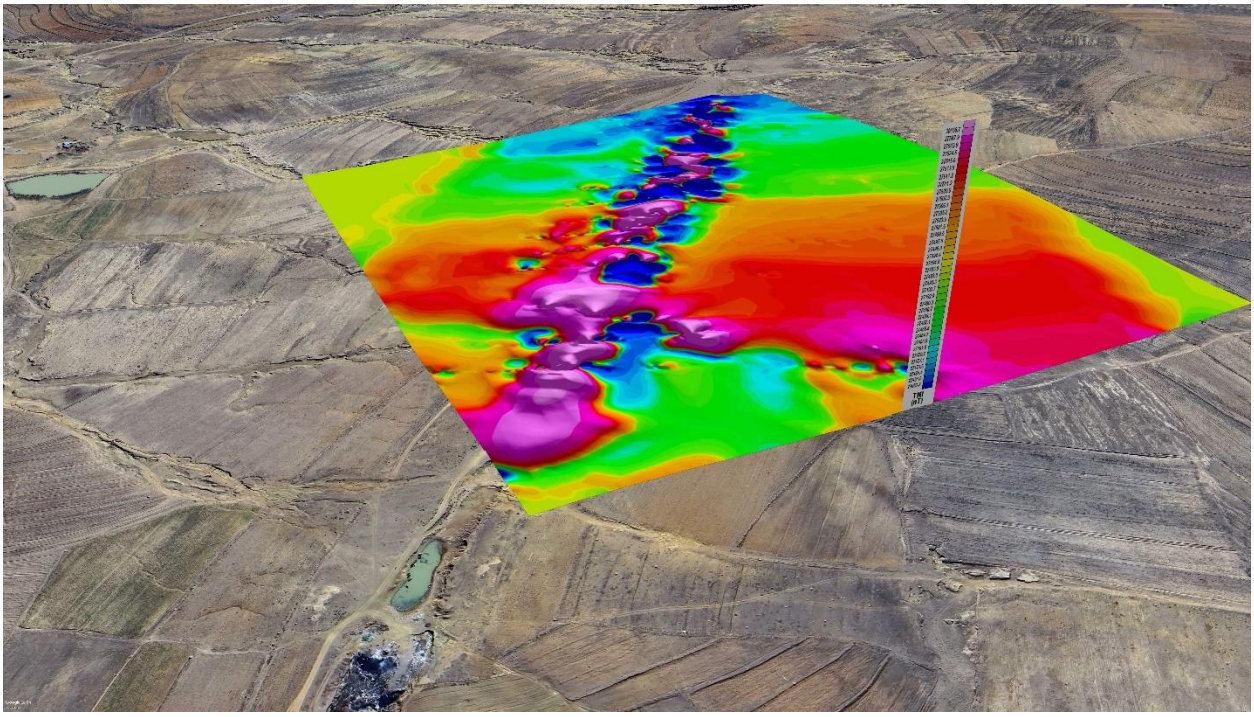

NW
SE
L-12
Magnetic Intensity (nT)
27900
27800
27700
27600
27500
27400
27300
27200
0
Distance (m)
507
NW
SE
L-13
Magnetic Intensity (nT)
27700
27600
27500
27400
27300
27200
27100
27000
0
Profile Length (m)
433
NW
SE
L-14
Magnetic Intensity (nT)
28500
28000
27500
27000
26500
26000
25500
25000
24500
24000
0
Profile Length (m)
529
NW
SE
L-15
Magnetic Intensity (nT)
28500
28000
27500
27000
26500
26000
0
Profile Length (m)
481

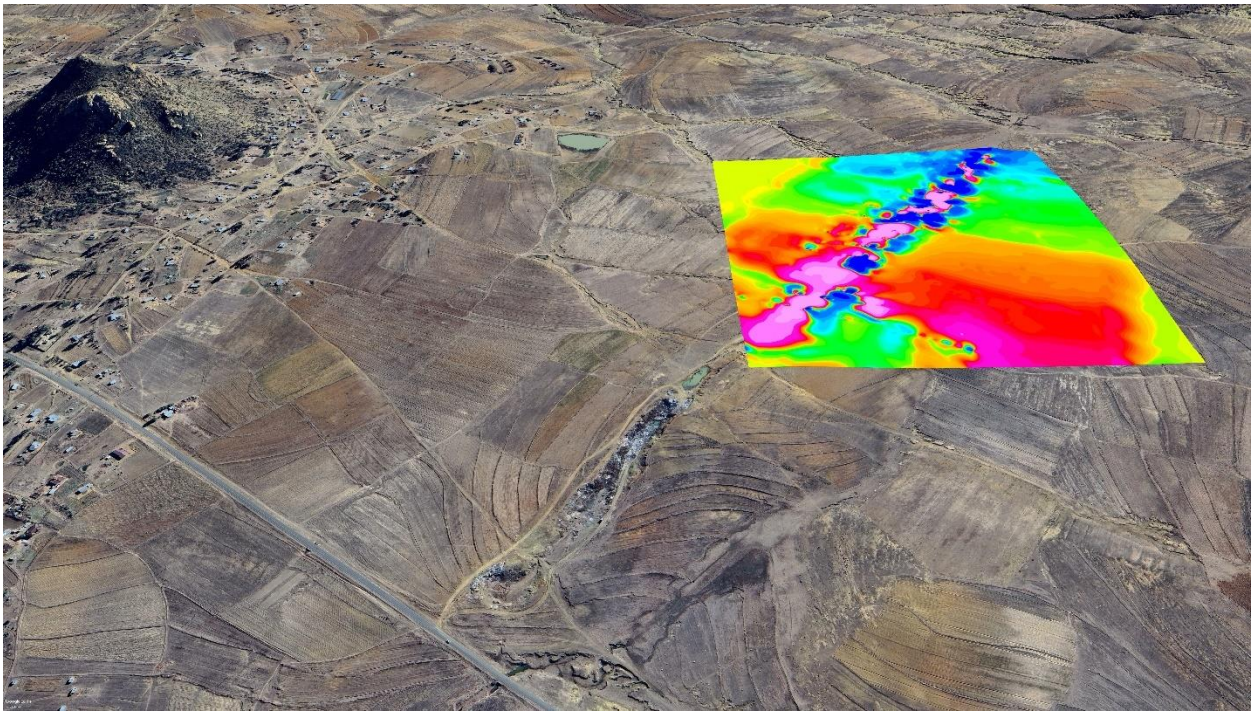

NW
SE
28500
28000
27500
27000
26500
26000
Magnetic Intensity (nT)
L-16
0
576
Profile Length (m)

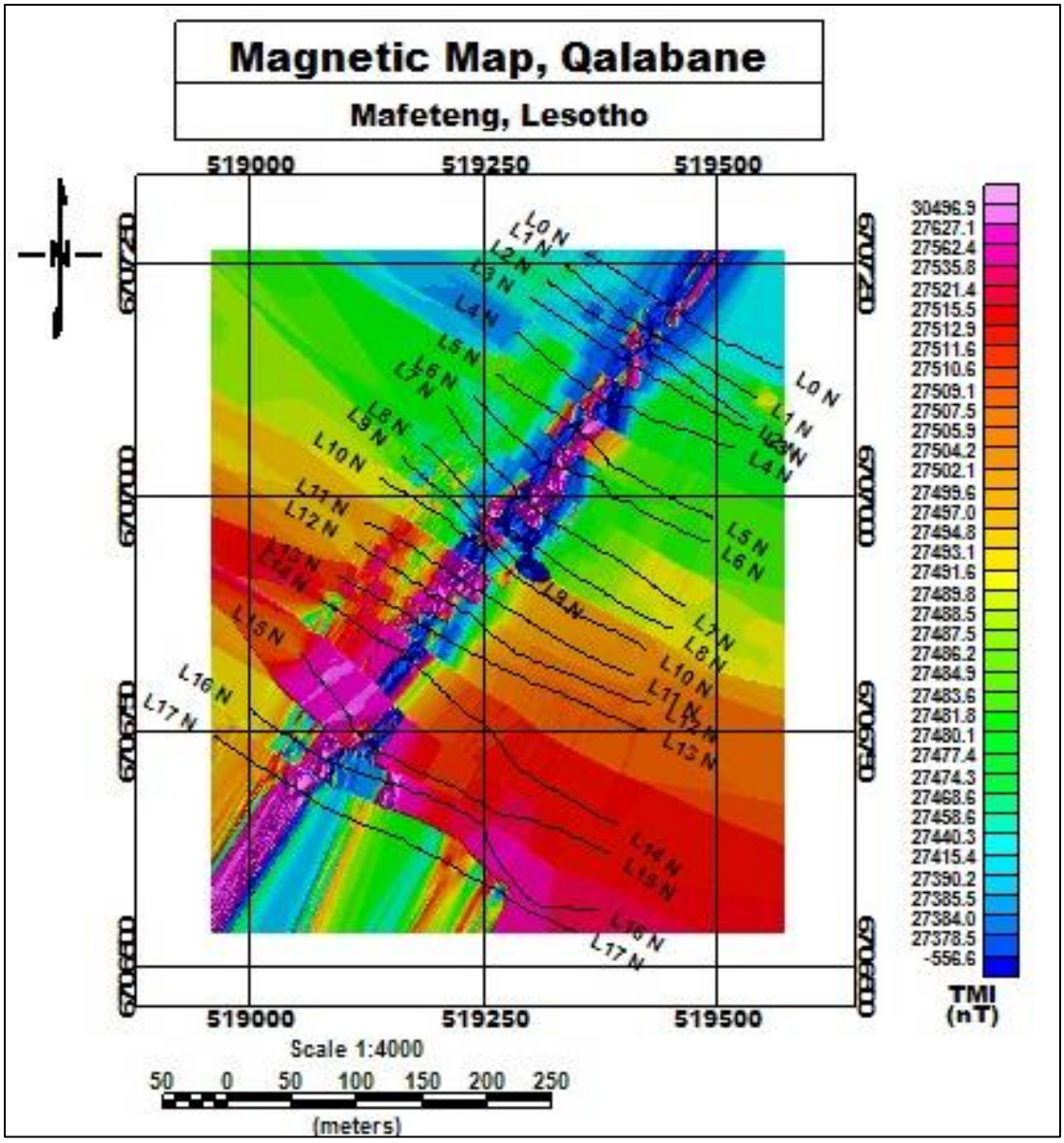

NW
SE
28400
28200
28000
27800
27600
27400
27200
27000
26800
Magnetic Intensity (nT)
L-17
0
530
Profile Length (m)

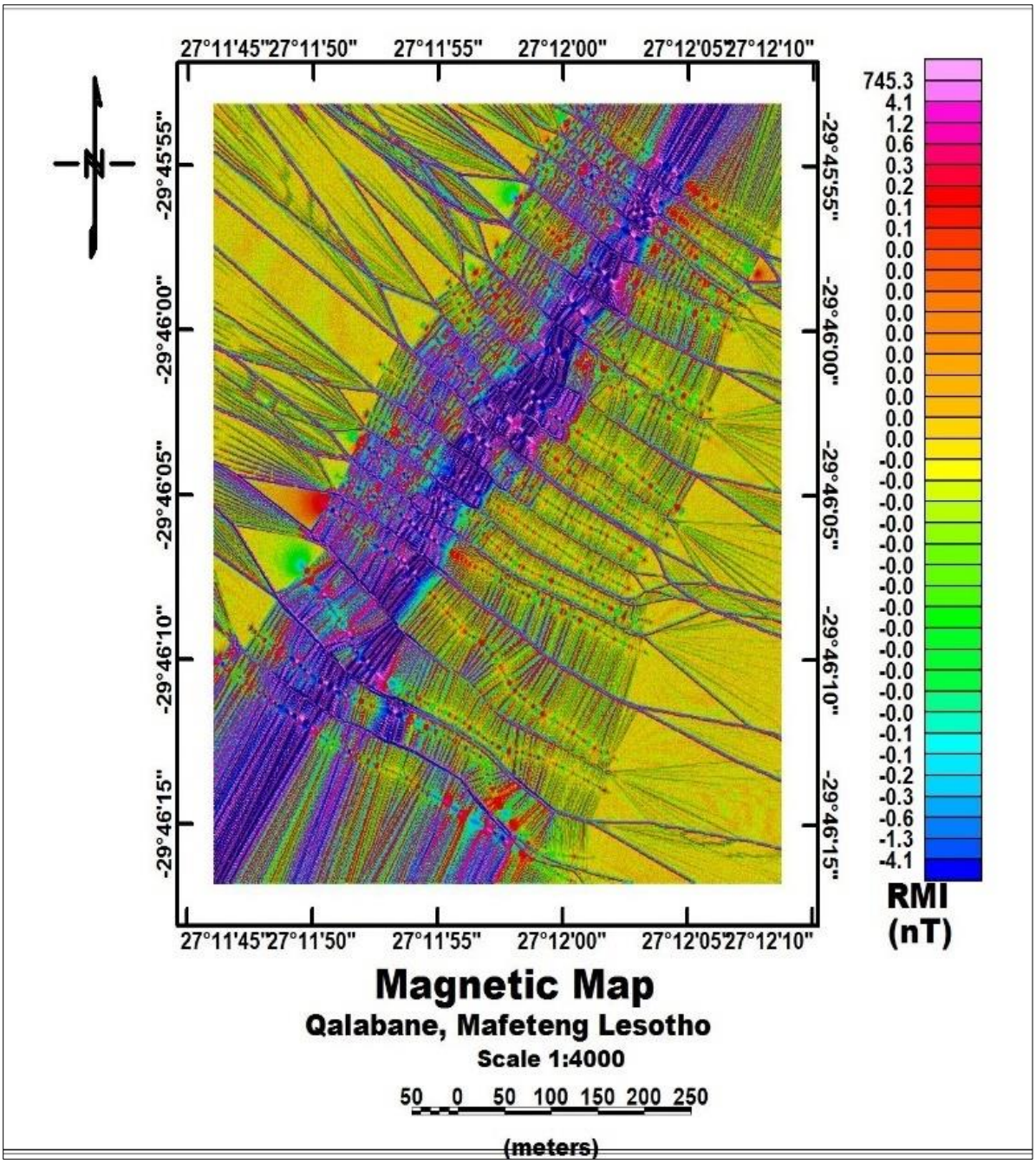









Magnetic Map, Qalabane
Mafeteng, Lesotho
519000
519250
519500
6707250
6707000
6706750
6706500
L0 N
L1 N
L2 N
L3 N
L4 N
L5 N
L6 N
L7 N
L8 N
L9 N
L10 N
L11 N
L12 N
L13 N
L14 N
L15 N
L16 N
L17 N
30496.9
27627.1
27562.4
27535.8
27521.4
27515.5
27512.9
27511.6
27510.6
27509.1
27507.5
27505.9
27504.2
27502.1
27499.6
27497.0
27494.8
27493.1
27491.6
27489.8
27488.5
27487.5
27486.2
27484.9
27483.6
27481.8
27480.1
27477.4
27474.3
27468.6
27458.6
27440.3
27415.4
27390.2
27385.5
27384.0
27378.5
-556.6
TMI
(nT)
Scale 1:4000
50 0 50 100 150 200 250
(meters)


27°11'45"
27°11'50"
27°11'55"
27°12'00"
27°12'05"
27°12'10"
-29°45'55"
-29°46'00"
-29°46'05"
-29°46'10"
-29°46'15"
N
745.3
4.1
1.2
0.6
0.3
0.2
0.1
0.1
0.0
0.0
0.0
0.0
0.0
0.0
0.0
0.0
0.0
0.0
-0.0
-0.0
-0.0
-0.0
-0.0
-0.0
-0.0
-0.0
-0.0
-0.0
-0.0
-0.0
-0.0
-0.0
-0.1
-0.1
-0.2
-0.3
-0.6
-1.3
-4.1
RMI
(nT)
Magnetic Map
Qalabane, Mafeteng Lesotho
Scale 1:4000
50 0 50 100 150 200 250
(meters)

## 8.2 CONSTANT DISCHARGE DATA SHEETS

| PUMPING BOREHOLE-QALABNE | | | |
|---|---|---|---|
| Depth of pump (m) | 79 | | |
| Collor Height (m) | 0.19 | | |
| Borehole Diameter (m) | 0.14 | | |
| Depth of Borehole (m) | 80 | | |
| Static Water Level (m) | 3.15 | | |
| **Time** | **Drawdown** | **Time** | **Recovery** |
| **(min)** | **s(m)** | **(min)** | **s'(m)** |
| 1 | 3.7 | 1 | 22.57 |
| 2 | 4.23 | 2 | 22.3 |
| 3 | 4.64 | 3 | 21.98 |
| 4 | 5.01 | 4 | 21.73 |
| 5 | 5.49 | 5 | 21.51 |
| 6 | 5.71 | 6 | 21.31 |
| 7 | 6.09 | 7 | 21.11 |
| 8 | 6.39 | 8 | 20.96 |
| 9 | 6.66 | 9 | 20.79 |
| 10 | 6.87 | 10 | 20.65 |
| 11 | 7.12 | 11 | 20.49 |
| 12 | 7.36 | 12 | 20.38 |
| 13 | 7.58 | 13 | 20.23 |
| 14 | 7.8 | 14 | 20.12 |
| 15 | 8.02 | 15 | 19.99 |
| 16 | 8.26 | 16 | 19.88 |
| 17 | 8.42 | 17 | 19.78 |
| 18 | 8.6 | 18 | 19.69 |
| 19 | 8.79 | 19 | 19.58 |
| 20 | 8.97 | 20 | 19.49 |
| 25 | 9.81 | 25 | 18.99 |
| 30 | 10.44 | 30 | 18.63 |
| 40 | 11.53 | 40 | 18.25 |
| 50 | 12.45 | 50 | 17.84 |
| 60 | 13.29 | 60 | 17.14 |
| 75 | 14.38 | 75 | 16.44 |
| 90 | 15.19 | 90 | 15.83 |

| | | | |
|---|---|---|---|
| 120 | 16.51 | 120 | 14.41 |
| 150 | 17.56 | 150 | 13.1 |
| 180 | 18.23 | 180 | 12.31 |
| 240 | 19.21 | 240 | 10.49 |
| 300 | 20.26 | 300 | 9.04 |
| 360 | 21.31 | 360 | 8.47 |
| 420 | 21.76 | 420 | 7.88 |
| 480 | 21.99 | 480 | 7.31 |
| 600 | 22.69 | 600 | 6.91 |
| 720 | 23.06 | | |

| **PUMPING BOREHOLE-Thabana Mohlomi** | |
|---|---|
| Depth of pump (m) | 81 |
| Collor Height (m) | 0.22 |
| Borehole Diameter (m) | 0.14 |
| Depth of Borehole (m) | 100 |
| Static Water Level (m) | 14.4 |

| **Time** | **Drawdown** | **Time** | **Recovery** |
|---|---|---|---|
| **(min)** | **s(m)** | **(min)** | **s'(m)** |
| 1 | 16.35 | 1 | 27.34 |
| 2 | 17.63 | 2 | 26.45 |
| 3 | 18.88 | 3 | 25.58 |
| 4 | 19.58 | 4 | 24.91 |
| 5 | 19.86 | 5 | 24.21 |
| 6 | 19.96 | 6 | 23.52 |
| 7 | 19.99 | 7 | 22.78 |
| 8 | 19.9 | 8 | 22.32 |
| 9 | 20.01 | 9 | 21.79 |
| 10 | 20.31 | 10 | 21.33 |
| 11 | 20.68 | 11 | 20.86 |
| 12 | 21.01 | 12 | 20.45 |
| 13 | 21.34 | 13 | 20.08 |
| 14 | 21.54 | 14 | 19.78 |
| 15 | 21.91 | 15 | 19.48 |
| 16 | 22.13 | 16 | 19.18 |
| 17 | 22.37 | 17 | 18.96 |
| 18 | 22.73 | 18 | 18.76 |

| | | | |
|---|---|---|---|
| 19 | 23.02 | 19 | 18.6 |
| 20 | 23.29 | 20 | 18.43 |
| 25 | 24.43 | 25 | 17.84 |
| 30 | 24.99 | 30 | 17.49 |
| 40 | 26.15 | 40 | 17.12 |
| 50 | 26.84 | 50 | 16.92 |
| 60 | 27.5 | 60 | 16.78 |
| 75 | 28.15 | 75 | 16.52 |
| 90 | 28.5 | 90 | 16.31 |
| 120 | 28.5 | 120 | 16.07 |
| 150 | 28.51 | 150 | |
| 180 | 28.52 | 180 | |
| 240 | 28.53 | 240 | |
| 300 | 28.53 | 300 | |
| 360 | 28.54 | 360 | |
| 420 | 28.77 | 420 | |
| 480 | 28.52 | 480 | |
| 600 | 31.68 | 600 | |
| 720 | 28.18 | | |

| **PUMPING BOREHOLE-Ha Lenonyane** | |
|---|---|
| Depth of pump (m) | 49 |
| Collor Height (m) | 0.22 |
| Borehole Diameter (m) | 0.14 |
| Depth of Borehole (m) | 80 |
| Static Water Level (m) | 6.84 |

| **Time** | **Drawdown** | **Time** | **Recovery** |
|---|---|---|---|
| **(min)** | **s(m)** | **(min)** | **s'(m)** |
| 1 | 8.4 | 1 | 28.53 |
| 2 | 9.84 | 2 | 26.51 |
| 3 | 11.61 | 3 | 24.18 |
| 4 | 12.23 | 4 | 22.72 |
| 5 | 12.96 | 5 | 21.56 |
| 6 | 13.42 | 6 | 19.92 |
| 7 | 13.35 | 7 | 19.12 |
| 8 | 14.66 | 8 | 17.99 |
| 9 | 15.33 | 9 | 16.19 |

| | | | |
|---|---|---|---|
| 10 | 15.93 | 10 | 15.14 |
| 11 | 16.74 | 11 | 15.38 |
| 12 | 17.13 | 12 | 14.88 |
| 13 | 17.71 | 13 | 14.28 |
| s | 18.22 | 14 | 13.88 |
| 15 | 18.66 | 15 | 13.6 |
| 16 | 19.06 | 16 | 13.34 |
| 17 | 19.46 | 17 | 13.12 |
| 18 | 19.75 | 18 | 12.87 |
| 19 | 20.04 | 19 | 12.63 |
| 20 | 20.25 | 20 | 12.36 |
| 25 | 21.47 | 25 | 11.12 |
| 30 | 22.17 | 30 | 10.48 |
| 40 | 23.51 | 40 | 9.87 |
| 50 | 24.57 | 50 | 9.45 |
| 60 | 25.32 | 60 | 9.27 |
| 75 | 26.12 | 75 | 9.00 |
| 90 | 26.67 | 90 | 8.87 |
| 120 | 27.47 | 120 | 8.68 |
| 150 | 28.01 | 150 | 8.54 |
| 180 | 28.48 | 180 | 8.44 |
| 240 | 29.11 | 240 | 8.26 |
| 300 | 29.62 | 300 | 8.24 |
| 360 | 30.00 | 360 | 8.10 |
| 420 | 30.16 | 420 | 8.02 |
| 480 | 30.02 | 480 | 7.95 |
| 600 | 30.86 | 600 | 7.88 |
| 720 | 31.25 | | |

| **PUMPING BOREHOLE-Ha Lumisi** | | | |
|---|---|---|---|
| Depth of pump (m) | 42 | | |
| Collor Height (m) | 0.4 | | |
| Borehole Diameter (m) | 0.14 | | |
| Depth of Borehole (m) | 45 | | |
| Static Water Level (m) | 4.55 | | |
| **Time** | **Drawdown** | **Time** | **Recovery** |
| **(min)** | **s(m)** | **(min)** | **s'(m)** |

| | | | |
|---|---|---|---|
| 1 | 4.79 | 1 | 7.97 |
| 2 | 4.88 | 2 | 7.92 |
| 3 | 4.98 | 3 | 7.87 |
| 4 | 5 | 4 | 7.79 |
| 5 | 5.08 | 5 | 7.65 |
| 6 | 5.13 | 6 | 7.62 |
| 7 | 5.18 | 7 | 5.57 |
| 8 | 5.25 | 8 | 7.5 |
| 9 | 5.29 | 9 | 7.45 |
| 10 | 5.32 | 10 | 7.4 |
| 11 | 5.37 | 11 | 7.37 |
| 12 | 5.42 | 12 | 7.35 |
| 13 | 5.46 | 13 | 7.31 |
| 14 | 5.48 | 14 | 7.28 |
| 15 | 5.51 | 15 | 7.24 |
| 16 | 5.57 | 16 | 7.2 |
| 17 | 5.6 | 17 | 7.16 |
| 18 | 5.63 | 18 | 7.12 |
| 19 | 5.65 | 19 | 7.09 |
| 20 | 5.69 | 20 | 7.07 |
| 25 | 5.82 | 25 | 6.94 |
| 30 | 5.93 | 30 | 6.82 |
| 40 | 6.12 | 40 | 6.63 |
| 50 | 6.27 | 50 | 6.55 |
| 60 | 6.49 | 60 | 6.41 |
| 75 | 6.55 | 75 | 6.24 |
| 90 | 6.69 | 90 | 6.14 |
| 120 | 6.86 | 120 | 6.03 |
| 150 | 7.01 | 150 | 5.92 |
| 180 | 7.12 | 180 | 5.88 |
| 240 | 7.32 | 240 | 5.74 |
| 300 | 7.48 | 300 | 5.64 |
| 360 | 7.61 | 360 | 5.56 |
| 420 | 7.75 | 420 | 5.51 |
| 480 | 7.86 | 480 | 5.41 |
| 600 | 8.05 | 600 | 5.36 |

| | | | |
|---|---|---|---|
| 720 | 8.23 | | |
| **PUMPING BOREHOLE-Malumeng** | | | |
| Depth of pump (m) | 65 | | |
| Collor Height (m) | 0.14 | | |
| Borehole Diameter (m) | 0.14 | | |
| Depth of Borehole (m) | 80 | | |
| Static Water Level (m) | 5.58 | | |
| **Time** | **Drawdown** | **Time** | **Recovery** |
| **(min)** | **s(m)** | **(min)** | **s'(m)** |
| 1 | 6.20 | 1 | 28.39 |
| 2 | 6.46 | 2 | 26.23 |
| 3 | 7.28 | 3 | 24.32 |
| 4 | 8.38 | 4 | 22.14 |
| 5 | 9.24 | 5 | 20.40 |
| 6 | 9.92 | 6 | 18.98 |
| 7 | 10.86 | 7 | 17.28 |
| 8 | 11.82 | 8 | 16.57 |
| 9 | 12.84 | 9 | 15.46 |
| 10 | 13.54 | 10 | 14.53 |
| 11 | 14.22 | 11 | 13.78 |
| 12 | 14.78 | 12 | 13.06 |
| 13 | 15.34 | 13 | 12.46 |
| 14 | 15.85 | 14 | 11.92 |
| 15 | 16.32 | 15 | 11.42 |
| 16 | 16.80 | 16 | 10.99 |
| 17 | 17.16 | 17 | 10.63 |
| 18 | 17.50 | 18 | 10.36 |
| 19 | 17.83 | 19 | 10.16 |
| 20 | 18.17 | 20 | 9.97 |
| 25 | 19.34 | 25 | 9.17 |
| 30 | 20.18 | 30 | 8.54 |
| 40 | 21.40 | 40 | 7.66 |
| 50 | 22.33 | 50 | 7.14 |
| 60 | 23.05 | 60 | 6.80 |
| 75 | 23.61 | 75 | 5.50 |
| 90 | 24.38 | 90 | 6.39 |

| | | | |
|---|---|---|---|
| 120 | 25.49 | 120 | 6.28 |
| 150 | 26.32 | 150 | 6.20 |
| 180 | 26.86 | 180 | 6.15 |
| 240 | 27.61 | 240 | 6.13 |
| 300 | 28.44 | 300 | 6.10 |
| 360 | 29.07 | 360 | 6.08 |
| 420 | 29.49 | 420 | |
| 480 | 29.92 | 480 | |
| 600 | 30.55 | 600 | |
| 720 | 31.08 | | |